ISSN 2658-3518

LIMNOLOGY & FRESHWATER BIOLOGY

2026, № 2

> abiotic and biotic water components;
> ecosystem-level studies;
> systematics and aquatic ecology;
> paleolimnology and environmental histories;
> laboratory experiments and modeling

Diatom ecological guilds as environmental indicators for biomonitoring in a tropical river basin of Southeast Asia

Original Article

LIMNOLOGY FRESHWATER BIOLOGY

Hallazgo C.I.J.S.[1]*, Sinco A.L.[1,2], Sendaydiego J.P.[1], Saab L.L.[1], Ladera R.A.[1], Raagas E.L.[3]

[1] *Biology Department, College of Arts and Sciences, Xavier University – Ateneo de Cagayan, Cagayan de Oro City, Misamis Oriental, 9000 Philippines*
[2] *McKeough Advancement for Environment, Resilience, and Sustainability Center, Xavier University – Ateneo de Cagayan, Cagayan de Oro City, Misamis Oriental, 9000 Philippines*
[3] *Xavier University – Ateneo de Cagayan, Cagayan de Oro City, Misamis Oriental, 9000 Philippines*

ABSTRACT. Functional traits are widely used in ecological studies to better understand diatom assemblages. This study examined the relationship between diatom ecological guilds (low-profile, high-profile, motile, and planktonic) and environmental parameters across 28 rivers and streams in the Tagoloan River Basin, Northern Mindanao, Philippines. The aim was to assess whether these guilds serve as effective indicators for biomonitoring. Canonical correspondence analysis (CCA) revealed a significant relationship ($p = 0.015$), indicating that phosphate (PO_4^{3-}), nitrate (NO_3^-), nitrite (NO_2^-), ammonium (NH_4^+), turbidity, pH, temperature, total dissolved solids (TDS), total suspended solids (TSS), conductivity, dissolved oxygen (DO), and flow influence diatom ecological guilds. The CCA explained 98.27% of the variance in two axes, demonstrating that diatom ecological guilds respond to environmental variables and may serve as useful indicators for river basin biomonitoring, which is useful for tropical countries like the Philippines where physicochemical analyses can be costly.

Keywords: biomonitoring, diatoms, diversity, ecological guilds, Tagoloan River Basin

For citation: Hallazgo C.I.J.S., Sinco A.L., Sendaydiego J.P., Saab L.L., Ladera R.A., Raagas E.L. Diatom ecological guilds as environmental indicators for biomonitoring in a tropical river basin of Southeast Asia // Limnology and Freshwater Biology. 2026. - № 2. - P. 63-77. DOI: 10.31951/2658-3518-2026-A-2-63

1. Introduction

Diatoms are considered one of the best bioindicators for aquatic systems (Bešta et al., 2015) because their assemblages are connected to the changes happening to their environment (Ladera et al., 2025; Porter et al., 2013). Most studies identify diatoms down to the species level to preserve the information shown by the assemblage and species complexes (Lane, 2007; Lange et al., 2016; Passy, 2007a). Some authors argued that identification to species level is critical because it improves classification within the ecoregion due to the presence of endemic and cosmopolitan diatoms (Morin et al., 2009; Ponader and Potapova, 2007). However, Rimet and Bouchez (2012) stated that genus-level identification is sufficient and has proven efficient and robust for bioassessment, as shown by other authors (Marcel et al., 2013; Pandey et al., 2017; Verleyen et al., 2009).

Using functional groups based on genus-level identification is another option to assess ecological quality (Berthon et al., 2011; Rimet and Bouchez, 2011) to complement biodiversity metrics (Pandey et al., 2017). This option reduces the strains in taxonomic identification, supplying a more cost and time effective method (Riato et al., 2017). Functional traits that reduce taxonomic resolution give good assessment on the pollution status much like species level resolution (Berthon et al., 2011; Passy, 2007b). A functional group is composed of organisms which share similar ecological features including morphology and physiology called functional traits (Tapolczai et al., 2016). Ecological guilds are examples of such groups which is defined as a group of taxa sharing the same environ-

*Corresponding author. E-mail address: challazgo@xu.edu.ph (I.J.S. Hallazgo)

Received: July 27, 2025;
Accepted after revised: February 27, 2026;
Available online: April 24, 2026

ment and utilize available resources similarly through various adaptations to abiotic factors (B-Béres et al., 2014; Passy, 2007b; Rimet and Bouchez, 2011) which can be applied to diatoms. These functional traits are used as adaptive strategies and growth morphologies by diatoms to provide more interpretation on the diatom assemblage variation. The use of such biological traits provides more robust ecological profiles because diatoms occur in biofilms. Understanding biofilm structure enhances the ecological interpretation of diatom guilds in biomonitoring, as guild composition reflects how diatoms interact with and adapt to environmental conditions within these structured communities (Cibic et al., 2012).

Passy (2007b) introduced three ecological guilds. The low-profile guild was comprised of species of short stature which include prostrate, adnate, erect, solitary centrics and slow-moving species (e.g., *Achnanthes*, *Achnanthidium*, *Amphora*, *Cocconeis*, *Cyclotella*, *Cymbella*, *Hannaea*, *Meridion*, *Opephora*, and *Reimeria*). Low-profile resists the change done by physical disturbance but cannot that of nutrient enrichment. The high-profile guild was composed of species of tall stature which include erect, filamentous, branched, chain-forming, tube-forming, stalked and colonial centrics (e.g., *Diatoma*, *Ellerbeckia*, *Eunotia*, *Fragilaria*, *Gomphoneis*, *Gomphonema*, *Melosira* and *Synedra*). Passy further explained their ability to make colonies allows them to exploit resources which are unavailable to the low-profile guild. High-profile guild does not resist the change done by physical disturbance but resists that of nutrient enrichment. The motile guild was constituted of fast-moving species from the *Navicula*, *Nitzschia*, *Sellaphora*, and *Surirella* genera. The motile guild shows similar pattern to that of high-profile but its members are able to move to a more suitable habitat. Rimet and Bouchez (2011) added a planktonic guild which are primarily diatoms which have adapted to the lentic environment through their adaptations that enable them to withstand sedimentation. Since different guilds show varying tolerances to nutrient enrichment, they can serve as effective indicators of trophic states. The high-profile and motile guilds, which are not limited by nutrients, may dominate in eutrophic waters, where nutrient levels are high (Passy, 2007b). On the other hand, the low-profile guild, which is sensitive to nutrient enrichment, may be more abundant in oligotrophic or less nutrient-rich environments (Passy, 2007b). The planktonic guild's presence can indicate slower-moving or standing waters where sedimentation is a concern (Rimet and Bouchez, 2011).

In order to assess the water quality and the disturbances in streams, diatom ecological guilds have been used in biomonitoring studies around the world (B-Béres et al., 2017; Marcel et al., 2017; Riato et al., 2017). However, no study was still done about using diatom functional-based approach as a means of assessing the conditions of aquatic systems in the Philippines. This study aims to evaluate the relationship between diatom ecological guilds and environmental variables, and to determine whether they can be used for biomonitoring in the Tagoloan River Basin.

2. Materials and Methods

Samples were collected at 28 rivers and streams of the Tagoloan River Basin (Fig. 1), encompassing the municipalities of Tagoloan, Villanueva, and Claveria in Misamis Oriental; and Malitbog, Manolo Fortich, Sumilao, Impasug-ong, and Malaybalay City in Bukidnon from August until December 2018. Three sampling points were established, representing the upstream, midstream and downstream regions of each river or tributary. In each sampling point, there were three replicates where the measurement of physical and chemical parameters and the collection of diatoms were done. Water depth (m) and the width (m) of the rivers and streams were measured using a meter stick while water flow (m/s) was measured using a drogue and a stopwatch. Water temperature (ºC), pH, total dissolved solids (mg/L), conductivity (µs/cm) and dissolved oxygen (mg/L) were measured in situ using a portable multiparameter digital meter (HACH water ecology, limnology Model AL-36DT). Water samples of 1000 mL were kept in coolers at 4 ºC while being transported to the laboratory for concentration measurements (mg/L) of nitrite (NO_2^-), nitrate (NO_3^-), phosphate (PO_4^{3-}), ammonium (NH_4^+), iron (Fe^+), biological oxygen demand (BOD_5), total suspended solids (TSS),

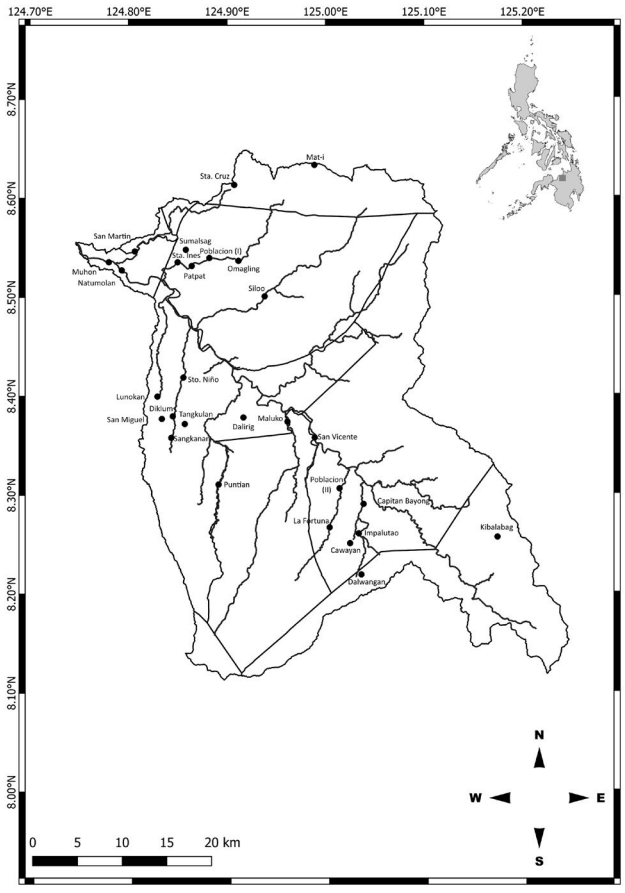

Fig.1. The sampling sites in the Tagoloan River Basin in the region of Northern Mindanao, Philippines. Black inner squiggly lines: The rivers and streams in the Tagoloan River Basin. Black dots: The sampling sites in the Tagoloan River Basin.

and water hardness using the guidelines of the Standard Methods for the Examination of Water and Wastewater 18th Edition (American Public Health Association et al., 2012). Turbidity (NTU) was measured in the laboratory with the Thermo Scientific Genesys 10 UV-Visible spectrometer.

Ten cobble-sized stones were collected in each one of the three replicate points in each sampling site, and were scrubbed with a clean toothbrush covering a surface area of 10 cm^2. The diatoms collected were placed in amber bottles fixed with 5% buffered solution made of 37% formaldehyde diluted with distilled water. In the laboratory, the diatom valves were cleaned and prepared using the hot hydrogen-peroxide method (EN13946:2003) before embedding in a Naphrax synthetic resin. Swift Optical M10DB-MP Phase Contrast microscope with 1000x magnification was then used for the counting and identification of 400 diatom frustules (EN 14407:2004). Identification down to genus level was done using the taxonomic keys of Gell (1999), Taylor et al. (2007), and other specialized keys as needed. There were 756 slides of diatom samples that were analyzed with parallel environmental parameters collected.

The identified diatom genera were classified according to the ecological guilds of Passy (2007b) and Rimet and Bouchez (2011) as shown in Table 1. Principal Component Analysis (PCA) was used to identify the most influential environmental variables (Stenger-Kovács et al., 2013), with 12 environmental variables determined to be the key factors. Canonical correspondence analyses (CCA) were conducted to examine the relationship between key environmental variables (identified through PCA) and diatom assemblages, both in terms of taxonomic composition and ecological guild structure. Environmental variables were incorporated into the CCA using a weighted averaging approach. Multivariate analysis was done using the PAST software version 4.16 (Hammer, 2023).

3. Results

There were 29 identified diatom genera in the 28 sampling areas of the Tagoloan River Basin; of which *Navicula* (19.24%), *Cocconeis* (16.34%), and *Achnanthidium* (12.78%) were the most abundant genera (Table 2). Across the said sampling areas, *Cocconeis* was the most abundant in 12 sites, followed by *Navicula* in 7 sites; *Achnanthidium* in 3 sites; *Gomphonema* in 2 sites; and *Encyonema*, *Fragilaria*, *Gomphoneis*, and *Nitzschia* in 1 site each (Table 3). In terms of diversity values, the sampling areas had a Simpson's index of diversity (1-D) ranging from 0.7727 (Lunokan) to 0.8907 (Muhon), indicating that the sites sampled were diverse in diatom assemblages (Table 3).

Table 1. Taxa assignment to the four ecological guilds adapted from Passy (2007b) and Rimet and Bouchez (2011).

Ecological guilds	Guild Description	Taxa composition
Low-profile	Comprised of species of short stature, including prostrate (species with their whole valve area directly attached to the substrate), adnate (species with their apex attached in parallel to the substrate), erect (species with perpendicular attachment to the substrate), solitary centrics, and slow- moving species	*Achnanthes* Bory 1822 *Achnanthidium* Kutzing 1844 *Amphora* Ehrenberg ex Kutzing 1844 *Cocconeis* Ehrenberg 1837 *Cymbella* Agardh 1830 *Diploneis* Cleve 1894 *Planothidium* Round and Bukhtiyarova 1996
High-profile	Comprised of species of tall stature, including erect, filamentous, branched, chain-forming, tubeforming, stalked, and colonial centrics	*Encyonema* Kutzing 1833 *Eunotia* Ehrenberg 1837 *Fragilaria* Lyngbye 1819 *Frustulia* Rabenhorst 1583 *Gomphoneis* Cleve 1894 *Gomphonema* Ehrenberg 1832 *Melosira* Agardh 1824 *Pleurosira* San Leon 1848
Motile	Comprised of species which are capable of motility in sediments	*Bacillaria* Gmelin 1791 *Epithemia* Kutzing 1844 *Gyrosigma* Hassall 1845 *Hantzschia* Grunow 1877 *Luticola* Mann 1990 *Navicula* Bory 1822 *Nitzschia* Hassall 1845 *Pinnularia* Ehrenberg 1843 *Rhopalodia* Muller 1895 *Sellaphora* Mereschkowsky 1902 *Stauroneis* Ehrenberg 1843 *Surirella* Turpin 1828 *Tryblionella* Smith 1853
Planktonic	Corresponds to taxa adapted to lentic environments with morphological adaptations that enable them to resist sedimentation	*Cyclotella* Kutzing ex Brebisson 1838

Out of the 17 physical and chemical parameters measured, 12 variables (NO_2^-, NO_3^-, PO_4^+, NH_4^+, turbidity, pH, temperature, conductivity, flow, TDS, TSS, and DO) turned out to be the main components based on the PCA done (Fig. 2). The first two axes of the PCA explained 96.82% of variance. The dominant factors were TSS (0.9749), flow (0.1185), TDS (0.0839), pH (0.0543), and conductivity (0.0456).

Tables 4 to 6 show the range and mean values of the measured physical and chemical conditions in the 28 sampling areas. Not all rivers and tributaries sampled in the river basin received a water body classification from the Department of Environment and Natural Resources (DENR) Region 10. However, Tagoloan River which is a major river, and Malitbog River which is a principal river, both received a Class A classification which meant that they are intended as sources of water supply requiring conventional treatment to meet the national standards (DENR Administrative Order 2016-08, 2016). Going by such classification, the rivers of the Tagoloan River Basin can be considered as Class A. Based on the water quality guidelines (WQG) by DENR, some sites had measurements of phosphate, nitrate, pH, TSS, and temperature which were beyond the standard values. These are indicated by the values in red.

The 28 sampling areas can be grouped according to the relative abundances of the ecological guilds (Table 7). Seventeen of the sampling areas were primarily composed of low-profile diatoms (Capitan Bayong, Dalirig, Impalutao, Kibalabag, La Fortuna, Lunokan, Maluko, Muhon, Omagling, Poblacion (I), Puntian, Sangkanan, San Martin, San Vicente, Silo-o, Sto. Niño, and Sumalsag) while 8 sites were mainly composed of motile diatoms (Cawayan, Dalwangan, Diklum, Natumolan, Patpat, Poblacion (II), San Miguel, and Sta. Ines). Three areas were mainly defined by

Table 2. Relative abundance of diatom genera in the Tagoloan River Basin. Values in red indicate the top three most abundant genera.

Diatom Genera	Relative Abundance (%)
Achnanthes	4.15
Achnanthidium	12.78
Amphora	0.86
Bacillaria	0.01
Cocconeis	16.34
Cyclotella	0.27
Cymbella	2.94
Diploneis	0.01
Encyonema	2.70
Epithemia	0.02
Eunotia	0.14
Fragilaria	3.69
Frustulia	0.31
Gomphoneis	5.97
Gomphonema	9.96
Gyrosigma	0.91
Hantzschia	0.08
Luticola	2.80
Melosira	0.77
Navicula	19.24
Nitzschia	8.52
Pinnularia	1.17
Planothidium	3.60
Rhopalodia	0.15
Sellaphora	0.01
Stauroneis	1.05
Surirella	0.88
Pleurosira	0.06
Tryblionella	0.62

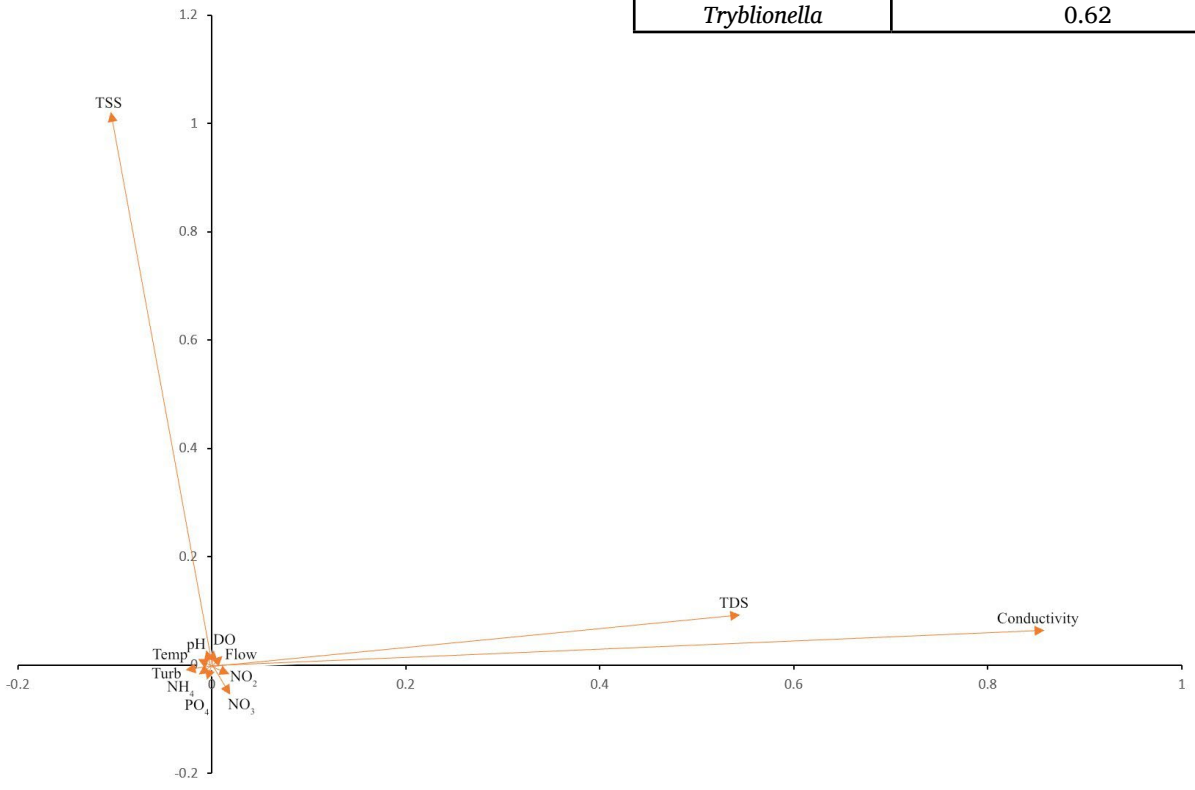

Fig.2. Principal component analysis diagram with ordination of axis 1 and 2 of measured environmental variables of the Tagoloan River Basin (Axis 1: 78.68%; Axis 2: 19.59%).

Table 3. Dominant diatom genera and their relative abundances, and Simpson's index of diversity (1-D) values in each of the 28 sampling areas of the Tagoloan River Basin.

Sampling Area	Dominant Genera	Relative Abundance (%)	Simpson (1-D)
Kibalabag	*Nitzschia*	18.78	0.8690
Mat-i	*Encyonema*	34.00	0.8164
Dalwangan	*Fragilaria*	18.78	0.8835
Cawayan	*Gomphoneis*	26.42	0.8470
La Fortuna	*Cocconeis*	25.36	0.8498
Impalutao	*Cocconeis*	24.78	0.8524
Sta. Cruz	*Navicula*	28.47	0.8294
Puntian	*Cocconeis*	23.94	0.8492
Sangkanan	*Navicula*	19.08	0.8599
San Miguel	*Gomphonema*	23.97	0.8314
Capitan Bayong	*Cocconeis*	25.94	0.8338
Tangkulan	*Gomphonema*	29.72	0.8002
Poblacion (I)	*Cocconeis*	26.19	0.8461
Diklum	*Navicula*	35.08	0.8050
Lunokan	*Cocconeis*	42.28	0.7727
Sto. Niño	*Cocconeis*	26.06	0.8514
Dalirig	*Cocconeis*	22.08	0.8801
San Vicente	*Cocconeis*	28.06	0.8336
Maluko	*Cocconeis*	29.00	0.8320
Silo-o	*Cocconeis*	32.28	0.7949
Omagling	*Cocconeis*	25.47	0.8365
Poblacion (II)	*Achnanthidium*	28.94	0.8239
Sumalsag	*Achnanthidium*	29.44	0.8281
Patpat	*Navicula*	22.69	0.8789
Sta. Ines	*Navicula*	28.39	0.8565
San Martin	*Navicula*	19.17	0.8759
Muhon	*Achnanthidium*	17.14	0.8907
Natumolan	*Navicula*	22.56	0.8822

high-profile diatoms (Mat-i, Sta. Cruz, and Tangkulan). Since the planktonic guild was only represented by one genus, 8 of the sampling sites had no planktonic diatoms.

A significant relationship between the 12 environmental variables and the diatom ecological guilds was indicated in the CCA (Fig. 3). The correlation between the guilds and environmental variables across the first two axes was 98.27%, with statistical significance confirmed by a Monte Carlo permutation test ($N = 999$, $p = 0.015$). The low-profile guild was positively associated with DO, pH, and conductivity and was negatively associated with NO_3, NO_2, and turbidity. In contrast, the high-profile guild was positively associated with turbidity and was negatively associated with TDS, DO, and conductivity. The motile guild was positively associated with NO_3, NO_2, PO_4, TSS, and temperature; and was negatively associated with DO and conductivity. The planktonic guild was positively associated with TDS and conductivity and was negatively associated with NH_4, flow, and turbidity.

In terms of diatom generic composition (Fig. 4), low-profile guild members were strongly correlated with DO and flow, especially *Achnanthes* (Achn) while *Cocconeis* (Cocc) and *Planothidium* (Plano) had a weak correlation with flow and DO. *Achnanthidium* (Achndm) and *Cymbella* (Cymb) were weakly associated with conductivity, TDS, and TSS while *Amphora* (Amph) and *Diploneis* (Dipl) were negatively associated with temperature. *Pleurosira* (Pleura), a member of the high-profile guild, was strongly positively correlated with PO_4^{3-} and turbidity while *Gomphonema* (Gopma) was positively associated with NO_2^- and NO_3^-. *Eunotia* (Euno) was weakly associated with NH_4^+ and pH while *Frustulia* (Frus) was weakly associated with conductivity, TDS, and TSS. *Encyonema* (Ency), *Fragilaria* (Frag), *Gomphoneis* (Gomeis), and *Melosira* (Melo) were all positively associated with DO and flow. The motile guild was correlated with high NO_2^- and NO_3^-, especially *Bacillaria* (Bacil), *Pinnularia* (Pinn), and *Surirella* (Suri). *Navicula* (Navi) and *Stauroneis* (Stau) were positively correlated with PO_4^{3-}, turbidity, NO_3^-, and NO_2^-. *Hantzschia* (Hantz) was positively associated with PO_4^{3-} and flow while *Sellaphora* (Sella) was positively correlated with PO_4^{3-} and turbidity. *Epithemia* (Epit), *Luticola* (Luti), and *Nitzschia* (Nitz) were strongly positively associated with DO and flow. On the other hand, *Gyrosigma* (Gyro), *Rhopalodia* (Rhop), and *Tryblionella* (Tryb) had a weak correlation with conductivity, TDS, and TSS. *Cyclotella* (Cyclo), the lone member of the planktonic guild, was strongly positively correlated with DO and flow.

Table 4. Range and mean physicochemical conditions (Flow, pH, Temperature, and TDS) of sampled rivers and streams. Values in red indicate that they are above or below the standard value or are out of range.

Sampling Area	Parameter							
	Flow (m/s)		pH Standard range = 6.50 - 8.50		Temperature (ºC) Standard range = 26.00 - 30.00		TDS (mg/L)	
	Range	Mean (sd)	Range	Mean (sd)	Range	Mean (sd)	Range	Mean (sd)
Kibalabag	3.90–14.25	8.44 ± 0.74	7.96–8.76	8.37 ± 0.30	20.8–22.30	21.44 ± 0.55	177.00–250.00	205.44 ± 28.77
Mat-i	1.35–6.19	3.63 ± 0.69	7.00–7.90	7.36 ± 0.25	21.50–22.10	21.57 ± 0.20	34.00–78.00	41.33 ± 13.86
Dalwangan	1.53–9.53	4.44 ± 0.68	7.20–8.18	7.70 ± 0.32	23.30–24.50	24.00 ± 0.46	167.00–170.00	168.11 ± 0.93
Cawayan	1.80–6.80	3.68 ± 0.00	7.64–7.79	7.72 ± 0.05	26.20–28.10	26.76 ± 0.63	60.00–65.00	61.11 ± 1.54
La Fortuna	1.60–6.80	3.76 ± 0.58	7.83–8.09	7.94 ± 0.08	25.90–26.70	26.31 ± 0.25	51.00–59.00	52.44 ± 2.51
Impalutao	1.84–6.00	3.72 ± 0.18	7.16–8.10	7.76 ± 0.41	23.00–25.60	24.03 ± 0.85	103.00–133.00	114.67 ± 14.16
Sta. Cruz	2.00–6.00	3.86 ± 0.30	7.70–7.78	7.75 ± 0.03	23.30–24.00	23.64 ± 0.26	47.00–54.00	48.11 ± 2.26
Puntian	0.22–7.47	2.84 ± 0.15	7.70–7.78	5.73 ± 0.02	23.30–24.00	22.88 ± 0.51	47.00–54.00	103.67 ± 0.50
Sangkanan	2.08–3.45	2.62 ± 0.73	7.67–7.79	7.73 ± 0.04	23.10–24.00	23.58 ± 0.26	56.00–68.00	65.78 ± 3.73
San Miguel	3.75–4.60	4.04 ± 0.48	7.07–7.31	7.16 ± 0.07	25.20–26.00	25.53 ± 0.24	110.00–121.00	116.11 ± 3.92
Capitan Bayong	0.72–4.59	2.77 ± 0.70	8.28–8.42	8.37 ± 0.04	22.60–24.40	23.26 ± 0.61	144.00–200.00	150.44 ± 18.59
Tangkulan	2.47–10.5	4.47 ± 1.60	7.57–7.84	7.65 ± 0.09	25.40–26.30	25.72 ± 0.39	78.00–115.00	82.67 ± 12.13
Poblacion (I)	1.68–4.41	2.81 ± 0.32	8.46–8.55	8.50 ± 0.03	24.60–26.10	25.13 ± 0.55	132.00–145.20	134.69 ± 4.69
Diklum	3.56–5.80	4.92 ± 1.19	6.79–7.08	6.97 ± 0.09	25.70–26.70	26.12 ± 0.41	57.00–82.00	63.22 ± 8.38
Lunokan	1.93–12.00	6.11 ± 1.66	7.87–8.40	8.07 ± 0.14	26.40–27.80	26.61 ± 0.46	247.00–272.00	250.89 ± 7.96
Sto. Nino	1.65–2.97	2.52 ± 0.75	7.95–8.15	8.08 ± 0.06	23.90–24.20	24.09 ± 0.09	139.00–144.00	140.33 ± 1.87
Dalirig	1.60–11.00	6.42 ± 0.82	7.71–8.21	8.06 ± 0.16	24.00–24.50	24.22 ± 0.19	293.00–346.00	301.00 ± 16.96
San Vicente	0.69–6.47	2.58 ± 0.64	5.73–5.79	5.76 ± 0.02	27.60–39.60	30.06 ± 3.68	163.00–167.00	166.11 ± 1.27
Maluko	0.40–16.00	4.04 ± 3.27	7.21–7.86	7.68 ± 0.21	22.50–27.70	23.34 ± 1.65	134.00–158.00	140.78 ± 9.46
Silo-o	1.00–4.60	2.71 ± 0.62	8.28–8.50	8.41 ± 0.07	22.80–26.80	24.40 ± 1.39	123.00–204.00	176.89 ± 22.25
Omagling	1.37–19.00	3.33 ± 0.66	8.58–8.69	8.63 ± 0.04	26.70–28.40	27.21 ± 0.53	165.00–189.00	175.22 ± 9.64
Poblacion (II)	1.05–5.67	2.18 ± 0.56	7.64–8.02	7.84 ± 0.17	24.50–24.70	24.60 ± 0.09	506.00–508.00	506.67 ± 1.00
Sumalsag	1.86–4.64	3.18 ± 1.39	7.74–8.16	7.97 ± 0.15	26.60–28.20	27.47 ± 0.55	495.00–554.00	513.33 ± 17.72
Patpat	3.30–4.43	3.91 ± 0.51	7.25–8.00	7.76 ± 0.22	26.10–27.30	26.63 ± 0.41	169.00–171.00	170.00 ± 0.71
Sta. Ines	2.45–3.45	2.89 ± 0.51	6.78–8.00	7.68 ± 0.36	24.20–25.50	24.54 ± 0.39	174.00–189.00	180.89 ± 3.82
San Martin	0.62–5.63	2.47 ± 1.13	8.72–8.82	8.79 ± 0.03	28.40–28.70	28.59 ± 0.11	191.00–195.00	192.00 ± 1.22
Muhon	2.90–10.75	5.44 ± 0.71	8.73–9.05	8.83 ± 0.11	29.40–30.30	29.91 ± 0.35	209.00–231.00	214.67 ± 6.91
Natumolan	1.70–6.16	4.03 ± 0.53	8.88–9.97	9.11 ± 0.33	29.20–30.40	29.53 ± 0.39	195.00–203.00	197.89 ± 2.85

Table 5. Range and mean of physicochemical conditions (Conductivity, DO, Turbidity, and TSS) of sampled rivers and streams. Values in red indicate that they are above or below the standard value or are out of range.

Sampling Area	Parameter							
	Conductivity (µs/cm)		DO (mg/L) Standard minimum value = 5.00		Turbidity (NTU)		TSS (mg/L) Standard value = 50.00	
	Range	Mean (sd)	Range	Mean (sd)	Range	Mean (sd)	Range	Mean (sd)
Kibalabag	176.90–250.00	205.56 ± 28.71	6.44–7.53	7.01 ± 0.41	0.00–6.00	1.00 ± 1.94	0.56.–795.40	262.01 ± 259.20
Mat-i	33.90–45.60	36.90 ± 3.57	7.18–7.33	7.26 ± 0.05	10.00–10.00	10.00 ± 0.00	1.80–281.28	98.81 ± 115.04
Dalwangan	167.60–172.80	169.17 ± 1.70	6.43–6.81	6.65 ± 0.15	0.30–6.00	1.48 ± 1.77	1.10–220.96	41.61 ± 70.86
Cawayan	57.20–62.80	58.51 ± 1.68	7.12–7.66	7.31 ± 0.19	2.00–6.00	3.22 ± 1.20	5.73–375.12	146.68 ± 140.57
La Fortuna	48.80–54.60	50.24 ± 1.73	7.27–7.40	7.31 ± 0.04	0.00–1.00	0.67 ± 0.50	1.08–232.64	29.80 ± 76.10
Impalutao	98.30–127.30	109.70 ± 13.27	6.31–7.60	7.19 ± 0.49	1.00–1.00	1.00 ± 0.00	2.22–126.78	45.48 ± 45.83
Sta. Cruz	45.00–48.60	45.88 ± 1.07	7.46–7.70	7.61 ± 0.09	7.00–10.00	8.33 ± 1.32	5.47–258.09	69.87 ± 99.20
Puntian	45.00–48.60	99.09 ± 0.86	7.46–7.70	7.46 ± 0.09	7.00–10.00	8.00 ± 1.73	5.47–258.09	18.49 ± 25.49
Sangkanan	62.70–67.60	64.27 ± 1.49	7.44–7.56	7.51 ± 0.04	5.00–6.00	5.67 ± 0.50	8.06–271.38	127.10 ± 100.17
San Miguel	105.20–116.30	111.23 ± 3.70	6.03–6.49	6.27 ± 0.18	6.00–18.00	11.00 ± 4.77	21.20–1091.00	478.11 ± 373.57
Capitan Bayong	136.30–140.00	137.79 ± 0.98	7.82–8.03	7.92 ± 0.07	0.00–1.00	0.78 ± 0.44	7.31–237.96	92.61 ± 97.66
Tangkulan	116.42–171.64	123.38 ± 18.11	7.04–7.24	7.15 ± 0.08	13.00–17.00	14.00 ± 1.41	14.81–89.11	45.42 ± 28.91
Poblacion (I)	126.60–137.90	129.23 ± 4.10	7.62–7.85	7.79 ± 0.07	1.00–1.00	1.00 ± 0.00	3.68–117.20	17.27 ± 37.49
Diklum	85.07–122.39	94.36 ± 12.50	7.01–7.12	7.05 ± 0.04	28.00–54.00	43.89 ± 6.97	29.20–48.80	37.60 ± 6.93
Lunokan	368.66–405.97	374.46 ± 11.88	6.80–7.08	7.01 ± 0.08	1.00–4.00	2.11 ± 1.27	2.33–127.26	38.29 ± 41.03
Sto. Nino	133.70–140.90	135.28 ± 2.61	7.41–7.61	7.53 ± 0.06	2.00–4.00	3.22 ± 0.97	16.60–752.00	350.16 ± 306.52
Dalirig	437.31–516.42	449.25 ± 25.31	7.41–7.64	7.54 ± 0.08	1.00–1.00	1.00 ± 0.00	3.22–119.22	46.48 ± 42.80
San Vicente	157.90–161.40	159.87 ± 1.07	7.30–7.68	7.49 ± 0.13	2.00–6.00	3.22 ± 1.20	8.47–91.33	19.61 ± 27.02
Maluko	200.00–235.82	210.12 ± 14.12	7.80–8.02	7.93 ± 0.08	1.00–2.00	1.11 ± 0.33	4.42–942.74	113.04 ± 311.17
Silo-o	167.10–194.30	176.34 ± 9.16	7.48–7.89	7.76 ± 0.14	0.00–7.00	1.78 ± 2.28	6.07–12.67	8.93 ± 2.36
Omagling	157.60–180.00	166.62 ± 8.52	7.37–7.67	7.54 ± 0.09	0.00–1.00	0.22 ± 0.44	1.26–12.07	7.00 ± 2.87
Poblacion (II)	755.22–758.21	756.22 ± 1.49	7.41–7.43	7.42 ± 0.01	1.00–4.00	1.56 ± 1.01	2.11–121.20	55.82 ± 36.88
Sumalsag	738.81–826.87	766.17 ± 26.45	7.25–7.58	7.41 ± 0.12	1.00 -1.00	1.00 ± 0.00	11.16–78.84	38.55 ± 22.89
Patpat	252.24–255.22	253.73 ± 1.06	7.13–7.55	7.39 ± 0.13	5.00–10.00	7.44 ± 1.67	5.89–26.77	13.32 ± 5.73
Sta. Ines	259.70–282.09	269.98 ± 5.71	7.62–7.85	7.75 ± 0.07	5.00–11.00	7.89 ± 1.69	10.84–21.16	15.99 ± 3.70
San Martin	183.80–189.70	185.49 ± 1.74	7.67–7.88	7.82 ± 0.06	7.00–10.00	8.00 ± 0.87	27.80–551.60	167.30 ± 185.76
Muhon	105.60–210.50	194.18 ± 33.36	7.40–10.96	8.76 ± 1.26	2.00–8.00	5.33 ± 2.18	35.20–106.80	68.06 ± 28.76
Natumolan	188.40–194.80	190.41 ± 2.29	8.34–11.22	9.55 ± 1.07	1.00–2.00	1.56 ± 0.53	7.78–102.67	23.35 ± 30.68

Table 6. Range and mean of physicochemical conditions (NO_2^-, NO_3^-, NH_4^+, and PO_4^{3-}) of sampled rivers and streams. Values in red indicate that they are above or below the standard value or are out of range.

Sampling Area	Parameter							
	NO_2^- (mg/L)		NO_3^- (mg/L) Standard value = 7.00		NH_4^+ (mg/L)		PO_4^{3-} (mg/L) Standard value = <0.05	
	Range	Mean (sd)	Range	Mean (sd)	Range	Mean (sd)	Range	Mean (sd)
Kibalabag	0.001–0.015	0.00 ± 0.00	1.00–13.00	6.33 ± 3.61	0.03–0.13	0.073 ± 0.04	0.01–0.02	0.01 ± 0.00
Mat-i	0.012–0.017	0.01 ± 0.00	1.00–2.00	1.67 ± 0.50	0.2–1.44	0.71 ± 0.56	0.03–0.09	0.05 ± 0.03
Dalwangan	0.001–0.016	0.01 ± 0.01	1.00–11.00	4.22 ± 2.95	0.01–0.12	0.04 ± 0.04	0.01–0.016	0.01 ± 0.00
Cawayan	0.021–0.029	0.02 ± 0.00	2.00–10.60	5.51 ± 2.74	0.01–0.10	0.04 ± 0.04	0.006–0.027	0.01 ± 0.01
La Fortuna	0.02–0.024	0.02 ± 0.00	1.00–9.00	5.56 ± 2.13	0.01–0.01	0.01 ± 0.00	0.002–0.218	0.04 ± 0.08
Impalutao	0.007–0.025	0.02 ± 0.01	1.00–5.00	3.11 ± 1.69	0.01–0.08	0.02 ± 0.02	0.004–0.051	0.01 ± 0.01
Sta. Cruz	0.013–0.14	0.06 ± 0.06	4.00–11.00	8.00 ± 3.12	0.03–0.25	0.17 ± 0.11	0.01–0.06	0.03 ± 0.02
Puntian	0.013–0.14	0.01 ± 0.00	4.00–11.00	7.44 ± 3.13	0.03–0.25	0.21 ± 0.02	0.01–0.06	0.01 ± 0.00
Sangkanan	0.017–0.02	0.02 ± 0.00	5.00–12.00	8.00 ± 2.83	0.10–0.30	0.16 ± 0.07	0.04- 0.06	0.05 ± 0.01
San Miguel	0.017–0.117	0.08 ± 0.03	30.00–34.00	32.44 ± 1.33	0.10–0.26	0.17 ± 0.07	0.033–0.056	0.04 ± 0.01
Capitan Bayong	0.02–0.025	0.02 ± 0.00	8.00–11.00	9.00 ± 1.00	0.01–0.06	0.03 ± 0.02	7.82–8.03	0.01 ± 0.00
Tangkulan	0.008–0.013	0.01 ± 0.00	1.00–5.00	4.11 ± 1.76	0.00–0.30	0.16 ± 0.09	0.01–0.18	0.07 ± 0.06
Poblacion (I)	0.017–0.024	0.02 ± 0.00	1.00–7.00	3.78 ± 2.54	0.01–0.07	0.02 ± 0.03	0.013–0.035	0.02 ± 0.01
Diklum	6.00–34.00	18.44 ± 10.50	45.00–200.00	106.44 ± 46.87	0.40–0.90	0.67 ± 0.16	0.68–15.30	8.34 ± 5.88
Lunokan	0.005–0.009	0.07 ± 0.00	6.00–23.00	15.78 ± 7.55	0.30–4.90	1.41 ± 1.40	0.35–0.59	0.43 ± 0.07
Sto. Nino	0.013–0.021	0.02 ± 0.00	5.00–15.00	8.11 ± 3.55	0.10–0.20	0.13 ± 0.05	0.021–0.048	0.03 ± 0.01
Dalirig	0.002–0.007	0.00 ± 0.00	4.00–56.00	32.11 ± 21.45	0.00–0.20	0.13 ± 0.09	0.03–0.23	0.11 ± 0.09
San Vicente	0.024–0.028	0.03 ± 0.00	7.00–15.00	10.00 ± 2.24	0.20–0.26	0.23 ± 0.03	0.017–0.02	0.02 ± 0.00
Maluko	0.005–0.30	0.04 ± 0.01	3.00–20.00	12.44 ± 6.67	0.00–0.50	0.17 ± 0.25	0.16–0.40	0.24 ± 0.07
Silo-o	0.012–0.017	0.01 ± 0.00	27.40–45.00	36.36 ± 5.80	0.01–1.10	0.30 ± 0.47	0.047–0.089	0.07 ± 0.01
Omagling	0.009–0.014	0.01 ± 0.00	28.20–42.50	33.68 ± 3.90	0.01–1.70	0.57 ± 0.85	0.014–0.026	0.02 ± 0.00
Poblacion (II)	1.00–19.00	7.56 ± 6.52	10.00–50.00	19.89 ± 15.28	0.00–0.50	0.17 ± 0.18	0.01–0.07	0.03 ± 0.02
Sumalsag	1.00–7.00	4.67 ± 2.00	14.00–35.00	26.67 ± 6.56	0.00–0.20	0.08 ± 0.06	0.01–0.05	0.03 ± 0.02
Patpat	1.00–1.00	1.00 ± 0.00	22.00–80.00	37.00 ± 17.20	0.10–0.72	0.50 ± 0.27	0.03–0.11	0.06 ± 0.03
Sta. Ines	0.50–1.00	0.94 ± 0.17	8.00–106.00	47.44 ± 33.56	0.00–1.00	0.19 ± 0.31	0.06–0.15	0.09 ± 0.03
San Martin	0.014–0.017	0.02 ± 0.00	10.00–51.00	27.33 ± 18.38	0.22–0.28	0.25 ± 0.03	0.01–0.51	0.20 ± 0.23
Muhon	0.01–0.017	0.01 ± 0.00	20.40–43.90	37.13 ± 7.19	0.05–0.17	0.09 ± 0.05	0.016–0.094	0.06 ± 0.02
Natumolan	0.01–0.016	0.01 ± 0.00	28.40–38.10	33.06 ± 3.22	0.01–0.07	0.03 ± 0.03	0.02–0.081	0.04 ± 0.02

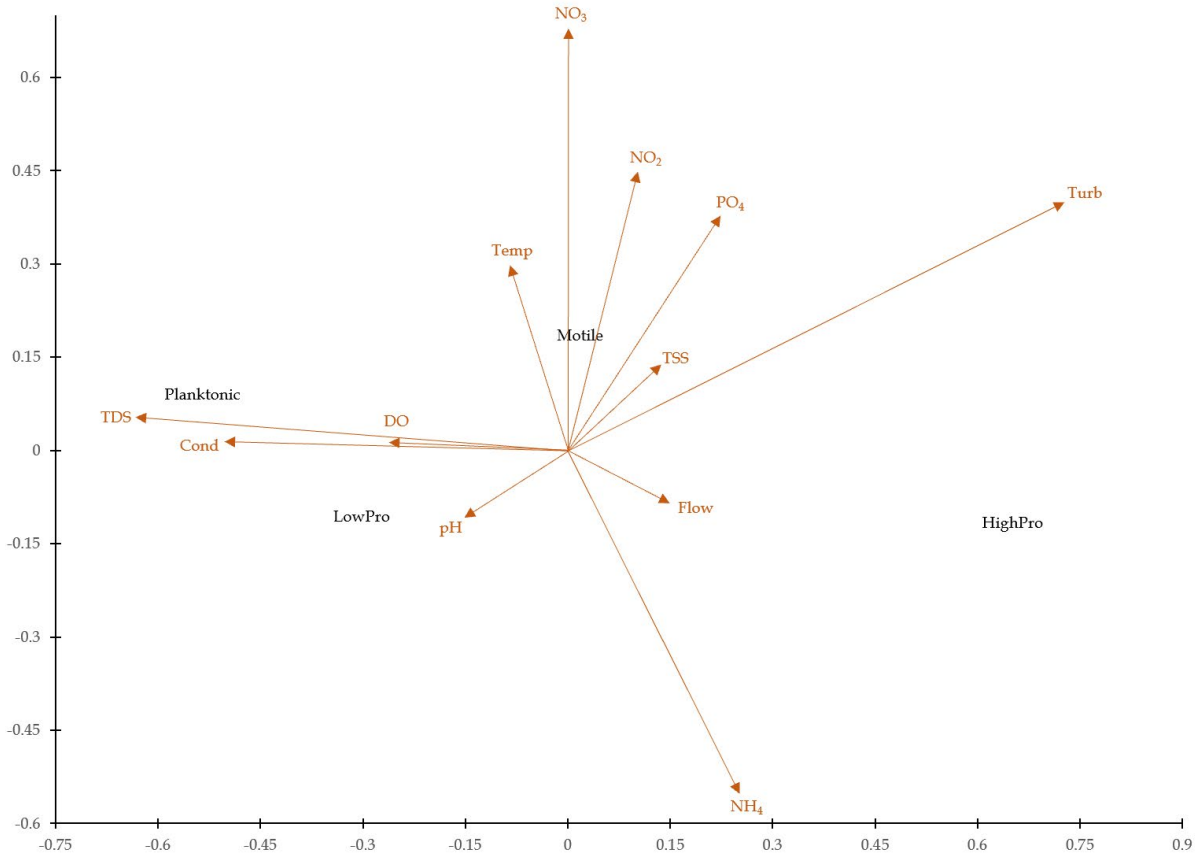

Fig.3. CCA showing the relation of diatom ecological guilds and the environmental variables based on guilds' relative abundances (Axis 1: 84.33%; Axis 2: 13.94%; p = 0.015).

4. Discussion

Navicula (19.24%), *Cocconeis* (16.34%), and *Achnanthidium* (12.78%) were the most abundant diatom genera in the Tagoloan River Basin (Table 2). These three genera were also the most abundant genera in 25 of the 28 sampling sites. *Navicula* was the most abundant in 7 sites (Diklum, Natumolan, Patpat, Sangkanan, San Martin, Sta. Cruz, and Sta. Ines); *Cocconeis* in 12 sites (Capitan Bayong, Dalirig, Impalutao, La Fortuna, Lunokan, Maluko, Omagling, Poblacion (I), Puntian, San Vicente, Silo-o, and Sto. Niño); and *Achnanthidium* in 3 sites (Muhon, Poblacion (II), and Sumalsag) as shown in Table 3. The cells of *Navicula* can be solitary, free living or motile and they were the most abundant in the river basin because they are tolerant across a huge range of pH levels, eutrophication, and conductivities (Taylor and Cocquyt, 2016). *Cocconeis*, on the other hand, is also found across a range of pH and trophic levels; they are also adapted to different substrate (Taylor and Cocquyt, 2016). *Achnanthidium* is usually attached via its mucilage stalk and is typically found in different trophic levels (Taylor and Cocquyt, 2016).

Total suspended solids (0.9749), flow (0.1185), total dissolved solids (0.0839), pH (0.0543), and conductivity (0.0456) were the dominant factors based on the PCA done (Table 4). Among the physicochemical conditions measured, pH, temperature, TSS, nitrate, and phosphate were the factors which had measurements that were above or below the standard value or were out of range based on the water quality guidelines of DENR (Tables 5 to 7).

There is a correlation between the total solids in the rivers and diatoms. The TSS are composed of the organic matter, substrate, and wastes in the water and these are significantly correlated with diatom assemblages (Dickman et al., 2005; Schroeder et al., 2016). The TDS, meanwhile, are comprised of ions, salts, and organic matter and these also relate to diatom communities (Bate et al., 2004; Kivrak and Uygun, 2012; Sudhakar et al., 1994). Both are associated with the pollution level of the river.

The potential of hydrogen (pH) plays a huge factor on diatom cell volume, growth and production rates (Berge et al., 2010; Dutkiewicz et al., 2015; Hervé et al., 2012; Kivrak and Uygun, 2012; Scholz, 2014) and the organisms disfavor acidic environments and flourish at a pH of 6.5-8.5. Acidic conditions change the internal pH of diatoms aside from altering the formation of their frustules (Hervé et al., 2012) The siliceous frustules of diatoms serve as pH buffer (Milligan and Morel, 2002). However, such impact still depends upon the species, given that diatoms have adaptations against acidification (Crawfurd et al., 2011).

Diatoms are also sensitive to flow alterations. Changes in flow modify nutrient concentration flux (Porter et al., 2013). Furthermore, the magnitude and duration of the flow are both important for diatom communities, contributing to their growth (Goldenberg-Vilar et al., 2022). At high flow, the community succession of diatoms is affected by the seasonal flood that may occur and thus, only those diatoms with a particular growth form (i.e. stalked) could thrive (Shibabaw et

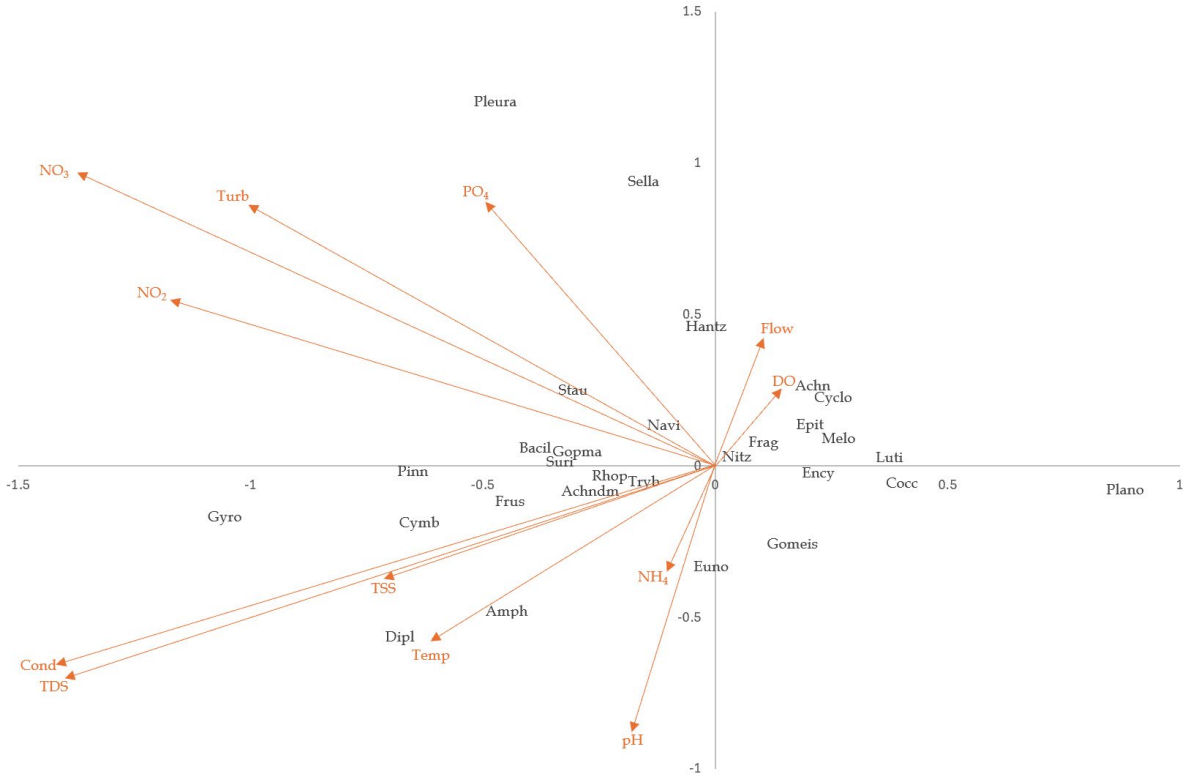

Fig.4. CCA showing the relation of diatom assemblage composition and the environmental variables based on genera abundances (Axis 2: 23.46%; Axis 8: 3.44%; p = 0.044).

al., 2021). However, the abundance and diversity of the algae will increase after some time once the community structure has been established once again.

Electrical conductivity indicates the entrance of an external discharge or pollution into the streams and rivers and is affected by temperature and dissolved solids. Diatom communities are affected by the said factor since they are sensitive to varying degrees of pollution (Bere and Tundisi, 2011; El-karim et al., 2016; Kivrak and Uygun, 2012; Pestryakova et al., 2018; Rioual et al., 2013; Teittinen et al., 2015). The parameter gives insights into the ions that could affect the availability of nutrients which the diatoms need during primary production (Saros and Fritz, 2000). Additionally, the presence of high conductivity and major ions had an impact on the distribution of diatom assemblages (Mangadze et al., 2017).

Diatoms have different responses when it comes to temperature changes; some decrease while other increase when temperature is increased (Cibic et al., 2012). Water temperature affects diatom growth where they favor environments with lower temperature (Javaheri et al., 2015; Necchi-Júnior et al., 2003; Nowrouzi and Valavi, 2011; Schabhüttl et al., 2013; Shatwell et al., 2013; Teittinen et al., 2015; Weckstrom et al., 1997; Xiao et al., 2018) thus hotter climates have a negative correlation with their growths. Diatom assemblages have a strong response to climate warming (Berthon et al., 2014). Temperature directly affects their biochemistry and metabolism (Ingebrigtsen et al., 2016).

Diatoms bloom when there is an increase in nutrient availability. Nutrients are derived from the nitrite (El-karim et al., 2016), nitrate (El-karim et al., 2016; Nowrouzi and Valavi, 2011), phosphates (El-karim et al., 2016; SE. Salomoni et al., 2011; Triest et al., 2001), ammonium (El-karim et al., 2016; S. E. Salomoni et al., 2006; Triest et al., 2001), nitrogen (S. E. Salomoni et al., 2006; SE. Salomoni et al., 2011), and phosphorus (El-karim et al., 2016; Shatwell et al., 2014) dissolved in the rivers and streams. From the said nutrients, nitrate and phosphate were the chemical factors which were included in the WQG by DENR. Nitrate is critical in the growth and survival of diatoms (Allen et al., 2011; Hockin et al., 2012; Kamp et al., 2011) and is one of the most important factors in structuring diatom assemblages (Dalu et al., 2017; Gottschalk and Kahlert, 2012). Nitrogen and phosphorus and their forms are the most important nutrients in the formation of diatom communities (Algarte et al., 2016; Wu et al., 2014). Diatom species respond differently to nutrient enrichment and pollution because of their varying tolerances and thus, the group serves as a useful bioindicator (Bere et al., 2016). They reflect the degree of anthropogenic activities occurring the area (Elias et al., 2015) since most of the sampling sites were agricultural in nature. The values which were above the standards could be associated with the agricultural runoff that the stream receives from the farms near it, leading to eutrophication. Agricultural land-use leads to surface run-off and in the process, allows additional nutrients to flow into the streams (Nhiwatiwa et al., 2017; Zhang et al., 2012). Nutrient enrichment just like that of phosphorus, is considered a precursor to eutrophication and water bodies highly enriched with the said nutrient bears decreased species richness (Jeppesen et al., 2000). Phosphorus not only drives the community composition but it is also a crucial element influencing

Table 7. Relative abundances of diatom ecological guilds in the 28 sampling areas of the Tagoloan River Basin. Values in red indicate the most abundant guild in each sampling site.

Sampling Area	Guild Relative Abundance (%)			
	Low-profile	High-profile	Motile	Planktonic
Kibalabag	50.89	14.19	34.89	0.03
Mat-i	10.31	75.61	14.06	0.03
Dalwangan	33.69	31.17	34.86	0.28
Cawayan	20.17	39.58	39.83	0.42
La Fortuna	51.17	13.06	35.64	0.14
Impalutao	51.47	11.81	36.61	0.11
Sta. Cruz	8.39	52.56	39.06	0.00
Puntian	52.89	8.61	38.08	0.42
Sangkanan	50.17	16.47	33.00	0.36
San Miguel	20.19	27.94	51.83	0.03
Capitan Bayong	52.17	16.36	30.72	0.75
Tangkulan	8.39	61.94	29.67	0.00
Poblacion (I)	41.53	25.67	32.72	0.08
Diklum	21.08	32.64	46.25	0.03
Lunokan	60.44	18.78	20.75	0.03
Sto. Niño	57.06	7.81	33.28	1.86
Dalirig	44.94	16.53	38.53	0.00
San Vicente	48.89	17.08	33.67	0.36
Maluko	69.28	5.42	25.31	0.00
Silo-o	60.44	8.19	31.36	0.00
Omagling	49.14	14.53	36.33	0.00
Poblacion (II)	43.50	8.42	47.97	0.11
Sumalsag	59.22	14.72	26.06	0.00
Patpat	34.19	20.42	45.36	0.03
Sta. Ines	31.94	20.61	47.44	0.00
San Martin	36.47	31.17	32.25	0.11
Muhon	38.42	25.14	35.36	1.08
Natumolan	32.56	24.14	41.97	1.33

how diatoms react to climate change and how sensitive they are to changes in the environment (Berthon et al., 2014). Nitrogen coupled with climate warming due to human-based activities, were found to cause some of the most changes in freshwater systems. Temperature regulates various ecological processes and thus it has a positive relationship with nitrogen concentrations (Marcarelli and Wurtsbaugh, 2006). In addition, higher temperatures also speed up nitrification processes, thereby negatively affecting the pH levels of the environment (Marcarelli and Wurtsbaugh, 2006). Their interaction drives higher biodiversity losses (Porter et al., 2013). In general, diatoms thrive in nutrient-rich environments particularly where phosphorus and nitrogen are high along with pH and conductivity (Algarte et al., 2016; Estadual De Maringá et al., 2015; Winter and Duthie, 2014).

Environmental variables strongly influence the growth and distribution of diatoms in aquatic ecosystems. Total phosphorus, electrical conductivity, nitrate, and pH are the primary drivers of diatom functional groups, with temperature, dissolved oxygen (DO), and organic matter also playing key roles (Marcel et al., 2017), serving as reliable predictors of diatom composition and shedding light on underlying ecological mechanisms (Lange et al., 2016; Riato et al., 2017). This study confirmed such pattern, revealing that pH, temperature, TDS, conductivity, DO, turbidity, TSS, and nutrient concentrations (NO_2^-, NO_3^-, PO_4^{3-}) significantly influenced diatom ecological guilds as shown in Fig. 2.

The positive association of the low-profile guild with DO, pH, and conductivity; and its negative association with nutrients and turbidity align with the results of Passy (2007b), confirming that low-profile diatoms tolerate high disturbance (Fig. 2). Although there was no clear alignment between the low-profile guild and flow (Fig. 2), representatives of the said guild (*Achnanthes*, *Cocconeis*, and *Planothidium*) showed a positive correlation to DO and flow (Fig. 3). Flow alterations impact nutrient availability and transport (Porter et al., 2013), with both magnitude and duration shaping diatom communities (Goldenberg-Vilar et al., 2022). Strong substrate attachment mechanisms allow species such as *Achnanthes* and *Planothidium* to persist in high-flow environments (Passy, 2007b). *Cocconeis* species, highly resilient to environmental disturbances, dominate lotic systems (B-Béres et al., 2014; Stenger-Kovács et al., 2013). DO plays a crucial role in respiration and organic matter (Salomoni et al., 2011; Takarina et al., 2017), supporting higher species richness in well-oxy-

genated environments (Dalu et al., 2017; Shibabaw et al., 2021; Teittinen et al., 2015). Low-profile diatoms prefer nutrient-poor environments, where limited biofilm formation prevents competitive exclusion (Lange et al., 2011; Passy, 2007b).

Contrary to low-profile diatoms, high-profile species thrive in nutrient-rich, low-flow environments where they form tall, multicellular structures that allow them to utilize important nutrients. High-profile guild members exhibited a strong positive association with turbidity and a negative correlation with flow (Fig. 2), supporting the work of Passy (2007b). Turbidity affects light availability and water quality (Nardelli et al., 2016), indirectly influencing diatom assemblages by limiting chlorophyll-a production (Shibabaw et al., 2021). Increased shading from TDS and TSS favors high-profile diatoms, reducing low-profile guild competition (Leira et al., 2015). Agricultural runoff, a key contributor to turbidity, introduces sediments and nutrients into streams, further benefiting high-profile diatoms (Shibabaw et al., 2021). *Pleurosira*, *Gomphonema*, and *Eunotia* showed strong correlations with NO_2^-, NO_3^-, PO_4^{3-}, and NH_4^+ (Fig. 3), consistent with findings from Sharifinia et al. (2016), Sinco and Metillo (2010), Taylor and Cocquyt (2016), and Van Dam and Mertens (2023). While nutrient tolerance varies among high-profile species (Taylor and Cocquyt, 2016), overall, they favor nutrient enrichment (Passy, 2007b).

Motile diatoms (*Epithemia*, *Hantzschia*, *Luticola*, *Navicula*, *Nitzschia*, *Pinnularia*, *Sellaphora*, *Stauroneis*, and *Surirella*) were positively associated with NO_2^-, NO_3^-, PO_4^{3-}, turbidity, DO, and flow (Fig. 3). Like high-profile diatoms, they prefer nutrient-rich, low-disturbance environments (Passy, 2007b). Fig. 2 confirmed their strong association with NO_2^-, NO_3^-, and PO_4^{3-}, indicating nutrient tolerance. Motile diatoms can actively relocate to optimize environmental conditions, allowing them to persist despite high flow rates. Nutrient supply is crucial in shaping motile guild composition (Larson and Passy, 2012; Stenger-Kovács et al., 2013).

Cyclotella was the sole representative of the planktonic guild, which was expected due to its preference for lentic waters. Its presence in the epilithon may be attributed to extracellular polymeric substances (EPS) or adhesive bacterial and fungal secretions, enabling substrate attachment (Wang et al., 2014). Planktonic diatoms resist sedimentation (Rimet and Bouchez, 2011), utilizing thin frustules and increased surface area for buoyancy and energy efficiency (Marcel et al., 2013). *Cyclotella* thrives in medium-to-high conductivity and high trophic levels (Taylor and Cocquyt, 2016), as indicated in Fig. 2.

The findings reinforce the ecological roles of diatom guilds and their strong associations with environmental parameters, highlighting their potential for biomonitoring in the Tagoloan River Basin as supported by Fig. 3. Low-profile diatoms, which thrive in high-flow, nutrient-poor environments, indicate pristine or less-disturbed sites. Seventeen of the sampling sites (Capitan Bayong, Dalirig, Impalutao, Kibalabag, La Fortuna, Lunokan, Maluko, Muhon, Omagling, Poblacion (I), Puntian, Sangkanan, San Martin, San Vicente, Silo-o, Sto. Niño, and Sumalsag) were mostly composed of low-profile diatoms. High-profile diatoms, on the other hand, signal nutrient enrichment and increased turbidity, often linked to runoff and sedimentation. Three sites (Mat-i, Sta. Cruz, and Tangkulan) were mostly composed of high-profile diatoms. Motile diatoms, correlated with organic pollution and elevated conductivity, suggest pollution stress. These guild-environment relationships confirm that diatom assemblages effectively reflect water quality changes. Eight sites (Cawayan, Dalwangan, Diklum, Natumolan, Patpat, Poblacion (II), San Miguel, and Sta. Ines) were mostly composed of motile diatoms. Though low-profile diatoms were the most abundant in San Martin (36.47%) and Muhon (38.42%), the close percentage of motile diatoms in the said sites (32.25% and 35.36%, respectively) could indicate increased pollution. On the contrary, though motile diatoms were the most abundant in Dalwangan (34.86%) and Cawayan (39.83%), the close percentage of low-profile diatoms in Dalwangan (33.69%) and of high-profile diatoms in Cawayan (39.83%) may indicate less disturbance and enriched nutrients in the said sites, respectively.

5. Conclusions

A functional group-based approach, particularly at the genus level, offers a fast and cost-effective alternative to species-level identification, reducing the need for specialized taxonomic expertise. This is especially valuable in developing tropical Southeast Asian countries like the Philippines, where physicochemical analyses can be costly. By assessing diatom guild composition, researchers and environmental managers can efficiently monitor ecosystem health, track water quality trends, and identify pollution sources, promoting the routine use of diatoms in freshwater assessments across Southeast Asian River basins.

Acknowledgements

The authors express their gratitude for the grant given by the Commission on Higher Education (CHED) under the Discovery-Applied Research and Extension for Trans/Inter-disciplinary Opportunities (DARE TO) program which facilitated the completion of this study.

Conflict of interest

The authors declare no conflicts of interest.

References

Algarte V.M., Dunck B., Leandrini J.A. et al. 2016. Periphytic diatom ecological guilds in floodplain: Ten years after dam. Ecological Indicators 69: 407–414. DOI: 10.1016/j.ecolind.2016.04.049

Allen A.E., Dupont C.L., Oborník M. et al. 2011. Evolution and metabolic significance of the urea cycle in photosynthetic diatoms. Nature 473(7346): 203–207. DOI: 10.1038/nature10074

American Public Health Association, American Water Works Association, & Water Environment Federation. 2012. Standard Methods for the Examination of Water and Wastewater. 22nd ed. Washington, DC: American Public Health Association.

Bate G., Smailes P., Adams J. 2004. A water quality index for use with diatoms in the assessment of rivers. Water South Africa 30(4): 493–498. DOI: 10.4314/wsa.v30i4.5101

B-Béres V., Török P., Kókai Z. et al. 2014. Ecological diatom guilds are useful but not sensitive enough as indicators of extremely changing water regimes. Hydrobiologia 738(1): 191–204. DOI: 10.1007/s10750-014-1929-y

B-Béres V., Török P., Kókai Z. et al. 2017. Ecological background of diatom functional groups: Comparability of classification systems. Ecological Indicators 82: 183–188. DOI: 10.1016/j.ecolind.2017.07.007

Bere T., Mangadze T., Mwedzi T. 2016. Variation partitioning of diatom species data matrices: Understanding the influence of multiple factors on benthic diatom communities in tropical streams. Science of The Total Environment 566–567: 1604–1613. DOI: 10.1016/j.scitotenv.2016.06.058

Bere T., Tundisi J.G. 2011. Influence of ionic strength and conductivity on benthic diatom communities in a tropical river (Monjolinho), São Carlos-SP, Brazil. Hydrobiologia 661: 261–276. DOI: 10.1007/s10750-010-0532-0

Berge T., Daugbjerg N., Andersen B.B. et al. 2010. Effect of lowered pH on marine phytoplankton growth rates. Marine Ecology Progress Series 416:79-91. DOI: 10.3354/meps08780

Berthon V., Alric B., Rimet F. et al. 2014. Sensitivity and responses of diatoms to climate warming in lakes heavily influenced by humans. Freshwater Biology 59(8): 1755–1767. DOI: 10.1111/fwb.12380

Berthon V., Bouchez A., Rimet F. 2011. Using diatom lifeforms and ecological guilds to assess organic pollution and trophic level in rivers: A case study of rivers in south-eastern France. Hydrobiologia 673(1): 259–271. DOI: 10.1007/s10750-011-0786-1

Bešta T., Muška M., Juggins S. et al. 2015. Comparison of diatom community structure from epilithon and fish guts: Implications for inferring past changes in water quality. Hydrobiologia 742(1): 233–248. DOI: 10.1007/s10750-014-1987-1

Cibic T., Comici C., Bussani A. et al. 2012. Benthic diatom response to changing environmental conditions. Estuarine, Coastal and Shelf Science 115: 158–169. DOI: 10.1016/j.ecss.2012.03.033

Crawfurd K.J., Raven J.A., Wheeler G.L. et al. 2011. The Response of Thalassiosira pseudonana to Long-Term Exposure to Increased CO2 and Decreased pH. PLoS ONE 6(10): e26695. DOI: 10.1371/journal.pone.0026695

Dalu T., Wasserman R.J., Magoro M.L. et al. 2017. Variation partitioning of benthic diatom community matrices: Effects of multiple variables on benthic diatom communities in an Austral temperate river system. Science of The Total Environment 601–602: 73–82. DOI: 10.1016/j.scitotenv.2017.05.162

Department of Environment and Natural Resources Administrative Order No. 2016-08 (DENR-DAO No. 2016-08). 2016. Water Quality Guidelines and General Effluent Standards of 2016. Diliman, Quezon City: Department of Environment and Natural Resources.

Dickman M.D., Peart M.R., Wai-Shu Yim W. 2005. Benthic Diatoms as Indicators of Stream Sediment Concentration in Hong Kong. International Review of Hydrobiology 90(4): 412–421. DOI: 10.1002/iroh.200410806

Dutkiewicz S., Morris J.J., Follows M.J. et al. 2015. Impact of ocean acidification on the structure of future phytoplankton communities. Nature Climate Change 5: 1002–1006. DOI: 10.1038/nclimate2722

Elias C.L., Calapez A.R., Almeida S.F.P. et al. 2015. Determining useful benchmarks for the bioassessment of highly disturbed areas based on diatoms. Limnologica 51: 83–93. DOI: 10.1016/j.limno.2014.12.008

El-karim M.S.A., Khafagi O.M.A., Belal D.M. 2016. Effect of substrate type on the response of diatoms to environmental gradients: Implication for bioassessment and biomonitoring programs. International Journal of Fisheries and Aquatic Studies 4(2): 361-369.

Estadual De Maringá U., Moresco B., Gubiani C. et al. 2015. Periphytic diatoms as bioindicators in a tropical stream: From urban to rural environments. Acta Scientiarum Biological Sciences 37(4): 427–437. DOI: 10.4025/actascibiolsci.v37i4.27426

Goldenberg-Vilar A., Delgado C., Peñas F.J. et al. 2022. The effect of altered flow regimes on aquatic primary producer communities: Diatoms and macrophytes. Ecohydrology 15(1): e2353. DOI: 10.1002/eco.2353

Gottschalk S., Kahlert M. 2012. Shifts in taxonomical and guild composition of littoral diatom assemblages along environmental gradients. Hydrobiologia 694(1): 41–56. DOI: 10.1007/s10750-012-1128-7

Hammer Ø. 2023. PAST - PAleontological STatistics, Version 4.16, Reference manual. URL: https://www.nhm.uio.no/english/research/resources/past/downloads/past4manual.pdf

Hervé V., Derr J., Douady S. et al. 2012. Multiparametric Analyses Reveal the pH-Dependence of Silicon Biomineralization in Diatoms. PLoS ONE 7(10): e46722. DOI: 10.1371/journal.pone.0046722

Hockin N.L., Mock T., Mulholland F. et al. 2012. The Response of Diatom Central Carbon Metabolism to Nitrogen Starvation Is Different from That of Green Algae and Higher Plants. Plant Physiology 158(1): 299–312. DOI: 10.1104/pp.111.184333

Ingebrigtsen R.A., Hansen E., Andersen J.H. et al. 2016. Light and temperature effects on bioactivity in diatoms. Journal of Applied Phycology 28(2): 939–950. DOI: 10.1007/s10811-015-0631-4

Javaheri N., Dries R., Burson A. et al. 2015. Temperature affects the silicate morphology in a diatom. Scientific Reports 5: 11652. DOI: 10.1038/srep11652

Jeppesen E., Peder Jensen J., SØndergaard M. et al. 2000. Trophic structure, species richness and biodiversity in Danish lakes: Changes along a phosphorus gradient. Freshwater Biology 45(2): 201–218. DOI: 10.1046/j.1365-2427.2000.00675.x

Kamp A., De Beer D., Nitsch J.L. et al. 2011. Diatoms respire nitrate to survive dark and anoxic conditions. Proceedings of the National Academy of Sciences 108(14): 5649–5654. DOI: 10.1073/pnas.1015744108

Kivrak E., Uygun A. 2012. The structure and diversity of the epipelic diatom community in a heavily polluted stream (the akarçay, Turkey) and their relationship with environmental variables. Journal of Freshwater Ecology 27(3): 443-457. DOI: 10.1080/02705060.2012.671147

Ladera R., Sinco A., Sendaydiego J. et al. 2025. Diatom-based Index: A tool for Assessing Water Quality in A Southeast Asian Tropical River Basin. Pollution 11(2): 298-311. DOI: 10.22059/poll.2024.378540.2437

Lane C.R. 2007. Assessment of isolated wetland condition in Florida using epiphytic diatoms at genus, species, and subspecies taxonomic resolution. EcoHealth 4(2): 219–230. DOI: 10.1007/s10393-007-0098-0

Lange K., Liess A., Piggott J.J. et al. 2011. Light, nutrients and grazing interact to determine stream diatom community composition and functional group structure. Freshwater Biology 56(2): 264–278. DOI: 10.1111/j.1365-2427.2010.02492.x

Lange K., Townsend C.R., Matthaei C.D. 2016. A trait-based framework for stream algal communities. Ecology and

Evolution 6(1): 23–36. DOI: 10.1002/ece3.1822

Larson C.A., Passy S.I. 2012. Taxonomic and functional composition of the algal benthos exhibits similar successional trends in response to nutrient supply and current velocity. FEMS Microbiology Ecology 80(2): 352–362. DOI: 10.1111/j.1574-6941.2012.01302.x

Leira M., Filippi M.L., Cantonati M. 2015. Diatom community response to extreme water-level fluctuations in two Alpine lakes: A core case study. Journal of Paleolimnology 53(3): 289–307. DOI: 10.1007/s10933-015-9825-7

Mangadze T., Wasserman R.J., Dalu T. 2017. Use of Diatom Communities as Indicators of Conductivity and Ionic Composition in a Small Austral Temperate River System. Water, Air, & Soil Pollution 228(11): 428. DOI: 10.1007/s11270-017-3610-3

Marcarelli A.M., Wurtsbaugh W.A. 2006. Temperature and nutrient supply interact to control nitrogen fixation in oligotrophic streams: An experimental examination. Limnology and Oceanography 51(5): 2278–2289. DOI: 10.4319/lo.2006.51.5.2278

Marcel R., Agnès B., Rimet F. 2013. Influence of herbicide contamination on diversity and ecological guilds of river diatoms. Cryptogamie, Algologie 34(2): 169–183. DOI: 10.7872/crya.v34.iss2.2013.169

Marcel R., Berthon V., Castets V. et al. 2017. Modelling diatom life forms and ecological guilds for river biomonitoring. Knowledge & Management of Aquatic Ecosystems 418: 1. DOI: 10.1051/kmae/2016033

Milligan A.J., Morel F.M.M. 2002. A Proton Buffering Role for Silica in Diatoms. Science 297(5588): 1848–1850. DOI: 10.1126/science.1074958

Morin S., Bottin M., Mazzella N. et al. 2009. Linking diatom community structure to pesticide input as evaluated through a spatial contamination potential (Phytopixal): A case study in the Neste river system (South-West France). Aquatic Toxicology 94(1): 28–39. DOI: 10.1016/j.aquatox.2009.05.012

Nardelli M.S., Bueno N.C., Ludwig T.A.V. et al. 2016. Structure and dynamics of the planktonic diatom community in the Iguassu River, Paraná State, Brazil. Brazilian Journal of Biology 76(2):374-86. DOI: 10.1590/1519-6984.16114

Necchi-Júnior O., Branco L.H.Z., Branco C.C.Z. 2003. Ecological distribution of stream macroalgal communities from a drainage basin in the Serra da Canastra National Park, Minas Gerais, Southeastern Brazil. Brazilian Journal of Biology 63(4): 635-646. DOI: 10.1590/S1519-69842003000400010

Nhiwatiwa T., Dalu T., Brendonck L. 2017. Impact of irrigation-based sugarcane cultivation on the Chiredzi and Runde Rivers quality, Zimbabwe. Science of The Total Environment 587–588: 316–325. DOI: 10.1016/j.scitotenv.2017.02.155

Nowrouzi S., Valavi H. 2011. Effects of Environmental Factors on Phytoplankton Abundance and Diversity in Kaftar Lake. Journal of Fisheries and Aquatic Science 6(2): 130-140. DOI: 10.3923/jfas.2011.130.140

Pandey L.K., Bergey E.A., Lyu J. et al. 2017. The use of diatoms in ecotoxicology and bioassessment: Insights, advances and challenges. Water Research 118: 39–58. DOI: 10.1016/j.watres.2017.01.062

Passy S.I. 2007. Community analysis in stream biomonitoring: What we measure and what we don't. Environmental Monitoring and Assessment 127(1–3): 409–417. DOI: 10.1007/s10661-006-9290-x

Passy S.I. 2007. Diatom ecological guilds display distinct and predictable behavior along nutrient and disturbance gradients in running waters. Aquatic Botany 86(2): 171–178. DOI: 10.1016/j.aquabot.2006.09.018

Pestryakova L.A., Herzschuh U., Gorodnichev R. et al. 2018. The sensitivity of diatom taxa from Yakutian lakes (north-eastern Siberia) to electrical conductivity and other environmental variables. Polar Research 37(1): 1485625. DOI: 10.1080/17518369.2018.1485625

Peter A.G., Janson A.S., Michael A.R. et al. 1999. An illustrated key to common diatom genera from southern Australia. Thurgoona, Australia: Cooperative Research Center for Freshwater Ecology.

Ponader K.C., Potapova M.G. 2007. Diatoms from the genus Achnanthidium in flowing waters of the Appalachian Mountains (North America): Ecology, distribution and taxonomic notes. Limnologica 37(3): 227–241. DOI: 10.1016/j.limno.2007.01.004

Porter E.M., Bowman W.D., Clark C.M. et al. 2013. Interactive effects of anthropogenic nitrogen enrichment and climate change on terrestrial and aquatic biodiversity. Biogeochemistry 114(1–3): 93–120. DOI: 10.1007/s10533-012-9803-3

Riato L., Della V., Leira M. et al. 2017. A diatom functional-based approach to assess changing environmental conditions in temporary depressional wetlands. Ecological Indicators 78: 205–213. DOI: 10.1016/j.ecolind.2017.03.018

Rimet F., Bouchez A. 2011. Use of diatom life-forms and ecological guilds to assess pesticide contamination in rivers: Lotic mesocosm approaches. Ecological Indicators 11(2): 489–499. DOI: 10.1016/j.ecolind.2010.07.004

Rimet F., Bouchez A. 2012. Biomonitoring river diatoms: Implications of taxonomic resolution. Ecological Indicators 15(1): 92–99. DOI: 10.1016/j.ecolind.2011.09.014

Rioual P., Lu Y., Yang H. et al. 2013. Diatom-environment relationships and a transfer function for conductivity in lakes of the Badain Jaran Desert, Inner Mongolia, China. Journal of Paleolimnology 50(2): 207-229. DOI: 10.1007/s10933-013-9715-9

Salomoni S.E., Rocha O., Callegaro V.L. et al. 2006. Epilithic diatoms as indicators of water quality in the Gravataí river, Rio Grande do Sul, Brazil. Hydrobiologia 559: 233–246. DOI: 10.1007/s10750-005-9012-3

Salomoni S.E., Rocha O., Hermany G. et al. 2011. Application of water quality biological indices using diatoms as bioindicators in the Gravataí river, RS, Brazil. Brazilian Journal of Biology 71(4): 949-959. DOI: 10.1590/S1519-69842011000500015

Saros J.E., Fritz S.C. 2000. Nutrients as a link between ionic concentration/composition and diatom distributions in saline lakes. Journal of Paleolimnology 23: 449–453.

Schabhüttl S., Hingsamer P., Weigelhofer G. et al. 2013. Temperature and species richness effects in phytoplankton communities. Oecologia 171: 527–536. DOI: 10.1007/s00442-012-2419-4

Scholz B. 2014. Effects of varying pH on the growth and physiology of five marine microphytobenthic diatoms isolated from the Solthörn tidal flat (southern North Sea, Germany). Phycologia 53(3):252-264. DOI: 10.2216/13-240.1

Schroeder L.A., Martin S.C., Kerns G.J. et al. 2016. Diatom assemblages in a reservoir sediment core track land-use changes in the watershed. Journal of Paleolimnology 55(1): 17-33. DOI: 10.1007/s10933-015-9860-4

Sharifinia M., Ramezanpour Z., Namin J.I. 2016. Distribution of benthic centric diatom Pleurosira laevis (Compère, 1982) in different substrate type and physical and chemical variables. Acta Limnologica Brasiliensia 28:e18. DOI: 10.1590/S2179-975X2416

Shatwell T., Köhler J., Nicklisch A. 2013. Temperature and photoperiod interactions with silicon-limited growth and competition of two diatoms. Journal of Plankton Research 35(5): 957-971. DOI: 10.1093/plankt/fbt058

Shatwell T., Köhler J., Nicklisch A. 2014. Temperature and photoperiod interactions with phosphorus-limited growth and competition of two diatoms. PLoS ONE 9(7):e102367. DOI: 10.1371/journal.pone.0102367

Shibabaw T., Beyene A., Awoke A. et al. 2021. Diatom community structure in relation to environmental factors in human influenced rivers and streams in tropical Africa. PLOS ONE 16(2): e0246043. DOI: 10.1371/journal.pone.0246043

Sinco A.L., Metillo E.B. 2010. Epilithic microalgal species discriminate low and high levels of dissolved phosphate in rivers of Northern Mindanao, Southern Philippines. In: 2010 International Conference on Environmental Engineering and Applications, pp. 22–25. DOI: 10.1109/ICEEA.2010.5596082

Stenger-Kovács C., Lengyel E., Crossetti L.O. et al. 2013. Diatom ecological guilds as indicators of temporally changing stressors and disturbances in the small Torna-stream, Hungary. Ecological Indicators 24: 138–147. DOI: 10.1016/j.ecolind.2012.06.003

Sudhakar G., Jyothi B., Venkateswarlu V. 1994. Role of diatoms as indicators of pollution gradients. Environmental Monitoring and Assessment 33: 85–99. DOI: 10.1007/BF00548591

Takarina N.D., Wardhana W., Soedjiarti T. 2017. Impact of oxygen depletion on planktonic community with emphasis temperature dynamics at aquaculture scale in Blanakan, West Java. AIP Conference Proceedings 1848(1): 020004. DOI: 10.1063/1.4983932

Tapolczai K., Bouchez A., Stenger-Kovács C. et al. 2016. Trait-based ecological classifications for benthic algae: Review and perspectives. Hydrobiologia 776: 1–17. DOI: 10.1007/s10750-016-2736-4

Taylor J.C., Cocquyt. 2016. Diatoms from the Congo and Zambesi Basins—Methodologies and Identification of the Genera (Vol. 16). Belgium: ABC Taxa and the Belgian Development Cooperation. URL: http://www.abctaxa.be/volumes/volume-16-diatoms-congoand-zambezi-basins

Teittinen A., Taka M., Ruth O. et al. 2015. Variation in stream diatom communities in relation to water quality and catchment variables in a boreal, urbanized region. Science of the Total Environment 530-531: 279-289. DOI: 10.1016/j.scitotenv.2015.05.101

Taylor J.C., Harding W.R., Archibald C.G.M. 2007. An illustrated guide to some common diatom species from South Africa. Pretoria: Water Research Commission.

Triest L., Kaur P., Heylen S. et al. 2001. Comparative monitoring of diatoms, macroinvertebrates and macrophytes in the Woluwe river (Brussels, Belgium). Aquatic Ecology 35: 183–194. DOI: 10.1023/A:1011468615246

Van Dam H., Mertens A. 2023. A century of diatom monitoring in acidified and warmed Dutch moorland pools. Limnologica 99: 126059. DOI: 10.1016/j.limno.2023.126059

Verleyen E., Vyverman W., Sterken M. et al. 2009. The importance of dispersal related and local factors in shaping the taxonomic structure of diatom metacommunities. Oikos 118(8): 1239–1249. DOI: 10.1111/j.1600-0706.2009.17575.x

Wang Q., Hamilton P.B., Kang F. 2014. Observations on attachment strategies of periphytic diatoms in changing lotic systems (Ottawa, Canada). Nova Hedwigia 99(1–2): 239–253. DOI: 10.1127/0029-5035/2014/0171

Weckstrom J., Korhola A., Blom T. 1997. Diatoms as quantitative indicators of pH and water temperature in subarctic Fennoscandian lakes. Hydrobiologia 347: 171–184. DOI: 10.1023/A:1003091923476

Winter J.G., Duthie H.C. 2014. Epilithic diatoms as indicators of stream total N and total P concentration Epilithic diatoms as indicators of stream total N and. Journal of the North American Benthological Society 19(1): 32–49.

Wu N., Cai Q., Fohrer N. 2014. Contribution of microspatial factors to benthic diatom communities. Hydrobiologia 732(1): 49–60. DOI: 10.1007/s10750-014-1843-3

Xiao W., Liu X., Irwin A.J. et al. 2018. Warming and eutrophication combine to restructure diatoms and dinoflagellates. Water Research 128: 206–216. DOI: 10.1016/j.watres.2017.10.051

Zhang Y., Wang B., Han M. et al. 2012. Relationships between the Seasonal Variations of Macroinvertebrates, and Land Uses for Biomonitoring in the Xitiaoxi River Watershed, China. International Review of Hydrobiology 97(3): 184–199. DOI: 10.1002/iroh.201111487

Original Article

LIMNOLOGY FRESHWATER BIOLOGY

Identification and comprehensive characterization of a new soil strain of carotenogenic microalgae *Chlorosarcinopsis* sp. VKM Al-296 (Chlorophyta)

Chubchikova I.N.[1]*, Dantsyuk N.V.[1], Drobetskaya I.V.[1], Temraleeva A.D.[2]

[1] *A. O. Kovalevsky Institute of Biology of the Southern Seas of RAS, 2 Nakhimov Ave., Sevastopol, 299011, Russian Federation*
[2] *All-Russian Collection of Microorganisms (VKM), G.K. Skryabin Institute of Biochemistry and Physiology of Microorganisms, Pushchino, Scientific Center for Biological Research, Russian Academy of Sciences, 142290 Pushchino, Russian Federation*

ABSTRACT. We conducted a complex study of the new green microalgae strain VKM Al-296, isolated from arable soil and identified as *Chlorosarcinopsis* sp. (Chlamydomonadales, Chlorophyta), using molecular phylogenetic analysis (18S rDNA and ITS2 sequences) and light and scanning electron microscopy. The strain's morphology, growth, and carotenogenesis during two-stage batch cultivation were studied. In a liquid medium, the cells occurred singly or in packages surrounded by extracellular mucilage, with cell sizes of 3-6 μm. By the end of the "green" stage (vegetative growth) lutein was the predominant pigment, accounting for >60% of the total carotenoids. Other primary carotenoids were also present: beta-carotene (14.6%), neoxanthin (11.1%), and antheraxanthin (7.1%). At the end of the "red" (secondary carotenogenesis) stage, the culture's dry biomass content was 1.92 ± 0.04 g/L, with carotenoids accounting for 0.3% of the dry biomass. The pigment profile was dominated by ketocarotenoids: astaxanthin (mono- and diesters), canthaxanthin, and adonixanthin monoesters (35%, 21% and 20% of the total carotenoid content, respectively). Over the entire cultivation period (17 days), the average biomass productivity and total carotenoid productivity were 0.10 g/L/day and 0.2 mg/L/day, respectively. *Chlorosarcinopsis* sp. VKM Al-296 may be a perspective object of further research aimed at optimizing cultivation conditions as a source of lutein at the "green" stage, as well as canthaxanthin and esters of astaxanthin and adonixanthin at the "red" stage.

Keywords: *Chlorosarcinopsis* sp., cell morphology, molecular phylogenetic analysis, two-stage batch culture, secondary carotenoids, thin-layer chromatography

For citation: Chubchikova I.N., Dantsyuk N.V., Drobetskaya I.V., Temraleeva A.D. Identification and comprehensive characterization of a new soil strain of carotenogenic microalgae *Chlorosarcinopsis* sp. VKM Al-296 (Chlorophyta) // Limnology and Freshwater Biology. 2026. - № 2. - P. 78-102. DOI: 10.31951/2658-3518-2026-A-2-78

1. Introduction

Chlorosarcinopsis is a genus of microalgae within the order Chlamydomonadales (Chlorophyta), commonly found in terrestrial environments, particularly in arid and semi-arid deserts (Friedmann and Ocampo-Paus, 1965; Andreeva, 1998; Lewis and Lewis, 2005; Hall et al., 2010; Khani-Juyabad et al., 2019).

Soil is home to a variety of microorganisms, including bacteria, fungi, protozoa, and microalgae. Unlike planktonic microalgae, whose habitat conditions, as a rule, vary insignificantly with the seasons and daytime, soil microalgae, living on the soil's surface or in its upper horizons, are subjected to permanent stress, enduring diurnal and seasonal fluctuations of environmental conditions. These are dramatic changes in irradiance, temperature, moisture, nutrient availability, etc. The key link in the survival strategy of soil species, including microalgae of the genus *Chlorosarcinopsis*, in conditions of severe abiotic stress is the ability to secondary carotenogenesis (SC) associated with the ability of cells to rapidly transition from the state of active vegetation to the resting stage and vice versa. Ketocarotenoids (KCar) are a group of pigments that are neither structurally nor functionally related to the photosynthetic apparatus (Lemoine and Schoefs, 2010; Solovchenko, 2013). Their functions include shielding the nucleus and cellular organelles, utilizing excess

*Corresponding author. E-mail address: chubchikova_in@ibss-ras.ru (I.N. Chubchikova)

Received: December 17, 2025;
Accepted after revised: February 27, 2026;
Available online: April 24, 2026

photosynthates, and "quenching" reactive oxygen species and preventing their formation (Solovchenko, 2013; Remias et al., 2016). The natural KCar astaxanthin is widely used in pharmaceuticals, nutraceuticals, cosmetics, dietetics, and aquaculture, and its range of applications is rapidly expanding. It is safe for human consumption, unlike its synthetic analogue, which is only approved for aquaculture (Nair et al., 2023).

Regarding this, in recent decades, much attention has been paid to the study of the SC process as a key adaptation mechanism in extremobiont green microalgae of different taxonomic and ecological groups. The bulk of information about SC patterns in unicellular microalgae was obtained from examples of a limited number of planktonic, soil and aerophytic species from the orders Chlamydomonadales and Sphaeropleales (*Haematococcus lacustris*, *Chromochloris zofingiensis*, *Coelastrella rubescens*, *Bracteacoccus pseudominor*, and *B. minor*) (Minyuk et al., 2014; 2017; Chelebieva et al., 2018; Minyuk et al., 2020; Malik et al., 2022). However, the diversity of carotenogenic microalgae species is much greater than is commonly believed. Advances in high-throughput whole-genome sequencing have identified orthologs of β-carotene ketolase, the key enzyme responsible for the synthesis of KCar from β-carotene, across the genomes of numerous microalgal species (Jeffers and Roth, 2021). Therefore, further search for commercially promising producers of KCar (astaxanthin and its metabolic precursors) and development of methods for their industrial cultivation remains relevant (Chubchikova et al., 2009; 2012; Minyuk et al., 2014; Chen et al., 2017; Minyuk et al., 2017; Marchenko et al., 2019; Minyuk et al., 2019; 2020; Doppler et al., 2022; Saito et al., 2023).

An additional adaptation mechanism enhances the survival strategy of sarcinoid microalgae, allowing them to successfully withstand abrupt changes in environmental conditions. This is the ability to produce copious amounts of mucilage–the so-called "mucous membranes" and "wrappers". The main component of mucilage is extracellular hydrophilic colloidal polysaccharides dominated by galactose, glucose, and rhamnose (Gollerbach and Shtina, 1969; Laroche, 2022). The matrix performs several functions. It ensures the attachment of cells to each other, protects them from contamination and abrupt biotic and abiotic stresses, smoothing out jumps in insolation, humidity, and temperature, especially for cells located within the cellular aggregate. In addition to polysaccharides, the mucus contains low-molecular protein compounds. There is information on the active growth of *Chlorosarcinopsis* spp. on mixo- and heterotrophic media under laboratory conditions (Cherdchukeattisak et al., 2018; Vasistha et al., 2021), which suggests the use of mucilage during periods of starvation as an available organic source of carbon and nitrogen.

These features of sarcinoid microalgae suggest that, under conditions of mass open cultivation, the survival rate of such species will be significantly higher than that of more sensitive planktonic species, which may have a positive effect on the KCar and biomass productivity.

The two-stage batch culture method (Boussiba, 2000; Fábregas et al., 2001; Minyuk et al., 2017) enables comprehensive studies of strains, including optical and scanning electron microscopy, molecular phylogeny, and evaluation of production characteristics during both active growth and secondary carotenogenesis.

The aim of this study was to investigate the strain VKM Al-296 using a polyphase method in a two-stage batch culture.

2. Material and Methods

2.1. Strain origin

The object of the study was a soil microalgal strain VKM Al-296 isolated from arable typical chernozem in the Stavropol Territory, Russian Federation (45°07′N, 42°01′E) in 2018. Unialgae culture was obtained as described by Temraleeva et al. (2014). The soil suspension was transferred to BG-11 agar plates (1.5% agar, pH 7.2) and incubated under constant conditions until cell colonies appeared. The cultivation regime was as follows: temperature 23–25 °C, photoperiod 12 h light: 12 h dark, and photosynthetic photon flux density (PPFD) 60–75 μmol photons/m^2/s provided by cool white fluorescent lamps. Individual colonies were scraped off and repeatedly subcultured under the same conditions until an algologically pure culture was obtained.

The strain was initially deposited in the Algological Collection (ACSSI) of the Institute of Physicochemical and Biological Problems in Soil Science, Russian Academy of Sciences (RAS), under the number ACSSI 296. Subsequently, it was transferred to the All-Russian Collection of Microorganisms (VKM) of the Institute of Biochemistry and Physiology of Microorganisms, RAS, where it was assigned the number VKM Al-296.

2.2. Morphological analysis

The morphological characteristics and life cycle of the strain VKM Al-296 were studied using light microscopy (LM) with a Leica DM750 microscope (Germany). Images were captured using a Leica Flexicam C3 color digital camera (Germany), and observations were conducted over a period ranging from two weeks to six months.

For scanning electron microscopy (SEM), the cells were fixed with 2% glutaraldehyde in 10-fold diluted 66.7 mmol Na-K phosphate buffer (pH 7.34) at 4°C for 24 hours. The sample was then postfixed with a 0.005% Lugol's iodine solution and dehydrated through a graded series of ethanol solutions with increasing concentrations, following the protocol described by Chubchikova et al. (2022). SEM imaging was performed using the Hitachi SU3500 scanning electron microscope (Japan).

2.3. DNA extraction, PCR, and sequencing

Total DNA was extracted using the DNeasy Plant Mini Kit (Qiagen, USA) following the manufacturer's

instructions. The nucleotide sequences of the 18S rDNA and ITS2 regions were amplified using the Screen Mix-HS reagent (Evrogen, Russia). The primers and amplification conditions were selected based on articles described by White et al. (1990) and Katana et al. (2001), with details provided in Table 1. PCR amplifications were carried out using a Gradient T100 thermal cycler (Bio-Rad, USA). The target PCR products were visualized by electrophoresis on a 1% agarose gel. Following electrophoresis, the PCR products were purified using the Cleanup Mini kit (Evrogen, Russia) according to the manufacturer's protocol. The purified PCR products were then sent for sequencing to Evrogen (Russia).

2.4. Phylogenetic analysis

The obtained nucleotide sequences were deposited in the GeneBank database under the following accession numbers: MT338814 (18S rDNA) and MT340909 (ITS2). To identify closely related sequences, the BLASTn algorithm from NCBI was utilized. For phylogenetic analysis, two datasets were constructed:

1. The 18S rDNA dataset included 70 sequences from various representatives of the order Chlamydomonadales, including clades such as Arenicolinia, Stephanosphaerinia, and Chlorogonia. Authentic strains of the genus *Gungnir* (Dunaliellinia clade) were used as the outgroup.
2. The ITS2 dataset included 66 sequences from all representatives of the Arenicolinia clade, including uncultured species, with authentic strains of *Chlorococcum isabeliense* (Stephanosphaerinia clade) serving as the outgroup.

Taxonomic names were standardized according to the AlgaeBase database (Guiry and Guiry, 2025).

Multiple sequence alignment was performed using the MAFFT online tool (https://www.ebi.ac.uk/jdispatcher/msa/mafft). The best-fitting evolutionary model for each locus (18S rDNA and ITS2) was determinated using the Akaike Information Criterion (AIC) implemented in jModelTest version 2.1.10 (Darriba et al., 2012). For maximum likelihood (ML) analysis, 1.000 bootstrap replicates were generated for each dataset using the PhyML program. Statistical support for the branches was assessed using bootstrap probabilities (BP). Bayesian inference (BI) was conducted using the BEAST software version 1.8.4. Two runs of 10^8 generations were performed, with sampling every 10^4 generations, and the first 25% were discarded as burn-in. Convergence of Markov chains was confirmed by ensuring ESS (Effective Sample Size) values > 200, and the results were visualized using the Tracer ver. 1.5 program. A consensus tree was generated using TreeAnnotator ver. 1.8.4, with branch support measured using Bayesian posterior probabilities (PP). Genetic distances were calculated in the MEGA 6 program using the Kimura 2-parameter model. For ITS2 secondary structure analysis, the sequences were folded using the RNAfold web server (https://rna.tbi.univie.ac.at/cgi-bin/RNAWebSuite/RNAfold.cgi), following the principle of minimum free energy. The accuracy of the predicted secondary structures was assessed based on guidelines from Caisová et al. (2013). Comparison of ITS2 secondary structures, identification of conserved motifs, and analysis of compensatory base changes (CBCs) were performed using the 4SALE 1.7 software (Seibel et al., 2006). CBC approach, as proposed by Coleman (2000; 2003; 2009), was employed to distinguish species based on ITS2 sequences. Finally, the ITS2 secondary structures were visualized using the PseudoViewer3 software (Byun and Han, 2009).

2.5. Cultivation condition

The strain was cultivated using a two-stage batch culture method (Boussiba, 2000; Fábregas et al., 2001) in BBM nutrient medium (Bischoff and Bold, 1963). Microalgae were grown in three biological replicates using 0.75 L plastic Tissue Culture Flasks ("Falcon", USA). The culture volume was 0.6 L, with initial dry biomass (DW) content 0.3 g/L.

The first ("green") stage lasted nine days and was conducted under the following cultivation conditions: unilateral illumination provided by cold-white LED lamps "Feron" DL 20W T4 6400K, (Russia), photosynthetic photon flux density (PPFD) of 130 μmol photons/m^2/s (as measured at the side surface of flasks), with a light mode of 15:9 h (light/dark), temperature

Table 1. Primers and amplification conditions for PCR.

Locus	Primers	Sequence (5'–3')	Amplification conditions
18S rDNA	F	AACCTGGTTGATCCTGCCAGT	95°C, 5 min; 95°C, 1 min, 55°C, 1 min, 72°C, 2 min, 35 cycles; 72°C, 5 min
	R	TGATCCTTCTGCAGGTTCACCTACG	
	402–23F*	GCTACCACATCCAAGGAAGGCA	
	1323–44F*	CGAACGAGACCTCAGCCTGCTA	
	416–37R*	ATTTGCGCGCCTGCTGCCTTCC	
	898–919R*	TAAATCCAAGAATTTCACCTCT	
	1308–39R*	CTCGTTCGTTAACGGAATTAACC	
	1636–57R*	GGTAGGAGCGACGGGCGGTGTG	
ITS2	ITS3	GCATCGATGAAGAACGCAGC	95°C, 3 min; 95°C, 30s, 52–57°C, 30 s, 72°C, 40 s, 35 cycles; 72°C, 10 min
	ITS4	TCCTCCGCTTATTGATATGC	

Note: * internal sequencing primers.

28 ± 0.5 °C, and continuous air bubbling at a rate of 0.44 L/min/L. The culture pH was maintained at 7.0 ± 0.05 with CO_2 supply from a gas cylinder during 8 h, controlled by an Aqua Medic pH2001C system (Germany) equipped with a Camozzi A7E solenoid valve (Italy).

To induce the "red" stage, the culture was transferred to bilateral 24-hour illumination with the same PPFD on each side and a temperature of 28–29 °C. The CO_2 supply remained unchanged. Additionally, a 1% NaCl solution was added to a final concentration of 5 mmol. The "red" stage lasted 8 days.

2.6. Monitoring of the culture growth

Growth characteristics of the strain were evaluated by monitoring biomass dynamics. DW content (g/L) was determined gravimetrically on nitrocellulose membrane filters "Sartorius" (Germany) with a pore size of 3.0 μm (Vonshak, 1985). The biomass on the filters was washed with distilled water (three or four times, 15 mL each) to remove mucilage. The specific growth rate (μ) and productivity of cultures (*P*) were calculated using the method described by Wood et al. (2005).

$$\mu = \ln(DW_1 / DW_0) / (t_1 - t_0) \quad (1)$$

$$P = (DW_1 - DW_0) / (t_1 - t_0) \quad (2)$$

where *P* is the average productivity, g/L/day;

DW_0–initial DW, g/L;

DW_1–the final DW, g/L;

t_1–t_0–growth period, days;

μ–specific growth rate, day^{-1}.

2.7. Pigment assay

Pigment concentrations were determined spectrophotometrically (spectrophotometer SF-2000 UV/Vis, OKB Spectr, Russia). The content of chlorophylls *a* and *b* and total carotenoids throughout the experiment was determined in biomass dimethylsulfoxide extacts (Merck, ACS grade) and calculated as described by Solovchenko et al. (2010).

The composition of carotenoids in the acetone extracts at the end of "green" and "red" stages was investigated by thin-layer chromatography (TLC) on silica gel (Britton, 2008). Extracts from "green" biomass were analyzed on reversed phase TLC plates, Silica gel 60 RP-18 (Merck, Germany) in the solvent system ethylacetate-methanol-water (50:40:10) (Henry et al., 1983). For the analysis of pigments from "red" biomass, normal-phase TLC Silica gel 60 plates (Merck, Germany) and two sequential solvent systems were used: I–hexane-acetone 9:1; II–hexane-benzene-acetone 5:3.75:0.8 (Minyuk and Solovchenko, 2018). Preliminary, in the acetone extract of each tested sample, the content of chlorophyll *a* (Chl*a*), chlorophyll *b* (Chl*b*), and total Car was calculated according to Lichtenthaler (1987).

Carotenoid fractions were identified by chemical, spectral and chromatographic tests for the presence and number of hydroxy- and ketogroups; position of absorption maxima in UV-VIS spectra in three solvents (hexane, benzene and acetone); and Rf matching of identified fractions and carotenoid standards in joint chromatography (Rodriguez-Amaya, 2001; Britton et al., 2004; Britton, 2008; Egeland et al., 2011; Minyuk and Solovchenko, 2018).

2.8. Statistics

All measurements were conducted in three biological and three analytical replicates. Average values ($\bar{x}$) and their standard errors (SE) were calculated using Microsoft Excel's statistical package. Data visualization was performed using Golden Software Grapher (version 17.3.454).

3. Results

3.1. Identification of the strain VKM Al-296: morphology and phylogenetic analysis

Based on LM and SEM observations, the strain VKM Al-296 was preliminarily identified as a member of the genus *Chlorosarcinopsis*. This assumption was supported by several key morphological features: the formation of cell packets, the presence of naked biflagellate zoospores, a parietal chloroplast, and a single pyrenoid with an interrupted starch sheath. Young vegetative cells were spherical and developed into dyads, tetrads, and more complex structures through desmoschisis. Pseudofilament clusters were not observed. A distinctive characteristic of the VKM Al-296 strain was small cell size (up to 6 μm) and the formation of multicellular packages surrounded by visible extracellular mucilage (Fig. 1).

During long-term storage of the culture (approximately six months), a noticeable shift in biomass color from green to reddish-brown was observed. This change indicates the synthesis of secondary carotenoids, a common response of carotenogenic algae to acute nutritional deficiency and desiccation.

18S rDNA analysis revealed that the strain VKM Al-296 belongs to the well-supported Arenicolinia clade (Fig. 2a), clustering closely with authentic strains such as *C. eremi* UTEX 1186, *C. arenicola* UTEX 1697, and *C. variabilis* UTEX 1600.

Within the Arenicolinia clade, the strain VKM Al-296 represents an independent phylogenetic lineage that does not cluster with any of the known representatives. Genetic distances within the clade ranged

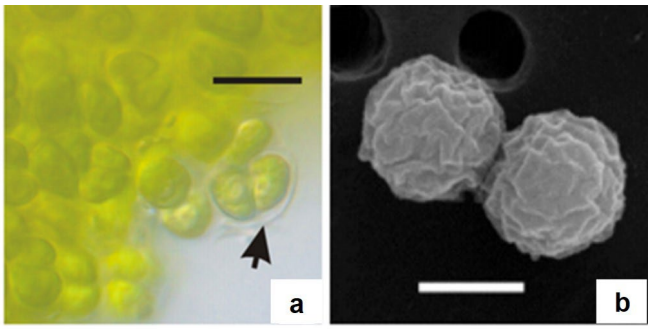

Fig.1. LM (a) and SEM (b) microscopy images of the strain *Chlorosarcinopsis* sp. VKM Al-296. Black arrow indicates extracellular mucilage. Scale: a–10 μm; b–3 μm.

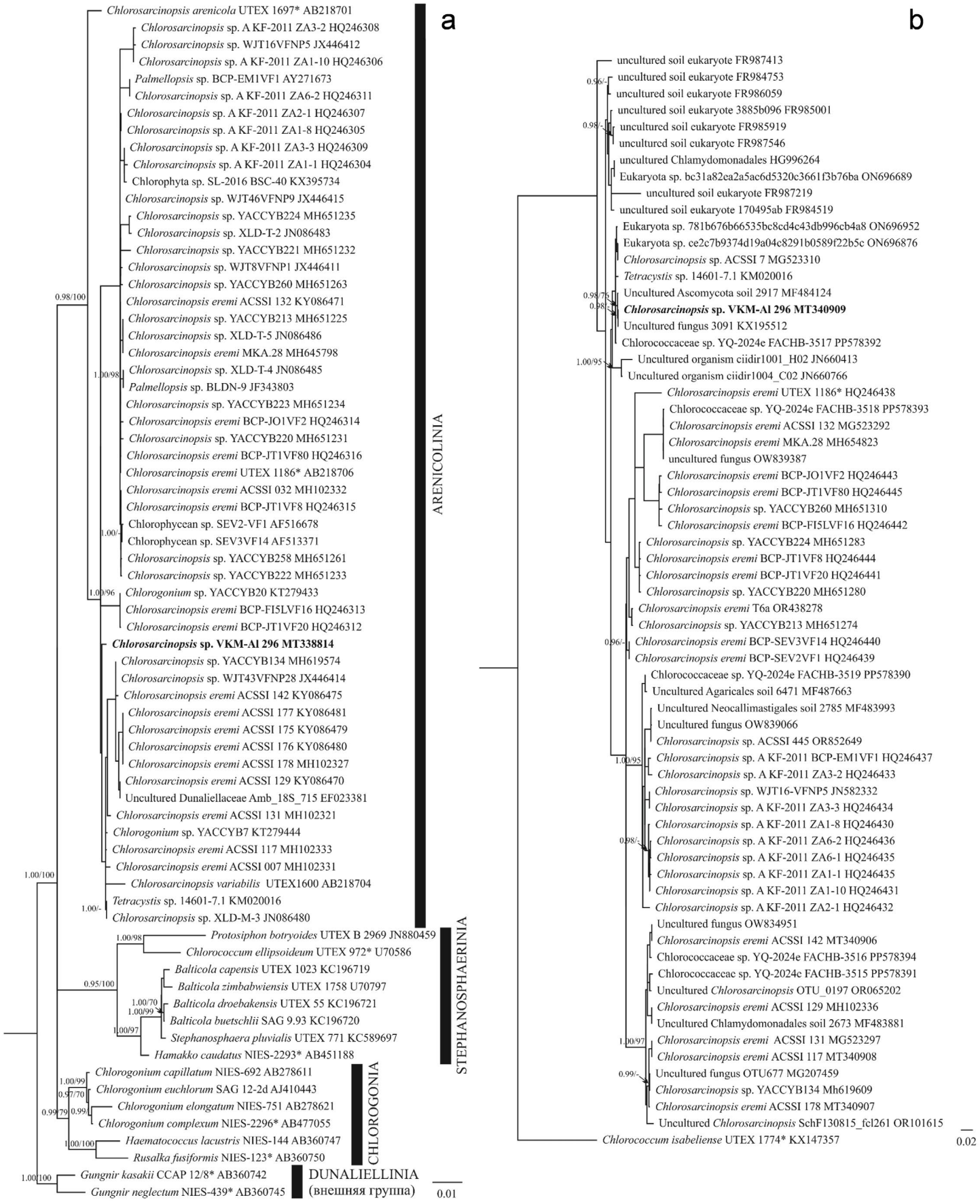

Fig.2. Bayesian phylogenetic trees of the strain VKM Al-296 based on the comparison of nucleotide sequences of 18S rDNA (a) and ITS2 (b). The best-fit evolutionary model for both markers was GTR + I + G. Statistical support for tree nodes is indicated by posterior probabilities (PP) and bootstrap values (BP); PP values < 0.9 and BP values < 70% are not shown. Note: The studied strain is highlighted in bold; * denotes authentic strains.

from 0 to 1.2%. Specifically, the studied strain differed by 0.1% from *C. eremi* UTEX 1186, by 0.9% from *C. arenicola* UTEX 1697, and by 0.4% from *C. variabilis* UTEX 1600. To enhance phylogenetic resolution, the variable ITS2 region was analyzed in addition to the conserved 18S rDNA (Fig. 2b). However, this did not improve clustering within the group. The strain VKM Al-296 grouped with algal sequences that had been misidentified as uncultured fungi. No differences were observed among these three sequences. The genetic distance between VKM Al-296 and *C. eremi* UTEX 1186 was 1.7%. The range of genetic variation within the Arenicolinia clade spanned from 0% to 12%. Based on the ITS2 species threshold of 10% (Hoshina and Fujiwara, 2013; Hoshina, 2014), it can be inferred that the clade includes several yet-to-be-described species. Unfortunately, the ITS2 sequences for *C. arenicola* UTEX 1697 and *C. variabilis* UTEX 1600 have not been deposited in GenBank. Comparison of the ITS2 secondary structures of VKM Al-296 and *C. eremi* UTEX 1186 revealed only hemi-compensatory base changes in helices I, II, and IV (Fig. 3).

No compensatory base changes were identified. Based on the morphological and genetic differences between the studied strain and *C. eremi*, the strain was classified as a *Chlorosarcinopsis* sp.

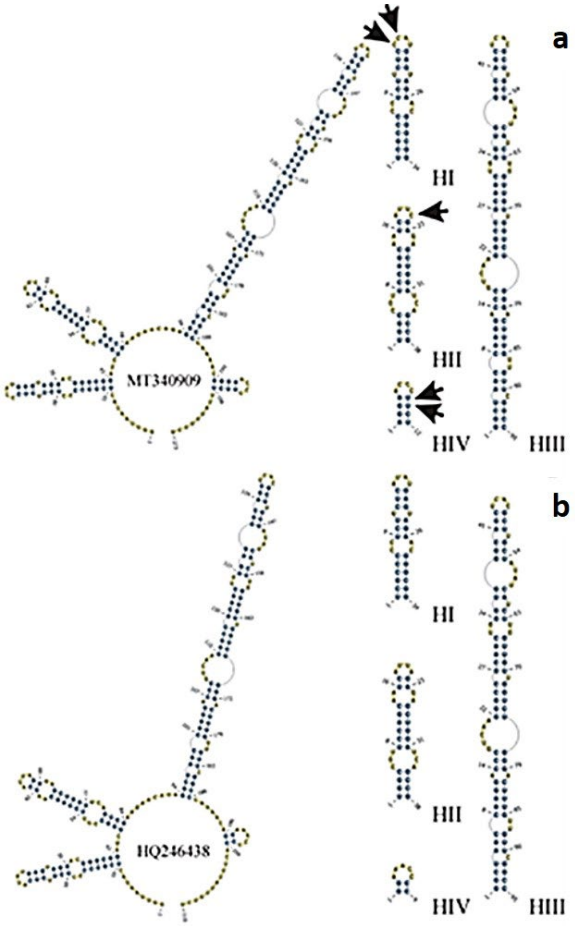

Fig.3. ITS2 secondary structure of *Chlorosarcinopsis* sp. VKM Al-296 (a) and *C. eremi* UTEX 1186 (b): general structure and helices. Black arrows indicate hemi-compensatory base changes.

3.2. Growth characteristics of the strain VKM Al-296 under two-stage cultivation

It should be noted that the active accumulation of biomass in the culture of *Chlorosarcinopsis* sp. did not stop throughout the experiment (Fig. 4a).

In the first two days, in addition to division by aplanospores, there was reproduction by zoospores. Numerous metabolic biflagellated zoospores were recorded in the cultures during the morning hours. By the mid-day, zoospores lost motility and became rounded. Sexual reproduction was not observed. The transfer of microalgae cultures to the “red” stage by adding NaCl to the nutrient medium and increasing illumination and temperature did not cause visually obvious cell death, which usually occurs in planktonic microalgae under similar stress conditions (Minyuk et al., 2007). Instead, the predominant mode of reproduction shifted to desmoschisis, leading to the formation of multicellular flat packets surrounded by mucilage (Fig. 1).

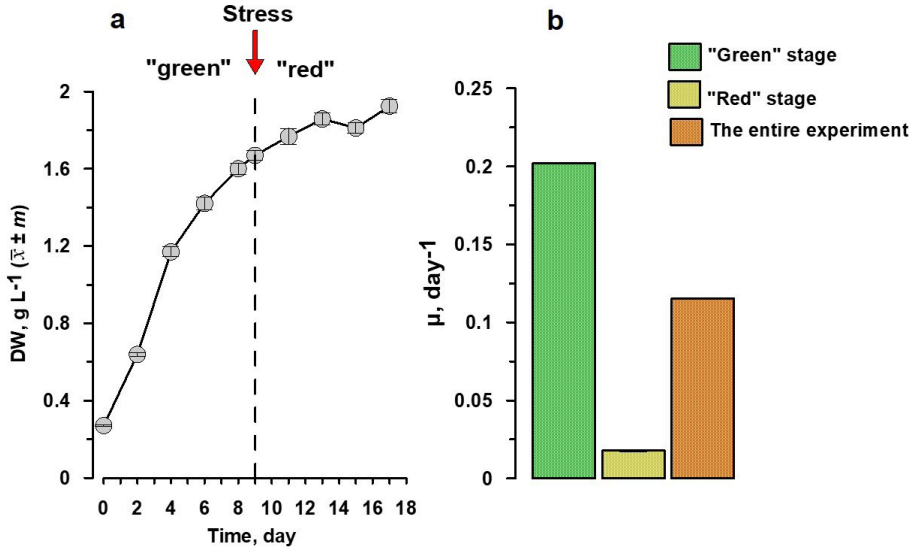

Fig.4. Dry weight dynamics (a) and specific growth rate (b) at the “green” and “red” stages and for entire experiment in *Chlorosarcinopsis* sp.

The VKM Al-296 strain culture grew faster at the "green" stage than the related *C. eremi* strain VKM Al-132 that was cultivated under natural light (Dantsyuk et al., 2024). At the SC stage, although both strains were subjected to the same stress, VKM Al-296 biomass accumulation was significantly slower, and, hence, its productivity over the entire experiment (0.10 g/L/day) was slightly lower than that of *C. eremi* VKM Al-132 (0.12 g/L/day) (Dantsyuk et al., 2024).

3.3. Pigment content of *Chlorosarcinopsis* sp. VKM Al-296 during cultivation

The chlorophyll content in *Chlorosarcinopsis* sp. changed in a manner typical for two-stage cultivation: during the "green" stage, with sufficient biogenic elements in the culture, it increased due to active cell division. By the end of the green stage, Chl*a* reached 7.50 ± 0.12 μg/mL (0.45 ± 0.01 % DW), and Chl*b* – 3.34 ± 0.05 μg/mL (0.20 ± 0.01 % DW). After stress, as a result of the destruction of chlorophyll molecules, their content sharply decreased by an order of magnitude (Fig. 5).

In contrast, the total Car content in the culture increased due to active biomass accumulation (Fig. 6a). The percentage of total Car in DW decreased sharply by the fourth day and remained relatively constant (0.3% of dry weight) until the end of the experiment. (Fig. 6b).

An increase in the Car/Chl*a* ratio from 0.33 to 0.64 by the ninth day (Fig. 6c) served as a key criterion for assessing the culture's readiness to transition to the secondary carotenogenesis stage. Visually, this readiness was marked by a change in the culture's color from green to a marsh yellow hue.

During the "red" stage, the Chl*a* content in the culture decreased 10-fold, while Chl*b* content decreased 5-fold. In contrast, the total Car content increased 1.3-fold (Fig. 5a, c; Fig. 6a). The total carotenoid productivity calculated for the entire experiment was 0.20 ± 0.01 mg/L/day, which was comparable to that of the related strain *C. eremi* VKM Al-132 (Dantsyuk et al., 2024).

3.4. Thin Layer Chromatography and carotenoid composition

Although the total Car content in microalgal biomass remained relatively constant from day 4 of the "green" stage, the qualitative composition of carotenoids changed significantly throughout the subsequent period. The application of TLC allowed for a detailed comparison of the carotenoid profiles at the end of the "green" and "red" stages.

In green cultures, lutein was the dominant carotenoid, accompanied by significant amounts of β-carotene and neoxanthin (Fig. 7a, 8a). However, following stress exposure, the culture's primary carotenoids characteristic of the "green" stage were replaced by secondary carotenoids (KCar), which were synthesized during the "red" stage (Fig. 7b, 8b). By the end of the experiment, the content of lutein and β-carotene in *Chlorosarcinopsis* sp. cells had decreased by an order of magnitude. In red cultures, canthaxanthin, adonixanthin monoesters, and astaxanthin esters were the predominant carotenoids (Fig. 8a, b).

Overall, these fractions accounted for 75–80% of the total Car (Fig. 8a, b). Notably, the fractions of astaxanthin esters alone reached nearly 35% of the total Car. The carotenoid profile of the studied strain *Chlorosarcinopsis* sp. VKM Al-296 at the "red" stage was similar to that of the strain *C. eremi* VKM Al-132, previously presented by Dantsyuk et al. (2024).

Despite the relatively low total carotenoid content (approximately 0.3% DW), the carotenoid composition of *Chlorosarcinopsis* sp. VKM Al-296 is notable for its high-value KCar, including canthaxanthin, and esters of adonixanthin, adonirubin, and astaxanthin, which together account for ~80% of the total carotenoids.

4. Discussion

The taxonomy of *Chlorosarcinopsis* has a complex and convoluted history since 1958 (Herndon, 1958). Initially, 21 species were grouped into the genus, with *C. minor* as the type species. Over time, some species were reclassified into the genera *Neochlorosarcina*,

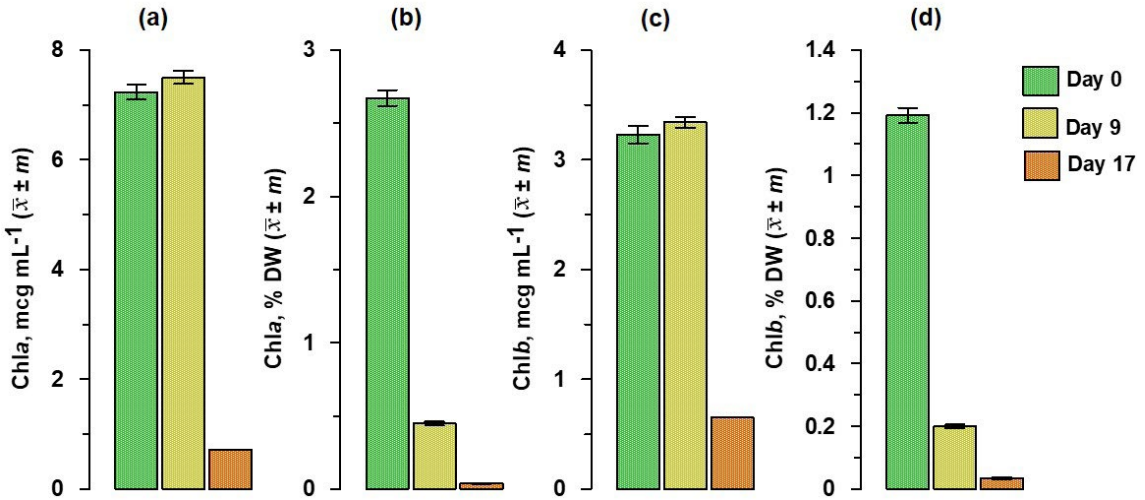

Fig.5. Chlorophyll content in the culture (a, c) and dry biomass (b, d) of *Chlorosarcinopsis* sp. at the beginning of experiment (day 0) and at the end of "green" (day 9) and "red" (day 17) stages.

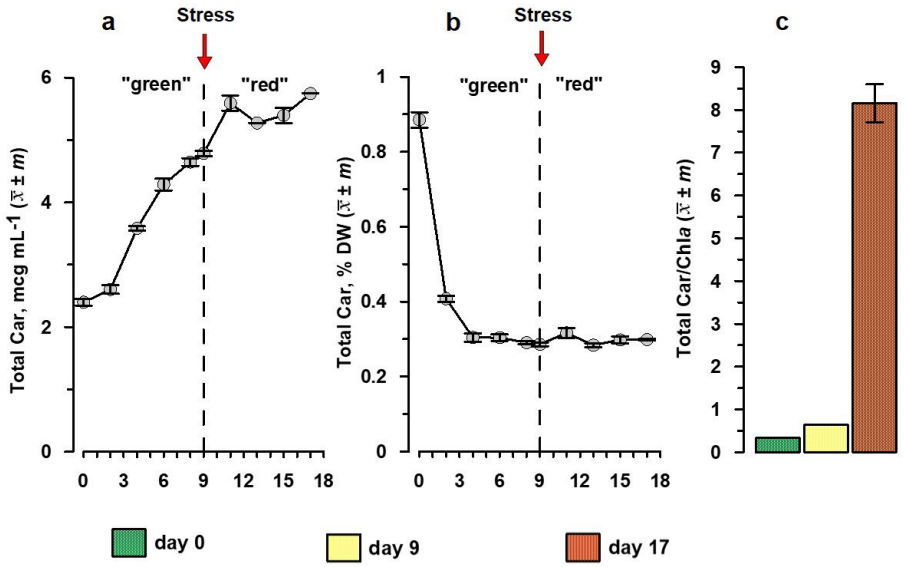

Fig.6. Total carotenoids content in culture (a) and dry biomass (b) in *Chlorosarcinopsis* sp., and total Car/Chl *a* ratio (c).

Desmotetra, and *Desmochloris*. Molecular studies later revealed that genus *Chlorosarcinopsis* is polyphyletic, with its members distributed across at least two phylogroups: Arenicolinia, including *C. arenicola*, *C. eremi*, and *C. variabilis*, and Stephanosphaerinia, including *C. minor*, *C. aggregata*, *C. bastropiensis*, and *C. dissociata* (Watanabe et al., 2006; Nakada et al., 2008). Since the holotype of *C. minor* forms an independent phylogenetic lineage within the Stephanosphaerinia clade, the other groups do not belong to the true *Chlorosarcinopsis* genus and should be described as new genera with a *Chlorosarcinopsis*-like morphology. The taxonomy of *Chlorosarcinopsis* remains unresolved, as some species (*C. angulosa*, *C. caeca*, and *C. superba*) have not yet been sequenced, and others lack sufficient sequence diversity, particularly in more variable loci. A key challenge is the choice of molecular markers to improve the clustering of the Arenicolinia phylogroup. Species delimitation based on the 18S rDNA and the ITS2 regions has proven problematic, suggesting that the *rbc*L gene might be more suitable.

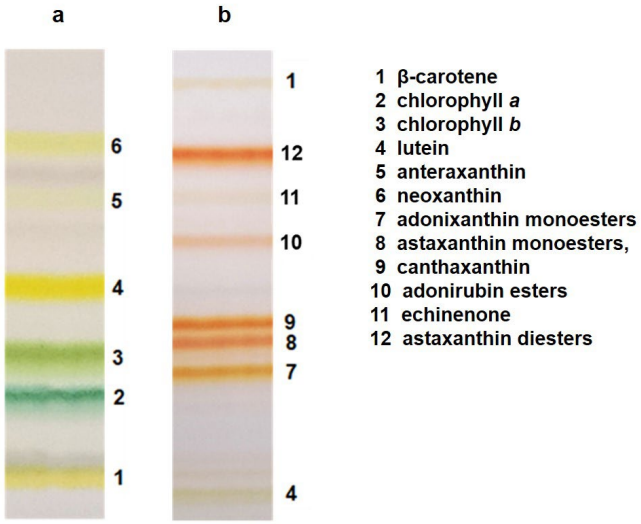

Fig.7. *Chlorosarcinopsis* sp. thin-layer chromatogram at the end of "green" (a) and "red" (b) stages of cultivation.

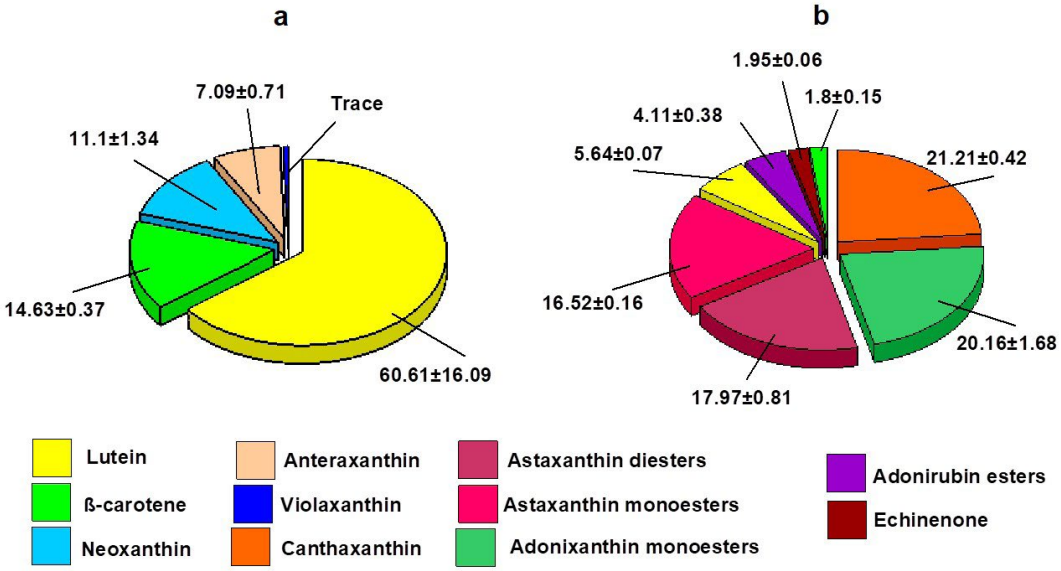

Fig.8. Carotenoid composition of *Chlorosarcinopsis* sp. at the "green" (a) and "red" (b) stages of the experiment ($\bar{x}+m$).

The application of the two-stage batch culture method to sarcinoid microalgae has its own peculiarities. Cell aggregation into three-dimensional clusters does not allow evaluating the state of the culture by cell division rate. Due to deformation of cells within aggregates, cell sizes are distorted. Thus, the assessment of the productive qualities of *Chlorosarcinopsis* is based solely on the measurement of the DW content in the culture. The presence of a mucilage matrix (mucilage) consisting of complex polysaccharide and protein components determines the peculiarities of DW dynamics (Domozych and LoRicco, 2024). Vesicles of mucilage form inside the cell within the Golgi apparatus, through bulb-shaped pores, and mucilage is then released outside, enveloping *Chlorosarcinopsis* cells and aggregating them (Domozych and Rogers-Domozych, 1993). The formation of multicellular packets as a result of cell division, as well as the shielding effect of the mucus matrix, rapidly deteriorates light conditions, which distinguishes sarcinoid microalgae from planktonic species. Therefore, bubbling (continuous aeration) of cultures is a necessary for the cultivation of these species.

Growth characteristics of the studied strain reflect the broad environmental tolerance typical of soil microalgae. The observed over six-fold increase in the DW content during the "green" stage is consistent with the microalgae growth dynamics in nutrient-rich culture medium. The sustained growth, even under stress, confirms the presence of an adaptive mechanism for managing drastic changes in critical environmental factors (Doppler et al., 2022; Nayana et al., 2022), a hallmark of carotenogenic microalgae.

The production characteristics of *Chlorosarcinopsis* sp., adapted to laboratory cultivation conditions, were comparable to those of previously studied extremobionts. Specifically, the average biomass productivity of *Chlorosarcinopsis* sp. VKM Al-296 during the "green" stage exceeded that reported for the other strains, such as *Bracteacoccus minor*, *Coelastrella rubescens*, and *Chromochloris zofingiensis* (order Sphaeropleales), as well as *Pseudospongiococcum protococcoides* (order Chlamydomonadales), which exhibited productivities of 0.08–0.09 g/L/day (Chubchikova and Drobetskaya, 2020).

The observed changes in the pigment composition of *Chlorosarcinopsis* sp. VKM Al-296 following the transition to the "red" stage are characteristic of carotenogenic microalgae. These changes support the concept of secondary carotenogenesis as a survival strategy, enabling cells to maintain viability under stressful conditions through metabolic reorganization.

The analysis of the carotenoid composition confirmed that a defining characteristic of the genus *Chlorosarcinopsis* during the active growth ("green") stage is the absolute predominance of lutein, consistent with the findings by Cherdchukeattisak et al. (2018). The second most significant pigment was β-carotene, whose content in the culture at the end of the "green" stage reached 0.7 mg/L, comparable to the 0.543 mg/L reported by Wongsnansilp et al. (2007).

At the SC stage, the carotenoid profile was dominated by canthaxanthin, mono- and diesters of astaxanthin, and monoesters of adonixanthin. The percentage of esterified astaxanthin in total Car (34.5%) was similar to the data presented by Chekanov (2023) for *Chlainomonas rubra* (32–44.5 %).

The total Car average productivity throughout the experiment (0.20 ± 0.01 mg/L/day) was comparable to that of *Chromochloris zofingiensis* and *Neochloris wimmeri,* which exhibited productivities of 0.21 and 0.22 mg/L/day, respectively (Orosa et al., 2000).

The astaxanthin content in DW of *Chlorosarcinopsis* sp. VKM Al-296 (0.11%), was comparable to that of *Chromochloris zofingiensis* (0.17%) (Del Campo et al., 2004), *Coelastrella* sp. S6 (0.17–0.18%) (Corato et al., 2022), and *Halochlorella rubescens* (0.12–0.18%) (Chekanov, 2023).

The presence of astaxanthin's metabolic precursors, along with astaxanthin, in the carotenoid profile does not reduce the biological value of red biomass and its extracts. Additionally, the high content of lutein (60%) in the green biomass makes the strain a promising source of this pigment.

5. Conclusion

Microscopic and molecular genetic analyses of the 18S rDNA confirmed the taxonomic position of the strain VKM Al-296 within the Arenicolinia clade. Using the primary and secondary structures of ITS2, we identified the strain as *Chlorosarcinopsis* sp.

The growth, physiological, and biochemical characteristics of the *Chlorosarcinopsis* sp. VKM Al-296 strain during two-stage batch cultivation are comparable to those previously reported for carotenogenic green microalgae of the orders Sphaeropleales and Chlamydomonadales under similar conditions.

The carotenoid composition of "green" cells is dominated by lutein, while "red" cells contain a mixture of valuable ketocarotenoids, including canthaxanthin and esters of adonixanthin and astaxanthin. The similarity of the carotenoid profile of *Chlorosarcionopsis* sp. with that of other members of Sphaeropleales and Chlamydomonadales indirectly supports the similarity of astaxanthin biosynthesis pathways in these microalgae.

The strain *Chlorosarcinopsis* sp. VKM Al-296 is a potentially promising candidate for further research aimed at optimizing cultivation conditions (temperature, light intensity, nutrient supply, and stress type) to enhance biomass growth during the "green" stage and ketocarotenoid biosynthesis during the "red" stage. Successful solution of this problem could unlock opportunities for the biotechnological application of this strain as a producer of lutein or ketocarotenoids.

Acknowledgements

The authors thank Dr. G.S. Minyuk, scientific advisor at the A.O. Kovalevsky Institute of Biology of the Southern Seas, Russian Academy of Sciences, for the assistance in analyzing the obtained data and consultations regarding the text of the article.

This work was performed under the project "Complex Investigation of Functioning Mechanisms of Marine Biotechnological Complexes in Order to Produce Biologically Active Substances from Hydrobionts" (No. 124022400152-1). Morphological and molecular genetic analyses were carried out with the financial support of the Ministry of Science and Higher Education of the Russian Federation (State Assignment No. FMRM-2026-0015).

Conflict of interest

The authors declare no competing interests.

References

Andreeva V.M. 1998. Terrestrial and aerophilic green algae (Chlorophyta: Tetrasporales, Chlorococcales, Chlorosarcinales). Sankt-Peterburg: Nauka. (in Russian)

Bischoff H.W., Bold H.C. 1963. Some soil algae from enchanted rock and related algal species. Phycological Studies IV 6318:1–95.

Boussiba S. 2000. Carotenogenesis in the green alga Haematococcus pluvialis: cellular physiology and stress response. Physiologia Plantarum 108(2):111–117. DOI: 10.1034/j.1399-3054.2000.108002111.x

Britton G. 2008. TLC of carotenoids. In: Waksmundzka-Hajnos M., Sherma J., Kowalska T. (Eds.), Thin Layer Chromatography in Phytochemistry. New York, CRC Press, pp. 543–573. DOI: 10.1201/9781420046786

Britton G., Liaaen-Jensen S., Pfander H. 2004. Carotenoids Handbook. Basel, Birkhäuser Verlag.

Byun Y., Han K. 2009. PseudoViewer3: generating planar drawings of large-scale RNA structures with pseudoknots. Bioinformatics 25(11): 1435–1437. DOI: 10.1093/bioinformatics/btp252

Caisová L., Marin B., Melkonian M. 2013. A consensus secondary structure of ITS2 in the Chlorophyta identified by phylogenetic reconstruction. Protist 164(4): 482–496. DOI: 10.1016/j.protis.2013.04.005

Chekanov K. 2023. Diversity and distribution of carotenogenic algae in Europe: A Review. Marine Drugs 21: 108. DOI: 10.3390/md21020108

Chelebieva E.S., Dantsyuk N.V., Chekanov K.A. et al. 2018. Identification and morphological-physiological characterization of astaxanthin producer strains of *Haematococcus pluvialis* from the Black Sea region. Applied Biochemistry and Microbiology 54(6): 639–648. DOI: 10.1134/S0003683818060078

Chen J., Liu L., Wei D. 2017. Enhanced production of astaxanthin by *Chromochloris zofingiensis* in a microplate-based culture system under high light irradiation. Bioresource technology 245: 518–529. DOI: 10.1016/j.biortech.2017.08.102

Cherdchukeattisak P., Fraser P.D., Purton S. et al. 2018. Detection and enhancement of ketocarotenoid accumulation in the newly isolated sarcinoid green microalga *Chlorosarcinopsis* PY02. Biology 7: 1–14. DOI: 10.3390/biology7010017

Chubchikova I.N. 2012. Effect of medium composition on the content of secondary carotenoids in microalgae *Scotiellopsis rubescens* Vinatz. (Chlorophyceae). Morskoj Ekologicheskij Zhurnal [Marine Ecological Journal] 9(4): 95–101. (in Russian)

Chubchikova I.N., Minyuk G.S., Drobetskaya I.V. et al. 2009. Chlorococcal microalgae as source of natural secondary carotenoids. Ecologia morya [Marine Ecology] 77: 77–83. (in Russian)

Chubchikova I.N., Drobetskaya I.V. 2020. Antiradical activity estimation of secondary carotenoids of four green microalgae species from order Sphaeropleales in vitro. Trudy Karadagskoj nauchnoj stancii im. T.I. Vyazemskogo – prirodnogo zapovednika RAN [Proceedings of the T.I. Vyazemsky Karadag scientific station – Nature Reserve of the RAS] 2(14): 66–78. DOI: 10.21072/eco.2021.14.07 (in Russian)

Chubchikova I.N., Drobetskaya I.V., Dantsyuk N.V. et al. 2022. Optimization of freshwater microalgae (Scenedesmaceae, Chlorophyta) fixation method for primary taxonomic identification by scanning electron microscopy. Voprosy sovremennoj algologii [Issues of modern algology] 1(28): 102–109. DOI: 10.33624/2311-0147-2022-1(28)-102-109 (in Russian)

Coleman A.W. 2000. The significance of a coincidencebetween evolutionary landmarks found in mating affinity and a DNA sequence. Protist 151: 1–9. DOI: 10.1078/1434-4610-00002

Coleman A.W. 2003. ITS2 is a double-edged tool for eukaryote evolutionary comparisons. Trends in Genetics 19: 370–375. DOI: 10.1016/S0168-9525(03)00118-5

Coleman A.W. 2009. Is there a molecular key to the level of "biological species" in eukaryotes? A DNA guide. Molecular Phylogenetics and Evolution 50: 197–203. DOI: 10.1016/j.ympev.2008.10.008

Corato A., Le T.T., Baurain D. et al. 2022. A fast-growing oleaginous strain of *Coelastrella* capable of astaxanthin and canthaxanthin accumulation in phototrophy and heterotrophy. Life 12:334. DOI: 10.3390/life12030334

Dantsyuk N.V., Chubchikova I.N., Temraleeva A.D. et al. 2024. Morphological, physiological, and biochemical characteristics of the sarcinoid microalga *Chlorosarcinopsis eremi* (Chlorophyceae, Chlorophyta). Russian Journal of Plant Physiology 71: 131. DOI: 10.1134/S1021443724607328

Darriba D., Taboada G.L., Doallo R. et al. 2012. jModelTest 2: more models, new heuristics and parallel computing. Nature Methods 9(8): 772. DOI: 10.1038/nmeth.2109

Del Campo J.A., Rodríguez H., Moreno J. et al. 2004. Accumulation of astaxanthin and lutein in *Chlorella zofingiensis* (Chlorophyta). Applied Microbiology and Biotechnology 64: 848–854. DOI: 10.1007/s00253-003-1510-5

Domozych D.S., LoRicco J.G. 2024. The extracellular matrix of green algae. Plant Physiology 194: 15–32. DOI: 10.1093/plphys/kiad384

Domozych D.S., Rogers-Domozych C. 1993. Mucilage processing and secretion in the green alga *Closterium* II. Ultrastructureandimmunocytochemistry.JournalofPhycology 29: 659–667. DOI: 10.1111/j.0022-3646.1993.00659.x

Doppler P., Kriechbaum R., Käfer M. et al. 2022. *Coelastrella terrestris* for adonixanthin production: physiological characterization and evaluation of secondary carotenoid productivity. Marine Drugs 20(3): 175. DOI: 10.3390/md20030175

Egeland E.S., Garrido J.L., Clementson L. et al. 2011. Data sheets aiding identification of phytoplankton carotenoids and chlorophylls. In: Roy S., Llewellyn C., Egeland E.S. et al. (Eds.), Phytoplankton pigments: characterization, chemotaxonomy and applications in oceanography. Cambridge, pp. 665–822.

Fábregas J., Otero A., Maseda A. et al. 2001. Two-stage cultures for the production of astaxanthin from *Haematococcus pluvialis*. Journal of biotechnology 89(1): 65–71. DOI: 10.1016/S0168-1656(01)00289-9

Friedmann I., Ocampo-Paus R. 1965. A new *Chlorosarcinopsis* from the Negev Desert. Journal of Phycology 1(4): 185–191. DOI: 10.1111/j.1529-8817.1965.tb04581.x

Gollerbach M.M., Shtina E.A. 1969. Soil algae. Leningrad: Nauka. (in Russian)

Guiry M.D., Guiry G.M. 2025. AlgaeBase. World-wide electronic publication, National University of Ireland, Galway. URL: http://www.algaebase.org (accessed: 24 November 2025).

Hall J.D., Fučíková K., Lo C. et al. 2010. An assessment of proposed DNA barcodes in freshwater green algae. Cryptogamie, Algologie 31(4): 529–555.

Henry L.E.A., Mikkelsen J.D., Møller B.L. 1983. Pigment and acyl lipid composition of photosystem I and II vesicles and of photosynthetic mutants in barley. Carlsberg Research Communications 48: 131–148. DOI: 10.1007/bf02906174

Herndon W. 1958. Studies on chlorosphaeracean algae from soil. American Journal of Botany 45(4): 298–308.

Hoshina R. 2014. DNA analyses of a private collection of microbial green algae contribute to a better understanding of microbial diversity. BMC Research Notes 7: 592. DOI: 10.1186/1756-0500-7-592

Hoshina R., Fujiwara Y. 2013. Molecular characterization of *Chlorella* cultures of the National Institute for Environmental Studies culture collection with description of *Micractinium inermum* sp. nov., *Didymogenes sphaerica* sp. nov., and *Didymogenes soliella* sp. nov. (Chlorellaceae, Trebouxiophyceae). Phycological Research 61: 124–132. DOI: 10.1111/pre.12010

Jeffers T.L., Roth M.S. 2021. Revealing mechanisms of algal astaxanthin production and bioengineering potential using multiomics. In: Ravishankar G.A., Ambati R.R. (Eds.), Global perspectives on Astaxanthin: from industrial production to food, health, and pharmaceutical applications. Cambridge, pp. 181–208. DOI: 10.1016/B978-0-12-823304-7.00010-60

Katana A., Kwiatowski J., Spalik K. et al. 2001. Phylogenetic position of *Koliella* (Chlorophyta) as inferred from nuclear and chloroplast small subunit rDNA. Journal of Phycology 37(3): 443–451. DOI: 10.1046/j.1529-8817.2001.037003443.x

Khani-Juyabad F., Mohammadi P., Zarrabi M. 2019. Comparative analysis of *Chlorosarcinopsis eremi* mitochondrial genome with some Chlamydomonadales algae. Physiology and Molecular Biology of Plants 25(5): 1301–1310. DOI: 10.1007/s12298-019-00696-y

Lewis L.A., Lewis P.O. 2005. Unearthing the molecular phylodiversity of desert soil green algae (Chlorophyta). Systematic Biology 54(6): 936–947. DOI: 10.1080/10635150500354852

Laroche C. 2022. Exopolysaccharides from microalgae and cyanobacteria: diversity of strains, production strategies, and applications. Marine Drugs 20(5): 336. DOI: 10.3390/md20050336

Lemoine Y., Schoefs B. 2010. Secondary ketocarotenoid astaxanthin biosynthesis in algae: a multifunctional response to stress. Photosynthesis Research 106: 155–177. DOI: 10.1007/s11120-010-9583-3

Lichtenthaler H.K. 1987. Chlorophylls and carotenoids: pigments of photosynthetic membranes. Methods in Enzymology 148: 350–382.

Malik S., Ashraf M.U.F., Shahid A. et al. 2022. Characterization of a newly isolated self-flocculating microalga *Bracteacoccus pseudominor* BERC09 and its evaluation as a candidate for a multiproduct algal biorefinery. Chemosphere 304: 135346. DOI: 10.1016/j.chemosphere.2022.135346

Marchenko M.M., Dorosh I.V., Cheban L.M. 2019. Induction of carotenogenesis in *Desmodesmus armatus* (Chod.) Hegew cultivated on the closed waterside from recirculating aquaculture system. Biotechnologia Acta 12(2): 46–55. DOI: 10.15407/biotech12.02.046

Minyuk G.S., Terentyeva N.V., Drobetskaya I.V. 2007. A comparison of characteristics of morpho-physiological and biochemical traits in three strains of *Haematococcus pluvialis* Flotow (Chlorophyta, Chlamydomonadales). International Journal on Algae 9(2): 174–186. DOI: 10.1615/INTERJALGAE.v9.i2.70

Minyuk G.S., Chelebieva E.S., Chubchikova I.N. 2014. Secondary carotenogenesis of the green microalga *Bracteacoccus minor* (Chodat) Petrova (Chlorophyta) in a two-stage culture. International Journal on Algae 16(4): 354–368. DOI: 10.1615/InterJAlgae.v16.i4.50

Minyuk G., Chelebieva E., Chubchikova I. et al. 2017. Stress-induced secondary carotenogenesis in *Coelastrella rubescens* (Scenedesmaceae, Chlorophyta), a producer of value-added keto-carotenoids. Algae 32(3): 245–259. DOI: 10.4490/algae.2017.32.8.6

Minyuk G.S., Solovchenko A.E. 2018. Express analysis of microalgal secondary carotenoids by TLC and UV-Vis spectroscopy. In: Barriero C., Barriero J.-L. (Eds.), Microbial Carotenoids: Methods and Protocols. New York, pp. 73–95. DOI: 10.1007/978-1-4939-8742-9

Minyuk G., Dantsyuk N., Chelebieva E. et al. 2019. The effect of diverse nitrogen sources in the nutrient medium on the growth of the green microalgae *Chromochloris zofingiensis* in the batch culture. Marine Biological Journal 4: 41–52. DOI: 10.21072/mbj.2019.04.4.04

Minyuk G., Sidorov R., Solovchenko A. 2020. Effect of nitrogen source on the growth, lipid, and valuable carotenoid production in the green microalga *Chromochloris zofingiensis*. Journal of Applied Phcology 32: 923. DOI: 10.1007/s10811-020-02060-0

Nair A., Ahirwar A., Singh S. et al. 2023. Astaxanthin as a king of ketocarotenoids: structure, synthesis, accumulation, bioavailability and antioxidant properties. Marine Drugs 21(3): 176. DOI: 10.3390/md21030176

Nakada T., Misawa K., Nozaki H. 2008. Molecular systematics of Volvocales (Chlorophyceae, Chlorophyta) based on exhaustive 18S rRNA phylogenetic analyses. Molecular Phylogenetics and Evolution 48: 281–291. DOI: 10.1016/j.ympev.2008.03.016

Nayana K., Sudhakar M.P., Arunkumar K. 2022. Biorefinery potential of *Coelastrella* biomass for fuel and bioproducts—a review. Biomass Conversion and Biorefinery. DOI: 10.1007/s13399-022-02519-9

Orosa M., Torres E., Fidalgo P. et al. 2000. Production and analysis of secondary carotenoids in green algae. Journal of Applied Phcology 12: 553–556.

Remias D., Pichrtova M., Pangratz M. et al. 2016. Ecophysiology, secondary pigments and ultrastructure of *Chlainomonas* sp. (Chlorophyta) from the European Alps compared with *Chlamydomonas nivalis* forming red snow. Microbiology Ecology 92(4): fiw030. DOI: 10.1093/femsec/fiw030

Rodriguez-Amaya D.B. 2001. A guide to carotenoid analysis in foods. Washington: ILSI Press.

Saito M., Watanabe H., Sasaki M. et al. 2023. Coproduction of lipids and carotenoids by the novel green alga *Coelastrella* sp. depending on cultivation conditions. Biotechnology Reports 37: e00769. DOI: 10.1016/j.btre.2022.e00769

Seibel P.N., Müller T., Dandekar T. et al. 2006. 4SALE – a tool for synchronous RNA sequence and secondary structure alignment and editing. BMC Bioinformatics 7: 498. DOI: 10.1186/1471-2105-7-498

Solovchenko A. 2013. Physiology and adaptive significance of secondary carotenogenesis in green microalgae. Russian Journal of Plant Physiology 60(1): 1–13. DOI: 10.1134/S1021443713010081

Solovchenko A., Merzlyak M., Khozin-Goldberg I. et al. 2010. Coordinated carotenoid and lipid syntheses induced in *Parietochloris incisa* (Chlorophyta, Trebouxiophyceae) mutant deficient in Δ5 desaturase by nitrogen starvation and high light. Journal of Phycology 46: 763–772. DOI: 10.1111/j.1529-8817.2010.00849.x

Temraleeva A.D., Mincheva E.V., Bukin Y.S. et al. 2014. Modern methods of isolation, cultivation and identification

of green algae (Chlorophyta). Kostroma: Kostroma Printing House. (in Russian)

Vasistha S., Khanra A., Rai M.P. 2021. Influence of microalgae-ZnO nanoparticle association on sewage wastewater towards efficient nutrient removal and improved biodiesel application: An integrated approach. Journal of Water Process Engineering 39: 101711. DOI: 10.1016/j.jwpe.2020.101711

Vonshak A. 1985. Microalgae: Laboratory growth techniques and outdoor biomass production. In: Coombs J., Hall D., Long S. et al. (Eds.), Techniques in Bioproductivity and Photosynthesis. Oxford:Pergamon Press, pp. 188–203. DOI: 10.1016/B978-0-08-031999-5.50025-X

Watanabe S., Mitsui K., Nakayama T. et al. 2006. Phylogenetic relationships and taxonomy of sarcinoid green algae: *Chlorosarcinopsis*, *Desmotetra*, *Sarcinochlamys* gen. nov., *Neochlorosarcina*, and *Chlorosphaeropsis* (Chlorophyceae, Chlorophyta) Journal of Phycology 42: 679–695. DOI: 10.1111/j.1529-8817.2006.00196.x

White T.J., Bruns T., Lee S. et al. 1990. Amplification and direct sequencing of fungal ribosomal RNA genes for phylogenetics. In: Innis M.A., Gelfand D.H., Sninsky J.J. et al. (Eds.), PCR protocols. San Diego:Academic Press, pp 315–324.

Wongsnansilp T., Tansakul P., Arunyanart M. 2007. Factors affecting growth and betacarotene content of *Chlorosarcinopsis* sp. (PSU/CHL20) in batch culture. Kasetsart J (Nat Sci) 41(1):153–157.

Wood A.M., Everroad R.C., Wingard L.M. 2005. Measuring growth rates in microalgal cultures. In: Andersen R.A. (Ed.), Algal Culturing Techniques.Elsevier Academic Press, pp. 269-285. DOI: 10.1016/B978-012088426-1/50019-6

Оригинальная статья

LIMNOLOGY FRESHWATER BIOLOGY

Идентификация и комплексная характеристика нового почвенного штамма каротиногенной микроводоросли *Chlorosarcinopsis* sp. VKM Al-296 (Chlorophyta)

Чубчикова И.Н.[1]*, Данцюк Н.В.[1], Дробецкая И.В.[1], Темралеева А.Д.[2]

[1] *Институт биологии южных морей им. А. О. Ковалевского РАН, проспект Нахимова, 2, Севастополь, 299011, Российская Федерация*

[2] *Всероссийская коллекция микроорганизмов (ВКМ), Институт биохимии и физиологии микроорганизмов им. Г.К. Скрябина, Пущино, Научно-исследовательский центр биологических исследований Российской академии наук, 142290 Пущино, Российская Федерация*

АННОТАЦИЯ. Проведено комплексное исследование нового штамма зеленых микроводорослей VKM Al-296, выделенного из пахотной почвы. На основе молекулярно-филогенетического анализа последовательностей 18S рДНК и ITS2, а также данных световой и сканирующей электронной микроскопии штамм идентифицирован как *Chlorosarcinopsis* sp. (Chlamydomonadales, Chlorophyta). Изучены его морфология, рост и каротиногенез в условиях двухстадийного накопительного культивирования. Установлено, что в жидкой среде клетки размером 3-6 мкм присутствовали поодиночке или в пакетах, окруженных внеклеточной слизью. К концу «зеленой» стадии (вегетативный рост) преобладающим пигментом был лютеин, составляющий более 60% от общего количества каротиноидов. Также присутствовали другие первичные каротиноиды: бета-каротин (14,6%), неоксантин (11,1%) и антераксантин (7,1%). В конце «красной» стадии (вторичного каротиногенеза) содержание сухой биомассы в культуре составляло 1,92 ± 0,04 г/л, при этом каротиноиды составляли 0,3% от сухой биомассы. В пигментном профиле преобладали кетокаротиноиды: астаксантин (моно- и диэфиры), кантаксантин и моноэфиры адониксантина (35%, 21% и 20% от общего содержания каротиноидов, соответственно). За весь период культивирования (17 суток) средняя продуктивность культур по биомассе и общая продуктивность по каротиноидам составляли 0,10 г/л/сут и 0,2 мг/л/сут, соответственно. *Chlorosarcinopsis* sp. штамм VKM Al-296 может стать перспективным объектом дальнейших исследований, направленных на оптимизацию условий культивирования, в качестве источника лютеина на «зеленой» стадии, а также кантаксантина и эфиров астаксантина и адониксантина на «красной» стадии.

Ключевые слова: *Chlorosarcinopsis* sp., морфология клеток, молекулярно-филогенетический анализ, двухстадийное культивирование, вторичные каротиноиды, тонкослойная хроматография

Для цитирования: Чубчикова И.Н., Данцюк Н.В., Дробецкая И.В., Темралеева А.Д. Идентификация и комплексная характеристика нового почвенного штамма каротиногенной микроводоросли *Chlorosarcinopsis* sp. VKM Al-296 (Chlorophyta) // Limnology and Freshwater Biology. 2026. - № 2. - С. 78-102. DOI: 10.31951/2658-3518-2026-A-2-78

1. Введение

Chlorosarcinopsis — род микроводорослей, относящихся к отряду Chlamydomonadales (Chlorophyta), широко распространенный в наземных условиях, особенно в засушливых и полузасушливых пустынях (Friedmann and Ocampo-Paus, 1965; Андреева, 1998; Lewis and Lewis, 2005; Hall et al., 2010; Khani-Juyabad et al., 2019).

Почва является средой обитания для множества микроорганизмов, включая бактерии, грибы, простейшие и микроводоросли. В отличие от планктонных микроводорослей, условия обитания которых, как правило, незначительно меняются в зависимости от времени года и времени суток, почвенные микроводоросли, обитающие на поверхности почвы или в ее верхних горизонтах, подвергаются постоянному стрессу, выдерживая суточные и сезонные

*Автор для переписки. Адрес e-mail: chubchikova_in@ibss-ras.ru (И.Н. Чубчикова)

Поступила: 17 декабря 2025;
Принята после доработки: 27 февраля 2026;
Опубликована online: 24 апреля 2026

колебания условий окружающей среды. Это резкие изменения освещенности, температуры, влажности, доступности питательных веществ и т. д. Ключевым звеном в стратегии выживания почвенных видов, включая микроводоросли рода *Chlorosarcinopsis*, в условиях абиотического стресса является способность к вторичному каротиногенезу (ВКГ), связанная со способностью клеток быстро переходить из состояния активной вегетативной фазы в состояние покоя и наоборот. Кетокаротиноиды (ККар) — это группа пигментов, которые структурно и функционально не связаны с фотосинтетическим аппаратом (Lemoine and Schoefs, 2010; Solovchenko, 2013). Установлено, что их функции включают защиту ядра и клеточных органелл, использование избытка продуктов фотосинтеза, а также «гашение» активных форм кислорода и предотвращение их образования (Solovchenko, 2013; Remias et al., 2016). Природный ККар астаксантин широко используется в фармацевтике, нутрицевтике, косметике, диетологии и аквакультуре, и спектр его применения быстро расширяется. Он безопасен для употребления в пищу, в отличие от своего синтетического аналога, который разрешен для использования только в аквакультуре (Nair et al., 2023).

В связи с этим в последние десятилетия большое внимание уделяется изучению процесса ВКГ как ключевого механизма адаптации у экстремобионтных зеленых микроводорослей различных таксономических и экологических групп. Основная часть информации о закономерностях ВКГ у одноклеточных микроводорослей была получена на примерах ограниченного числа планктонных, почвенных и аэрофитных видов из порядков Chlamydomonadales и Sphaeropleales (*Haematococcus lacustris*, *Chromochloris zofingiensis*, *Coelastrella rubescens*, *Bracteacoccus pseudominor*, *B. minor*) (Minyuk et al., 2014; 2017; Chelebieva et al., 2018; Minyuk et al., 2020; Malik et al., 2022). Однако разнообразие видов каротиногенных микроводорослей намного больше, чем принято считать. Достижения в области высокопроизводительного полногеномного секвенирования позволили идентифицировать ортологи β-каротинкетолазы, ключевого фермента, ответственного за синтез ККар из β-каротина, в геномах многочисленных видов микроводорослей (Jeffers and Roth, 2021). Поэтому дальнейший поиск коммерчески перспективных продуцентов ККар (астаксантина и его метаболических предшественников) и разработка методов их промышленного культивирования остаются актуальными (Чубчикова и др., 2009; 2012; Minyuk et al., 2014; Chen et al., 2017; Minyuk et al., 2017; Marchenko et al., 2019; Minyuk et al., 2019; 2020; Doppler et al., 2022; Saito et al., 2023).

Стратегия выживания сарциноидных микроводорослей усиливается дополнительным адаптационным механизмом, позволяющим им успешно противостоять резким изменениям условий окружающей среды. Это способность производить большое количество слизи – так называемых «слизистых оболочек» и «оберток» (муцилажа). Основным компонентом муцилажа являются внеклеточные гидрофильные коллоидные полисахариды, в которых преобладают галактоза, глюкоза и рамноза (Голлербах и Штина, 1969; Laroche, 2022). Такой внеклеточный матрикс выполняет несколько функций. Он обеспечивает прикрепление клеток друг к другу, защищает их от контаминации и резких биотических и абиотических стрессов, сглаживая скачки инсоляции, влажности и температуры, особенно для клеток, расположенных внутри клеточного агрегата. Помимо полисахаридов, слизь содержит низкомолекулярные белковые соединения. Имеются данные об активном росте *Chlorosarcinopsis* spp. на миксо- и гетеротрофных средах в лабораторных условиях (Cherdchukeattisak et al., 2018; Vasistha et al., 2021), что позволяет предположить использование слизи в периоды голодания как доступного органического источника углерода и азота.

Эти особенности сарциноидных микроводорослей позволяют предположить, что в условиях массового открытого культивирования выживаемость таких видов будет значительно выше, чем у более чувствительных планктонных видов, что может положительно сказаться на продуктивности по биомассе и ККар.

Метод двухстадийной накопительной культуры (Boussiba, 2000; Fábregas et al., 2001; Minyuk et al., 2017) позволяет проводить комплексные исследования штаммов, включая световую и сканирующую электронную микроскопию, молекулярно-филогенетический анализ и оценку продукционных характеристик как в период активного роста, так и в процессе вторичного каротиногенеза.

Целью данного исследования было изучение штамма VKM Al-296 с использованием комплексного метода в условиях двухстадийной накопительной культуры.

2. Материалы и методы

2.1. Изоляция штамма

Объектом исследования являлся штамм почвенной микроводоросли VKM Al-296, выделенный в 2018 году из пахотного типичного чернозема в Ставропольском крае, Российская Федерация (45˚07′ с.ш., 42˚01′ в.д.). Альгологически чистую культуру получали методом, описанным Темралеевой и соавт. (2014). Почвенную суспензию высевали на поверхность плотной питательной среды BG-11 (1,5% агар, pH 7,2) в чашках Петри и инкубировали в контролируемых условиях (температура 23–25 ˚C, фотопериод 12 ч света/12 ч темноты, освещенность 60–75 мкмоль фотонов/м^2/с, обеспечиваемая люминесцентными лампами холодного белого света) до появления колоний. Далее отдельные колонии многократно пересевали и культивировали в тех же условиях до получения альгологически чистой культуры.

Первоначально штамм был депонирован в Альгологическую коллекцию Института физико-химических и биологических проблем почвоведения РАН (ACSSI) под номером ACSSI 296. Впоследствии

он был передан во Всероссийскую коллекцию микроорганизмов (VKM) Института биохимии и физиологии микроорганизмов РАН, где ему был присвоен номер VKM Al-296.

2.2. Морфологический анализ

Морфологию и жизненный цикл штамма VKM Al-296 исследовали методом световой микроскопии с использованием микроскопа Leica DM750 (Германия) и цифровой цветной камеры Leica Flexicam C3 (Германия) для документирования изображений. Наблюдения проводили в течение периода от двух недель до шести месяцев.

Для сканирующей электронной микроскопии (СЭМ) клетки фиксировали 2% раствором глутаральдегида в 10-кратно разбавленном 66,7 мМоль Na-K фосфатном буфере (pH 7,34) при 4°C в течение 24 часов. Затем образец дополнительно фиксировали 0,005% раствором Люголя и обезвоживали в градуированной серии растворов этанола с возрастающей концентрацией (Чубчикова и др., 2022). Для получения СЭМ-изображений клеток использовали сканирующий электронный микроскоп Hitachi SU3500 (Япония) на базе Лаборатории микроскопии ФИЦ ИнБЮМ.

2.3. Выделение ДНК, ПЦР и секвенирование

Суммарную ДНК экстрагировали с использованием набора DNeasy Plant Mini Kit (Qiagen, США) в соответствии с инструкцией производителя. Нуклеотидные последовательности регионов 18S рДНК и ITS2 амплифицировали с использованием готовой смеси Screen Mix-HS (Евроген, Россия). Праймеры и режимы амплификации были подобраны на основании методик, описанных White et al. (1990) и Katana et al. (2001), и приведены в Таблице 1. Амплификацию проводили с помощью термоциклера T100 (Bio-Rad, США). Целевые продукты ПЦР визуализировали методом электрофореза в 1% агарозном геле. После электрофореза ампликоны очищали с помощью набора Cleanup Mini (Евроген, Россия) по протоколу производителя. Далее очищенные продукты ПЦР были направлены для проведения секвенирования в компанию Евроген (Россия).

2.4. Молекулярно-филогенетический анализ

Полученные нуклеотидные последовательности депонированы в базу данных GenBank под номерами: MT338814 (18S рДНК) и MT340909 (ITS2). Для поиска близкородственных последовательностей использовали алгоритм BLASTn (NCBI). Филогенетический анализ проводили на основе двух независимо сформированных наборов данных:

1. Набор данных 18S рДНК включал 70 последовательностей от различных представителей порядка Chlamydomonadales, в том числе из клад Arenicolinia, Stephanosphaerinia и Chlorogonia. В качестве внешней группы использовали аутентичные штаммы рода *Gungnir* (клада Dunaliellinia).
2. Набор данных ITS2 включал 66 последовательностей от всех представителей клады Arenicolinia, включая некультивируемые виды. В качестве внешней группы использовали аутентичный штамм *Chlorococcum isabeliense* (= *Pleurastrum isabeliense*) из клады Stephanosphaerinia.

При анализе использовали современную таксономическую систему, принятую в базе данных AlgaeBase (Guiry and Guiry, 2025).

Множественное выравнивание последовательностей выполняли с помощью онлайн-сервиса MAFFT (https://www.ebi.ac.uk/jdispatcher/msa/mafft). Оптимальную эволюционную модель для каждого локуса (18S рДНК и ITS2) определяли с использованием информационного критерия Акаике (AIC), реализованного в программе jModelTest 2.1.10 (Darriba et al., 2012). В рамках анализа методом максимального правдоподобия (ML) для каждого набора данных было сгенерировано 1000 реплик бутстреп-анализа с использованием программы PhyML. Статистическую поддержку вет-

Таблица 1. Праймеры и условия амплификации.

Локус	Праймеры	Последовательность (5'–3')	Условия амплификации
18S рДНК	F	AACCTGGTTGATCCTGCCAGT	95°C, 5 мин; 95°C, 1 мин, 55°C, 1 мин, 72°C, 2 мин, 35 циклов; 72°C, 5 мин
	R	TGATCCTTCTGCAGGTTCACCTACG	
	402–23F*	GCTACCACATCCAAGGAAGGCA	
	1323–44F*	CGAACGAGACCTCAGCCTGCTA	
	416–37R*	ATTTGCGCGCCTGCTGCCTTCC	
	898–919R*	TAAATCCAAGAATTTCACCTCT	
	1308–39R*	CTCGTTCGTTAACGGAATTAACC	
	1636–57R*	GGTAGGAGCGACGGGCGGTGTG	
ITS2	ITS3	GCATCGATGAAGAACGCAGC	95°C, 3 мин; 95°C, 30 с, 52–57°C, 30 с, 72°C, 40 с, 35 циклов; 72°C, 10 мин
	ITS4	TCCTCCGCTTATTGATATGC	

Примечание: * внутренние секвенирующие праймеры.

вей оценивали по значениям вероятностей бутстрепа (BP). Байесовский вывод (BI) проводили с использованием программы BEAST 1.8.4. Выполняли два независимых прогона по 10^8 поколений каждый с отбором каждые 10^4 поколений; первые 25% поколений отбрасывали (burn-in). Сходимость цепей Маркова подтверждали, убедившись, что значения эффективного размера выборки (ESS) превышали 200, а результаты визуализировали в программе Tracer 1.5. Консенсусное дерево строили с помощью программы TreeAnnotator 1.8.4, где поддержка ветвей оценивалась по апостериорным вероятностям Байеса (PP). Генетические дистанции рассчитывали в программе MEGA 6 с использованием двухпараметрической модели Кимуры. Для анализа вторичной структуры ITS2 последовательности сворачивали с помощью веб-сервера RNAfold (https://rna.tbi.univie.ac.at/cgi-bin/RNAWebSuite/RNAfold.cgi) в соответствии с принципом минимальной свободной энергии. Достоверность предсказанных вторичных структур оценивали на основе критериев, предложенных Caisová et al. (2013). Сравнение вторичных структур ITS2, идентификацию консервативных мотивов и анализ полных компенсаторных замен (CBC) проводили с использованием программы 4SALE 1.7 (Seibel et al., 2006). Для разграничения видов по последовательностям ITS2 применяли CBC-подход, разработанный A. Coleman (2000; 2003; 2009). Визуализацию вторичных структур ITS2 выполняли в программе PseudoViewer3 (Byun and Han, 2009).

2.5. Условия культивирования

Штамм выращивали методом двухстадийной накопительной культуры (Boussiba, 2000; Fábregas et al., 2001) в питательной среде BBM (Bischoff and Bold, 1963). Микроводоросли выращивали в трех биологических повторностях, используя пластиковые культуральные флаконы объемом 0,75 л («Falcon», США). Объем культуры составлял 0,6 л; начальное содержание сухой биомассы (СБ) — 0,3 г/л.

Первая («зеленая») стадия культивирования, длительностью 9 суток, проходила в следующих условиях: одностороннее освещение, обеспечиваемое светодиодными лампами холодного белого света «Feron» DL 20W T4 6400K (Россия), плотность потока ФАР 130 мкмоль фотонов/м^2/с (измеренная на боковой поверхности колб), световой режим 15:9 ч (свет/темнота), температура $28 \pm 0{,}5$ °C и непрерывное барботирование воздухом со скоростью 0,44 л/мин/л. pH культуры поддерживали на уровне $7{,}0 \pm 0{,}05$ дозированной подачей CO_2 из газового баллона в течение 8 часов, контролируя системой Aqua Medic pH2001C (Германия), оснащенной электромагнитным клапаном Camozzi A7E (Италия).

Для индукции «красной» стадии культуру перевели на двустороннее 24-часовое освещение с той же самой плотностью потока ФАР с каждой стороны и температурой 28–29 °C. Подача CO_2 оставалась неизменной. Дополнительно был внесен 1% раствор NaCl до конечной концентрации в культуре 5 мМоль. «Красная» стадия длилась 8 дней.

2.6. Мониторинг роста культуры

Ростовые характеристики штамма оценивали по динамике биомассы. Содержание СБ (г/л) определяли гравиметрическим методом на нитроцеллюлозных мембранных фильтрах «Sartorius» (Германия) с размером пор 3,0 мкм (Vonshak, 1985). Биомассу на фильтрах промывали дистиллированной водой (три или четыре раза по 15 мл каждый) для удаления слизи. Удельную скорость роста (μ) и продуктивность культур (*P*) рассчитывали по методу, описанному Wood et al. (2005).

$$\mu = \ln(СБ_1 / СБ_0) / (T_1 - T_0) \quad (1)$$

$$P = (СБ_1 - СБ_0) / (T_1 - T_0) \quad (2)$$

где *P* – средняя продуктивность г/л/сут;

$СБ_0$ – начальная СБ, г/л;

DW_1 – конечная СБ, г/л;

$T_1 - T_0$ – период роста, сут;

μ – удельная скорость роста, сут$^{-1}$.

2.7. Анализ пигментов

Концентрации пигментов определяли спектрофотометрически (спектрофотометр СФ-2000 UV/Vis, ОКБ Спектр, Россия). Содержание хлорофиллов *a* и *b* и суммарных каротиноидов на протяжении всего эксперимента определяли в диметилсульфоксидных экстрактах биомассы (Merck, класс ACS) и рассчитывали, как описано у Solovchenko et al. (2010).

Состав каротиноидов в ацетоновых экстрактах в конце «зеленой» и «красной» стадий исследовали методом тонкослойной хроматографии (ТСХ) на силикагеле (Britton, 2008). Экстракты из «зеленой» биомассы анализировали на пластинах с обращенной фазой Silica gel 60 RP-18 (Merck, Германия) в системе растворителей этилацетат-метанол-вода (50:40:10) (Henry et al., 1983). Для анализа пигментов из «красной» биомассы использовали пластины Silica gel 60 (Merck, Германия) с нормальной фазой с последовательным использованием двух систем растворителей: I – гексан-ацетон 9:1; II – гексан-бензол-ацетон 5:3.75:0.8 (Minyuk and Solovchenko, 2018). Предварительно в ацетоновом экстракте каждого исследуемого образца определяли содержание хлорофилла *a* (Хл*a*), хлорофилла *b* (Хл*b*) и суммарных Кар по методу Lichtenthaler (1987).

Идентификацию каротиноидных фракций проводили с помощью химических, спектральных и хроматографических тестов на наличие и количество гидроксильных и кетогрупп; определения максимумов поглощения в УФ/видимых спектрах в трех растворителях (гексане, бензоле и ацетоне); сопоставления Rf идентифицированных фракций и стандартов каротиноидов в совместной хроматографии (Rodriguez-Amaya, 2001; Britton et al., 2004; Britton, 2008; Egeland et al., 2011; Minyuk and Solovchenko, 2018).

2.8. Статистика

Все измерения проводили в трех биологических и трех аналитических повторностях. Средние значения ($\bar{x}$) и их стандартные ошибки (SE) рассчитывали с помощью статистического пакета Microsoft Excel. Графическую визуализацию данных выполняли с помощью программы Golden Software Grapher (версия 17.3.454).

3. Результаты

3.1. Идентификация штамма VKM Al-296: морфология и филогенетический анализ

На основании наблюдений с помощью световой и сканирующей электронной микроскопии штамм VKM Al-296 был предварительно отнесен к роду *Chlorosarcinopsis*. Данное предположение подтверждалось несколькими ключевыми морфологическими признаками: образование пакетов клеток, наличие голых двужгутиковых зооспор, пристенного хлоропласта и одного пиреноида с прерывистой крахмальной обверткой. Молодые вегетативные клетки имели сферическую форму и в результате десмосхизиса формировали диады, тетрады и более сложные структуры. Формирование псевдонитей не наблюдалось. Отличительной особенностью штамма VKM Al-296 являлись малый размер клеток (до 6 мкм) и образование многоклеточных пакетов, окруженных видимым слоем внеклеточной слизи (Рис. 1).

При длительном хранении культуры (около 6 месяцев) наблюдали заметное изменение цвета биомассы с зеленого на красновато-коричневый. Данное изменение указывает на синтез вторичных каротиноидов – типичную реакцию каротиногенных водорослей на острую нехватку питательных веществ и дегидратацию.

18S рДНК анализ показал, что штамм VKM Al-296 относится к кладе Arenicolinia (Рис. 2а), формируя кластер с аутентичными штаммами, такими как *C. eremi* UTEX 1186, *C. arenicola* UTEX 1697 и C. *variabilis* UTEX 1600.

Внутри клады Arenicolinia штамм VKM Al-296 представляет собой независимую филогенетическую линию, которая не объединяется в кластер ни с одним из известных представителей. Генетические дистанции внутри клады варьировали от 0 до 1,2%. В частности, изучаемый штамм отличался на 0,1% от *C. eremi* UTEX 1186, на 0,9% от *C. arenicola* UTEX 1697 и на 0,4% от *C. variabilis* UTEX 1600. Для повышения филогенетического разрешения, помимо консервативного локуса 18S рДНК, был проанализирован вариабельный регион ITS2 (Рис. 2б). Однако это не улучшило кластеризацию внутри группы. Штамм VKM Al-296 образовал кластер с последовательностями водорослей, которые ранее были ошибочно идентифицированы как некультивируемые грибы. Между этими тремя последовательностями различий выявлено не было. Генетическая дистанция между VKM Al-296 и *C. eremi* UTEX 1186 составила 1,7%. Общий диапазон генетической

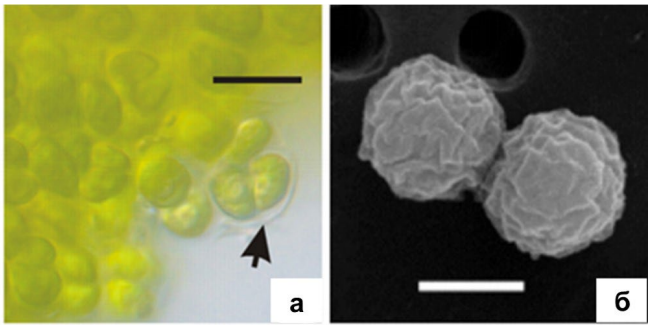

Рис.1. Фотографии световой (а) и сканирующей электронной (б) микроскопии штамма *Chlorosarcinopsis* sp. VKM Al-296. Черной стрелкой обозначена внеклеточная слизь. Шкала: а – 10 мкм; б – 3 мкм.

изменчивости внутри клады Arenicolinia составил от 0 до 12%. На основании установленного для ITS2 порога видового различия в 10% (Hoshina and Fujiwara, 2013; Hoshina, 2014) можно сделать вывод, что клада включает несколько еще не описанных видов. К сожалению, последовательности ITS2 для *C. arenicola* UTEX 1697 и *C. variabilis* UTEX 1600 не депонированы в GenBank. Сравнение вторичных структур ITS2 VKM Al-296 и *C. eremi* UTEX 1186 выявило лишь полукомпенсаторные замены нуклеотидных пар в спиралях I, II и IV (Рис. 3).

Полные компенсаторные замены нуклеотидных пар выявлены не были. На основании морфологических и генетических различий между VKM Al-296 и *C. eremi* UTEX 1186 исследуемый штамм был идентифицирован как *Chlorosarcinopsis* sp.

3.2. Ростовые характеристики штамма VKM Al-296 в условиях двухстадийного культивирования

Следует отметить, что активное накопление биомассы в культуре *Chlorosarcinopsis* sp. не прекращалось на протяжении всего эксперимента (Рис. 4а).

В первые два дня, помимо деления апланоспорами, наблюдалось размножение зооспорами. В утренние часы в культурах было обнаружено множество метаболичных двужгутиковых зооспор. К полудню зооспоры теряли подвижность и округлялись. Полового размножения не наблюдалось. Перевод культур микроводорослей на «красную» стадию путем добавления NaCl в питательную среду и увеличения освещения и температуры не вызывал визуально заметной гибели клеток, которая происходит у планктонных микроводорослей в аналогичных стрессовых условиях (Минюк и др., 2007). В новых условиях преобладающим способом размножения стал десмосхиз, приводящий к образованию многоклеточных плоских пакетов, окруженных слизью (Рис. 1).

Культура штамма VKM Al-296 на «зеленой» стадии росла быстрее, чем родственный штамм C. *eremi* VKM Al-132, культивируемый при естественном освещении (Данцюк и др., 2024). Несмотря на то, что оба штамма подвергались одинаковому стрессу, на стадии ВКГ накопление биомассы VKM

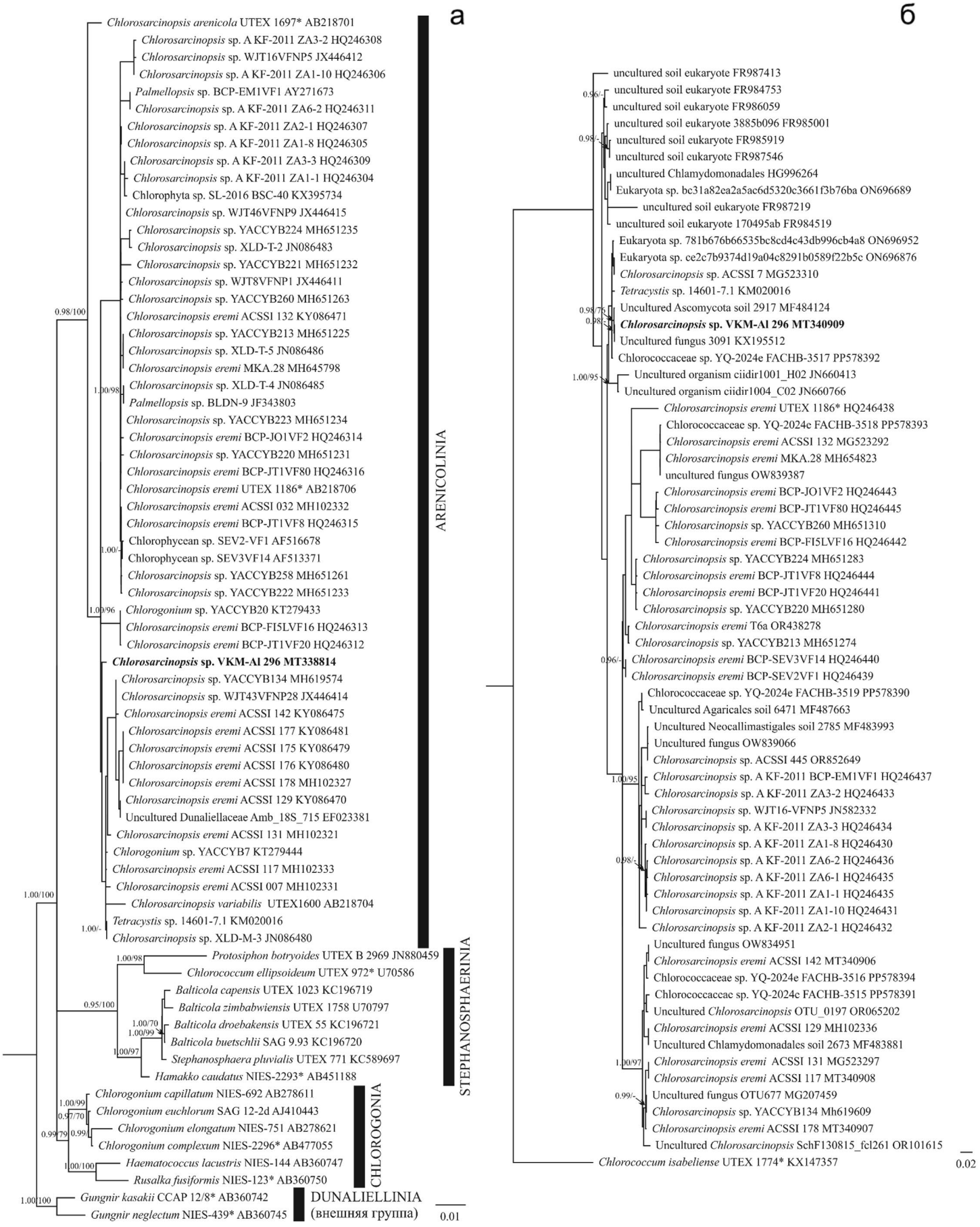

Рис.2. Байесовские филогенетические деревья штамма VKM Al-296, построенные на основе сравнения нуклеотидных последовательностей 18S рДНК (а) и ITS2 (б). Для обоих локусов оптимальной эволюционной моделью оказалась GTR + I + G. Статистическая поддержка узлов дерева указана в виде апостериорных вероятностей (PP) и значений бустрепа (BP); значения PP < 0.9 и BP < 70% не показаны.

Примечание: исследуемый штамм выделен полужирным шрифтом, звездочкой (*) отмечены аутентичные штаммы.

Al-296 происходило значительно медленнее, и, как следствие, его продуктивность на протяжении всего эксперимента (0,10 г/л/сут) была несколько ниже, чем у *C. eremi* VKM Al-132 (0,12 г/л/сут) (Данцюк и др., 2024).

3.3. Содержание пигментов в *Chlorosarcinopsis* sp. VKM Al-296 на протяжении культивирования

Содержание хлорофиллов у *Chlorosarcinopsis* sp. изменялось типичным для двухстадийного культивирования образом: на «зеленой» стадии, при достаточном количестве биогенных элементов в культуре, оно увеличивалось за счет активного деления клеток. К концу «зеленой» стадии содержание Хл*a* достигло 7,50 ± 0,12 мкг/мл (0,45 ± 0,01 % от СБ), Хл *b* – 3,34 ± 0,05 мкг/мл (0,20 ± 0,01 % от СБ) После стресса, в результате разрушения молекул хлорофиллов, их содержание снизилось на порядок (Рис. 5).

Напротив, содержание суммарных каротиноидов в культуре увеличилось за счет активного накопления биомассы (Рис. 6а). Массовая доля суммарных каротиноидов в сухой биомассе резко снизилась к четвертым суткам и оставалась относительно постоянной (0,3% от сухого веса) до конца эксперимента (Рис. 6б).

Увеличение соотношения Кар/Хл*a* с 0,33 до 0,64 к 9-м суткам (Рис. 6в) послужило ключевым критерием для оценки готовности культуры к переходу на стадию вторичного каротиногенеза. Визуально эта готовность проявилась в изменении цвета культуры с зеленого на болотно-желтый.

В течение «красной» стадии содержание Хл *a* в культуре снизилось в 10 раз, а содержание Хл *b* — в 5 раз. В то же время содержание суммарных каротиноидов увеличилось в 1,3 раза (Рис. 5а,в; Рис. 6а). Общая продуктивность каротиноидов, рассчитанная для всего эксперимента, составила 0,20 ± 0,01 мг/л/сут, что сопоставимо с показателем родственного штамма *C. eremi* VKM Al-132 (Данцюк и др., 2024).

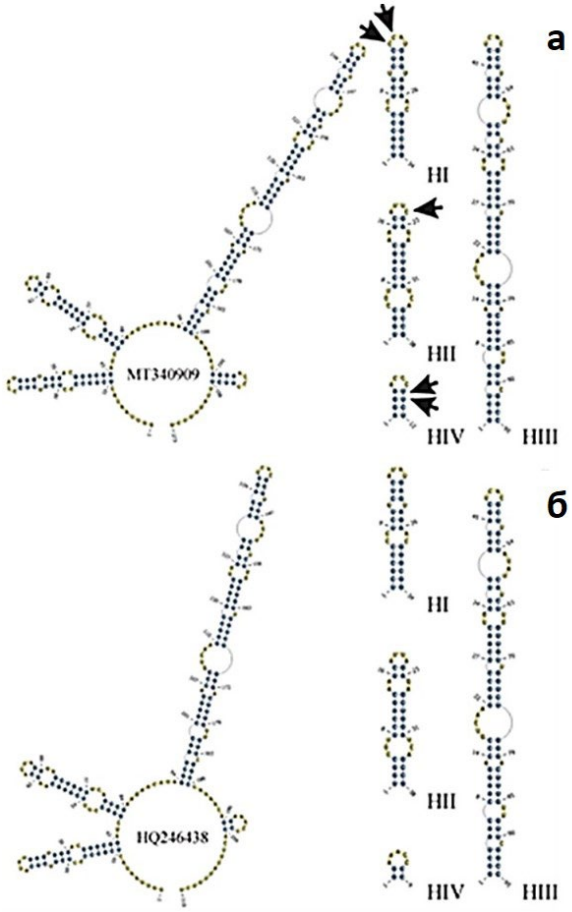

Рис.3. Вторичная структура ITS2 штаммов *Chlorosarcinopsis* sp. VKM Al-296 (а) и *C. eremi* UTEX 1186 (б): общая организация и спирали. Черными стрелками показаны полукомпенсаторные замены нуклеотидных пар.

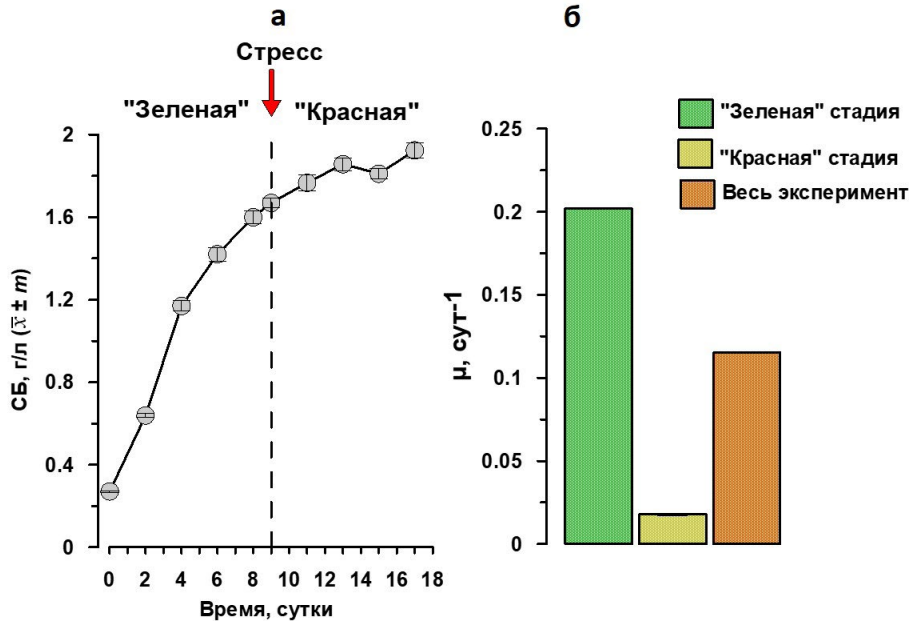

Рис.4. Динамика сухой биомассы (а) и удельная скорость роста (б) *Chlorosarcinopsis* sp. на «зеленой» и «красной» стадиях, а также на протяжении всего эксперимента.

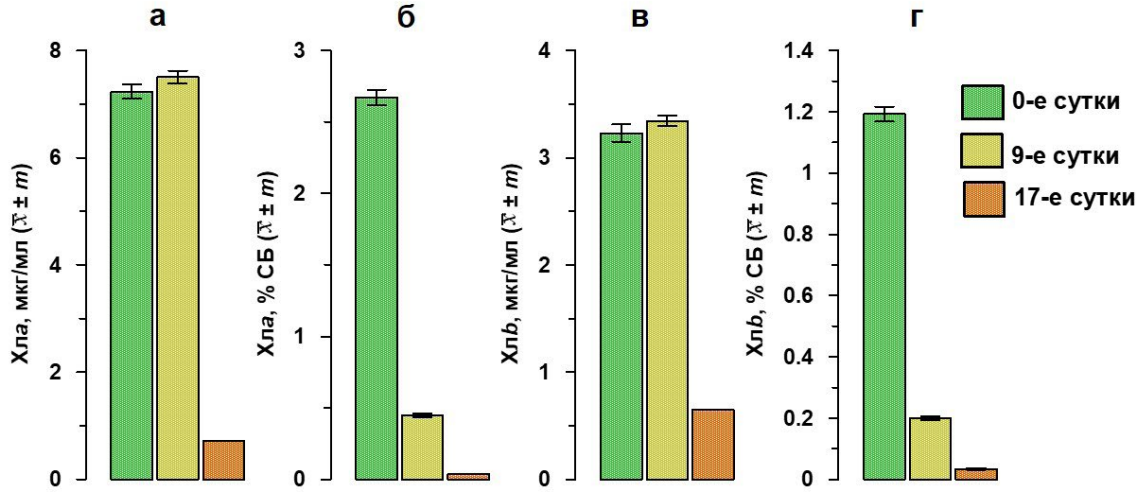

Рис.5. Содержание хлорофиллов в культуре (а, в) и сухой биомассе (б, г) *Chlorosarcinopsis* sp. в начале эксперимента (0-е сутки) и в конце «зеленой» (9-е сутки) и «красной» (17-е сутки) стадий.

3.4. Тонкослойная хроматография и состав каротиноидов

Хотя содержание суммарных каротиноидов в биомассе микроводорослей, начиная с 4-х суток «зеленой» стадии, оставалось относительно постоянным, качественный состав каротиноидов значительно изменился в течение последующего периода. Применение тонкослойной хроматографии позволило провести детальное сравнение профилей каротиноидов в конце «зеленой» и «красной» стадий.

В зеленых культурах доминирующим каротиноидом был лютеин при значительном количестве β-каротина и неоксантина (Рис. 7а, 8а). Однако после стрессирования культуры первичные каротиноиды, характерные для «зеленой» стадии, сменились вторичными каротиноидами (ККар), образующимися на «красной» стадии (Рис. 7б, 8б). К концу эксперимента содержание лютеина и β-каротина в клетках *Chlorosarcinopsis* sp. уменьшилось на порядок. В красных культурах преобладающими каротиноидами были кантаксантин, моноэфиры адониксантина и эфиры астаксантина (Рис. 8а, б).

В общей сложности эти фракции достигали 75–80 % от общего количества каротиноидов (Рис. 8а, б). Примечательно, что фракции эфиров астаксантина сами по себе составляли почти 35 % от общего количества каротиноидов. Каротиноидный профиль исследуемого штамма *Chlorosarcinopsis* sp. VKM Al-296 на «красной» стадии оказался сходным с профилем штамма *C. eremi* VKM Al-132, ранее представленным Данцюк и соавт. (2024).

Несмотря на относительно низкое содержание суммарных каротиноидов (приблизительно 0,3% от сухой биомассы), каротиноидный состав *Chlorosarcinopsis* sp. VKM Al-296 интересен содержанием ценных ККар, включая кантаксантин, а также эфиры адониксантина, адонирубина и астаксантина, которые в сумме составляют около 80% от суммарных каротиноидов.

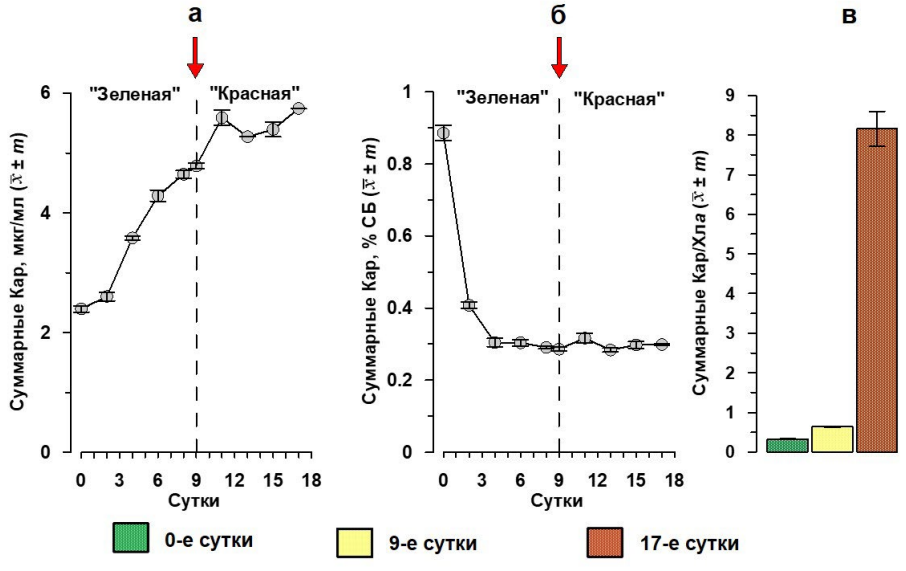

Рис.6. Содержание суммарных каротиноидов в культуре (а) и сухой биомассе (б) *Chlorosarcinopsis* sp., а также соотношение суммарных Кар/Хл*а* (в).

4. Обсуждение

Таксономия рода *Chlorosarcinopsis* имеет сложную и запутанную историю, начавшуюся в 1958 году (Herndon, 1958). Первоначально в род включали 21 вид, с *C. minor* в качестве типового. Со временем некоторые виды были переклассифицированы в роды *Neochlorosarcina*, *Desmotetra* и *Desmochloris*. Молекулярные исследования позднее показали, что род *Chlorosarcinopsis* является полифилетичным: его представители распределены по меньшей мере в две филогруппы – Arenicolinia (включая *C. arenicola*, *C. eremi* и *C. variabilis*) и Stephanosphaerinia (включая *C. minor*, *C. aggregata*, *C. bastropiensis* и *C. dissociata*) (Watanabe et al., 2006; Nakada et al., 2008). Поскольку голотип *C. minor* формирует независимую филогенетическую линию внутри клады Stephanosphaerinia, остальные группы не относятся к собственно роду *Chlorosarcinopsis* и должны быть описаны как новые роды, обладающие морфологией, сходной с *Chlorosarcinopsis*. Тем не менее, таксономия *Chlorosarcinopsis* до сих пор не разрешена, поскольку для некоторых видов (*C. angulosa*, *C. caeca* и *C. superba*) секвенирование еще не проведено, а для других отсутствует достаточный уровень генетического полиморфизма, особенно по более вариабельным локусам. Ключевой проблемой является выбор молекулярных маркеров для улучшения кластеризации филогруппы Arenicolinia. Разграничение видов на основе регионов 18S рДНК и ITS2 оказалось проблематичным, что указывает на возможную пригодность для этих целей пластидного гена *rbc*L.

Применение метода двухстадийной накопительной культуры к сарциноидным микроводорослям имеет свои особенности. Агрегация клеток в трехмерные кластеры не позволяет оценить состояние культуры по скорости деления клеток. Из-за деформации клеток внутри агрегатов размеры клеток искажаются. Таким образом, оценка продуктивных качеств *Chlorosarcinopsis* основывается исключительно на измерении содержания сухой биомассы

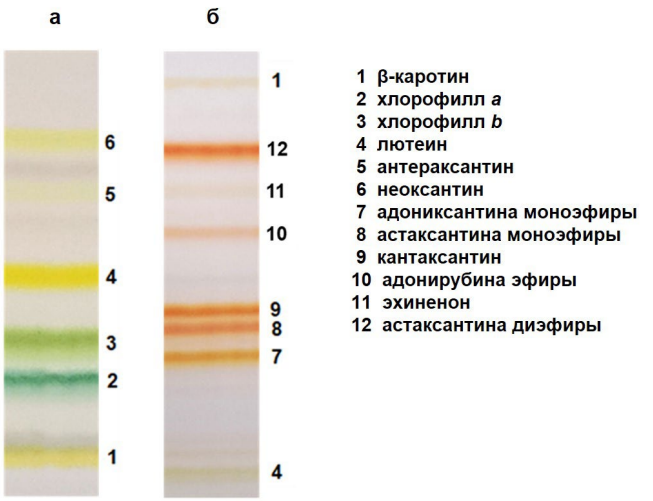

Рис.7. Тонкослойная хроматография *Chlorosarcinopsis* sp. в конце «зеленой» (а) и «красной» (б) стадий культивирования.

в культуре. Особенности динамики сухой биомассы определяются наличием слизистого матрикса (муцилажа), состоящего из сложных полисахаридных и белковых компонентов (Domozych and LoRicco, 2024). Везикулы муцилажа образуются внутри клетки в аппарате Гольджи, через поры в форме луковицы, а затем высвобождаются наружу, обволакивая клетки *Chlorosarcinopsis* и вызывая их агрегацию (Domozych and Rogers-Domozych, 1993). Образование многоклеточных скоплений в результате деления клеток, а также экранирующий эффект слизистого матрикса быстро ухудшают условия освещения, что отличает сарциноидные микроводоросли от планктонных видов. Поэтому барботирование (непрерывная аэрация) культур является необходимым условием для культивирования этих видов.

Ростовые характеристики изучаемого штамма отражают широкую экологическую устойчивость, характерную для почвенных микроводорослей.

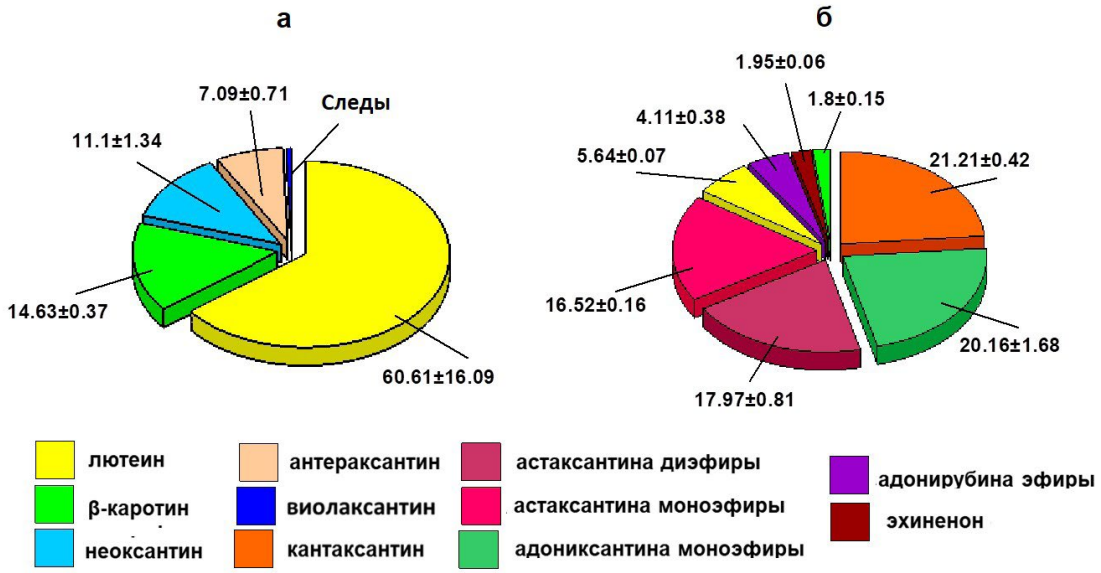

Рис.8. Состав каротиноидов *Chlorosarcinopsis* sp. на «зеленой» (а) и «красной» (б) стадиях эксперимента ($\bar{x}+m$).

Наблюдаемое более чем шестикратное увеличение содержания СБ в период «зеленой» стадии соответствует динамике роста микроводорослей в богатой питательными веществами питательной среде. Сохранение этой тенденции роста даже после воздействия стресса подтверждает наличие адаптационного механизма, позволяющего справляться с резкими изменениями критических факторов окружающей среды (Doppler et al., 2022; Nayana et al., 2022), что является отличительной чертой каротиногенных микроводорослей.

Продукционные характеристики *Chlorosarcinopsis* sp., адаптированного к лабораторным условиям культивирования, были сопоставимы с таковыми у ранее изученных экстремобионтов. В частности, средняя продуктивность по биомассе *Chlorosarcinopsis* sp. VKM Al-296 на «зеленой» стадии превысила показатели, зафиксированные для других штаммов, таких как *Bracteacoccus minor*, *Coelastrella rubescens* и *Chromochloris zofingiensis* (порядок Sphaeropleales), а также *Pseudospongiococcum protococcoides* (порядок Chlamydomonadales), продуктивность которых составила 0,08–0,09 г/л/сут (Чубчикова и Дробецкая, 2020).

Наблюдаемые изменения пигментного состава *Chlorosarcinopsis* sp. VKM Al-296 после перехода на «красную» стадию характерны для каротиногенных микроводорослей. Эти изменения подтверждают концепцию вторичного каротиногенеза как стратегии выживания, позволяющей клеткам сохранять жизнеспособность в стрессовых условиях за счет перестройки метаболизма.

Анализ состава каротиноидов подтвердил, что характерной чертой рода *Chlorosarcinopsis* в период активного роста («зеленой» стадии) является абсолютное преобладание лютеина, что согласуется с выводами Cherdchukeattisak et al. (2018). Вторым по значимости пигментом является β-каротин, содержание которого в культуре в конце «зеленой» стадии достигало 0,7 мг/л, что сопоставимо с 0,543 мг/л (Wongsnansilp et al., 2007).

На стадии ВКГ в профиле каротиноидов преобладали кантаксантин, моно- и диэфиры астаксантина, а также моноэфиры адониксантина. Доля эстерифицированного астаксантина в общем количестве каротиноидов (34,5%) согласуется с данными, представленными К. Чекановым (Chekanov, 2023) для *Chlainomonas rubra* (32–44,5 %).

Средняя продуктивность суммарных Кар за весь эксперимент ($0{,}20 \pm 0{,}01$ мг/л/сутки) оказалась сопоставима с таковой у *Chromochloris zofingiensis* и *Neochloris wimmeri* (0,21 и 0,22 мг/л/сут, соответственно) (Orosa et al., 2000).

Содержание астаксантина в сухой массе *Chlorosarcinopsis* sp. VKM Al-296 (0,11%) было сопоставимо с содержанием астаксантина у *Chromochloris zofingiensis* (0,17%) (Del Campo et al., 2004), *Coelastrella* sp. S6 (0,17–0,18 %) (Corato et al., 2022) и *Halochlorella rubescens* (0,12–0,18 %) (Chekanov, 2023).

Присутствие метаболических предшественников астаксантина, наряду с самим астаксантином, в каротиноидном профиле не снижает биологическую ценность красной биомассы и ее экстрактов. Кроме того, высокое содержание лютеина (60%) в зеленой биомассе делает этот штамм перспективным источником этого пигмента.

5. Заключение

Микроскопический и молекулярно-генетический анализ 18S рДНК подтвердил таксономическое положение штамма VKM Al-296 в пределах клады Arenicolinia. Анализ первичной и вторичной структур ITS2 позволил идентифицировать данный штамм как *Chlorosarcinopsis* sp.

Ростовые, физиологические и биохимические характеристики штамма *Chlorosarcinopsis* sp. VKM Al-296 в условиях двухстадийной накопительной культуры сопоставимы с ранее описанными характеристиками каротиногенных зеленых микроводорослей порядков Sphaeropleales и Chlamydomonadales в аналогичных условиях.

В составе каротиноидов «зеленых» клеток преобладает лютеин, тогда как «красные» клетки содержат смесь ценных кетокаротиноидов, включая кантаксантин и эфиры адониксантина и астаксантина. Сходство каротиноидного профиля *Chlorosarcionopsis* sp. с таковым у других представителей Sphaeropleales и Chlamydomonadales косвенно подтверждает предположение о сходных путях биосинтеза астаксантина у этих микроводорослей.

Штамм *Chlorosarcinopsis* sp. VKM Al-296 является потенциально перспективным кандидатом для дальнейших исследований, направленных на оптимизацию условий культивирования (температура, интенсивность света, снабжение питательными веществами и природа стресс-агента) с целью повышения роста биомассы на «зеленой» стадии и биосинтеза кетокаротиноидов на «красной» стадии. Успешное решение этой проблемы может открыть возможности для биотехнологического применения этого штамма в качестве продуцента лютеина или кетокаротиноидов.

Благодарности

Авторы выражают глубокую благодарность кандидату биологических наук Г.С. Минюк, научному консультанту Института биологии южных морей им. А.О. Ковалевского Российской академии наук, за помощь в анализе полученных данных и консультации по тексту статьи.

Данная работа выполнена в рамках государственного задания «Комплексное исследование механизмов функционирования морских биотехнологических комплексов с целью получения биологически активных веществ из гидробионтов» (проект № 124022400152-1). Морфологический и молекулярно-генетический анализы были выполнены при финансовой поддержке Министерства науки и высшего образования Российской Федерации (Госзадание №FMRM-2026-0015).

Конфликт интересов

Авторы заявляют об отсутствии конкурирующих интересов.

Список литературы

Андреева В.М. 1998. Почвенные и аэрофильные зеленые водоросли (Chlorophyta: Tetrasporales, Chlorococcales, Chlorosarcinales). Санкт-Петербург: Наука.

Голлербах М.М., Штина Э.А. 1969. Почвенные водоросли. Ленинград: Наука.

Данцюк Н.В., Чубчикова И.Н., Темралеева А.Д. и др. 2024. Морфофизиологические и биохимические характеристики сарциноидной микроводоросли *Chlorosarcinopsis eremi* (Chlorophyceae, Chlorophyta). Физиология растений 71(6): 820–829. DOI: 10.31857/S0015330324060159

Минюк Г.С., Терентьева Н.В., Дробецкая И.В. 2007. Сравнительная характеристика морфологических и физиолого-биохимических признаков трех штаммов *Haematococcus pluvialis* Flotow (Chlorophyta, Chlamydomonadales). Альгология 17(2): 148–159. DOI: 10.1615/INTERJALGAE.v9.i2.70

Темралеева А.Д., Миничева Е.В., Букин Ю.С. и др. 2014. Современные методы выделения, культивирования и идентификации зеленых водорослей (Chlorophyta). Кострома: Костромской печатный дом.

Чубчикова И.Н. 2012. Влияние состава среды на содержание вторичных каротиноидов у микроводоросли *Scotiellopsis rubescens* Vinatz. (Chlorophyceae). Морской экологический журнал 9(4): 95–101.

Чубчикова И.Н., Дробецкая И.В. 2020. Оценка антирадикальной активности вторичных каротиноидов у четырёх видов зёленых микроводорослей порядка Sphaeropleales в системе in vitro. Труды Карадагской научной станции им. Т.И. Вяземского - природного заповедника РАН 2(14): 66–78. DOI: 10.21072/eco.2021.14.07

Чубчикова И.Н., Дробецкая И.В., Данцюк Н.В. и др. 2022. Оптимизация метода фиксации пресноводных микроводорослей (Scenedesmaceae, Chlorophyta) для первичной идентификации с использованием сканирующей электронной микроскопии. Вопросы современной альгологии 1(28): 102–109. DOI: 10.33624/2311-0147-2022-1(28)-102-109

Чубчикова И.Н., Минюк Г.С., Дробецкая И.В. и др. 2009. Хлорококковые микроводоросли как потенциальный источник природных кето-каротиноидов. Экология моря 77: 77–83.

Bischoff H.W., Bold H.C. 1963. Some soil algae from enchanted rock and related algal species. Phycological Studies IV 6318:1–95.

Boussiba S. 2000. Carotenogenesis in the green alga *Haematococcus pluvialis*: cellular physiology and stress response. Physiologia Plantarum 108(2):111–117. DOI: 10.1034/j.1399-3054.2000.108002111.x

Britton G. 2008. TLC of carotenoids. In: Waksmundzka-Hajnos M., Sherma J., Kowalska T. (Eds), Thin Layer Chromatography in Phytochemistry. New York, CRC Press, pp. 543–573. DOI: 10.1201/9781420046786

Britton G., Liaaen-Jensen S., Pfander H. 2004. Carotenoids Handbook. Basel, Birkhäuser Verlag.

Byun Y., Han K. 2009. PseudoViewer3: generating planar drawings of large-scale RNA structures with pseudoknots. Bioinformatics 25(11): 1435–1437. DOI: 10.1093/bioinformatics/btp252

Caisová L., Marin B., Melkonian M. 2013. A consensus secondary structure of ITS2 in the Chlorophyta identified by phylogenetic reconstruction. Protist 164(4): 482–496. DOI: 10.1016/j.protis.2013.04.005

Chekanov K. 2023. Diversity and distribution of carotenogenic algae in Europe: A Review. Marine Drugs 21: 108. DOI: 10.3390/md21020108

Chelebieva E.S., Dantsyuk N.V., Chekanov K.A. et al. 2018. Identification and morphological-physiological characterization of astaxanthin producer strains of *Haematococcus pluvialis* from the Black Sea region. Applied Biochemistry and Microbiology 54(6): 639–648. DOI: 10.1134/S0003683818060078

Chen J., Liu L., Wei D. 2017. Enhanced production of astaxanthin by *Chromochloris zofingiensis* in a microplate-based culture system under high light irradiation. Bioresource technology 245: 518–529. DOI: 10.1016/j.biortech.2017.08.102

Cherdchukeattisak P., Fraser P.D., Purton S. et al. 2018. Detection and enhancement of ketocarotenoid accumulation in the newly isolated sarcinoid green microalga *Chlorosarcinopsis* PY02. Biology 7: 1–14. DOI: 10.3390/biology7010017

Coleman A.W. 2000. The significance of a coincidence between evolutionary landmarks found in mating affinity and a DNA sequence. Protist 151: 1–9. DOI: 10.1078/1434-4610-00002

Coleman A.W. 2003. ITS2 is a double-edged tool for eukaryote evolutionary comparisons. Trends in Genetics 19: 370–375. DOI: 10.1016/S0168-9525(03)00118-5

Coleman A.W. 2009. Is there a molecular key to the level of “biological species” in eukaryotes? A DNA guide. Molecular Phylogenetics and Evolution 50: 197–203. DOI: 10.1016/j.ympev.2008.10.008

Corato A., Le T.T., Baurain D. et al. 2022. A fast-growing oleaginous strain of *Coelastrella* capable of astaxanthin and canthaxanthin accumulation in phototrophy and heterotrophy. Life 12:334. DOI: 10.3390/life12030334

Darriba D., Taboada G.L., Doallo R. et al. 2012. jModelTest 2: more models, new heuristics and parallel computing. Nature Methods 9(8): 772. DOI: 10.1038/nmeth.2109

Del Campo J.A., Rodríguez H., Moreno J. et al. 2004. Accumulation of astaxanthin and lutein in *Chlorella zofingiensis* (Chlorophyta). Applied Microbiology and Biotechnology 64: 848–854. DOI: 10.1007/s00253-003-1510-5

Domozych D.S., LoRicco J.G. 2024. The extracellular matrix of green algae. Plant Physiology 194: 15–32. DOI: 10.1093/plphys/kiad384

Domozych D.S., Rogers-Domozych C. 1993. Mucilage processing and secretion in the green alga *Closterium* II. Ultrastructure and immunocytochemistry. Journal of Phycology 29: 659–667. DOI: 10.1111/j.0022-3646.1993.00659.x

Doppler P., Kriechbaum R., Käfer M. et al. 2022. *Coelastrella terrestris* for adonixanthin production: physiological characterization and evaluation of secondary carotenoid productivity. Marine Drugs 20(3): 175. DOI: 10.3390/md20030175

Egeland E.S., Garrido J.L., Clementson L. et al. 2011. Data sheets aiding identification of phytoplankton carotenoids and chlorophylls. In: Roy S., Llewellyn C., Egeland E.S. et al. (Eds.), Phytoplankton pigments: characterization, chemotaxonomy and applications in oceanography. Cambridge, pp. 665–822.

Fábregas J., Otero A., Maseda A. et al. 2001. Two-stage cultures for the production of astaxanthin from *Haematococcus pluvialis*. Journal of biotechnology 89(1): 65–71. DOI: 10.1016/S0168-1656(01)00289-9

Friedmann I., Ocampo-Paus R. 1965. A new *Chlorosarcinopsis* from the Negev Desert. Journal of Phycology 1(4): 185–191. DOI: 10.1111/j.1529-8817.1965.tb04581.x

Guiry M.D., Guiry G.M. 2025. AlgaeBase. World-wide electronic publication, National University of Ireland, Galway. URL: http://www.algaebase.org (Accessed: 24 November 2025).

Hall J.D., Fučíková K., Lo C. et al. 2010. An assessment of proposed DNA barcodes in freshwater green algae. Cryptogamie, Algologie 31(4): 529–555.

Henry L.E.A., Mikkelsen J.D., Møller B.L. 1983. Pigment and acyl lipid composition of photosystem I and II vesicles and of photosynthetic mutants in barley. Carlsberg Research Communications 48: 131–148. DOI: 10.1007/bf02906174

Herndon W. 1958. Studies on chlorosphaeracean algae from soil. American Journal of Botany 45(4): 298–308.

Hoshina R. 2014. DNA analyses of a private collection of microbial green algae contribute to a better understanding of microbial diversity. BMC Research Notes 7: 592. DOI: 10.1186/1756-0500-7-592

Hoshina R., Fujiwara Y. 2013. Molecular characterization of *Chlorella* cultures of the National Institute for Environmental Studies culture collection with description of *Micractinium inermum* sp. nov., *Didymogenes sphaerica* sp. nov., and *Didymogenes soliella* sp. nov. (Chlorellaceae, Trebouxiophyceae). Phycological Research 61: 124–132. DOI: 10.1111/pre.12010

Jeffers T.L., Roth M.S. 2021. Revealing mechanisms of algal astaxanthin production and bioengineering potential using multiomics. In: Ravishankar G.A., Ambati R.R. (Eds.), Global perspectives on Astaxanthin: from industrial production to food, health, and pharmaceutical applications. Cambridge, pp. 181–208. DOI: 10.1016/B978-0-12-823304-7.00010-60

Katana A., Kwiatowski J., Spalik K. et al. 2001. Phylogenetic position of *Koliella* (Chlorophyta) as inferred from nuclear and chloroplast small subunit rDNA. Journal of Phycology 37(3): 443–451. DOI: 10.1046/j.1529-8817.2001.037003443.x

Khani-Juyabad F., Mohammadi P., Zarrabi M. 2019. Comparative analysis of *Chlorosarcinopsis eremi* mitochondrial genome with some Chlamydomonadales algae. Physiology and Molecular Biology of Plants 25(5): 1301–1310. DOI: 10.1007/s12298-019-00696-y

Laroche C. 2022. Exopolysaccharides from microalgae and cyanobacteria: diversity of strains, production strategies, and applications. Marine Drugs 20(5): 336. DOI: 10.3390/md20050336

Lemoine Y., Schoefs B. 2010. Secondary ketocarotenoid astaxanthin biosynthesis in algae: a multifunctional response to stress. Photosynthesis Research 106: 155–177. DOI: 10.1007/s11120-010-9583-3

Lewis L.A., Lewis P.O. 2005. Unearthing the molecular phylodiversity of desert soil green algae (Chlorophyta). Systematic Biology 54(6): 936–947. DOI: 10.1080/10635150500354852

Lichtenthaler H.K. 1987. Chlorophylls and carotenoids: pigments of photosynthetic membranes. Methods in Enzymology 148: 350–382.

Malik S., Ashraf M.U.F., Shahid A. et al. 2022. Characterization of a newly isolated self-flocculating microalga *Bracteacoccus pseudominor* BERC09 and its evaluation as a candidate for a multiproduct algal biorefinery. Chemosphere 304: 135346. DOI: 10.1016/j.chemosphere.2022.135346

Marchenko M.M., Dorosh I.V., Cheban L.M. 2019. Induction of carotenogenesis in *Desmodesmus armatus* (Chod.) Hegew cultivated on the closed waterside from recirculating aquaculture system. Biotechnologia Acta 12(2): 46–55. DOI: 10.15407/biotech12.02.046

Minyuk G., Chelebieva E., Chubchikova I. et al. 2017. Stress-induced secondary carotenogenesis in *Coelastrella rubescens* (Scenedesmaceae, Chlorophyta), a producer of value-added keto-carotenoids. Algae 32(3): 245–259. DOI: 10.4490/algae.2017.32.8.6

Minyuk G., Dantsyuk N., Chelebieva E. et al. 2019. The effect of diverse nitrogen sources in the nutrient medium on the growth of the green microalgae *Chromochloris zofingiensis* in the batch culture. Marine Biological Journal 4: 41–52. DOI: 10.21072/mbj.2019.04.4.04

Minyuk G., Sidorov R., Solovchenko A. 2020. Effect of nitrogen source on the growth, lipid, and valuable carotenoid production in the green microalga *Chromochloris zofingiensis*. Journal of Applied Phcology 32: 923. DOI: 10.1007/s10811-020-02060-0

Minyuk G.S., Chelebieva E.S., Chubchikova I.N. 2014. Secondary carotenogenesis of the green microalga *Bracteacoccus minor* (Chodat) Petrova (Chlorophyta) in a two-stage culture. International Journal on Algae 16(4): 354–368.

Minyuk G.S., Solovchenko A.E. 2018. Express analysis of microalgal secondary carotenoids by TLC and UV-Vis spectroscopy. In: Barriero C., Barriero J.-L. (Eds.), Microbial Carotenoids: Methods and Protocols. New York, pp. 73–95. DOI: 10.1007/978-1-4939-8742-9

Nair A., Ahirwar A., Singh S. et al. 2023. Astaxanthin as a king of ketocarotenoids: structure, synthesis, accumulation, bioavailability and antioxidant properties. Marine Drugs 21(3): 176. DOI: 10.3390/md21030176

Nakada T., Misawa K., Nozaki H. 2008. Molecular systematics of Volvocales (Chlorophyceae, Chlorophyta) based on exhaustive 18S rRNA phylogenetic analyses. Molecular Phylogenetics and Evolution 48: 281–291. DOI: 10.1016/j.ympev.2008.03.016

Nayana K., Sudhakar M.P., Arunkumar K. 2022. Biorefinery potential of *Coelastrella* biomass for fuel and bioproducts—a review. Biomass Conversion and Biorefinery. DOI: 10.1007/s13399-022-02519-9

Orosa M., Torres E., Fidalgo P. et al. 2000. Production and analysis of secondary carotenoids in green algae. Journal of Applied Phcology 12: 553–556.

Remias D., Pichrtova M., Pangratz M. et al. 2016. Ecophysiology, secondary pigments and ultrastructure of *Chlainomonas* sp. (Chlorophyta) from the European Alps compared with *Chlamydomonas nivalis* forming red snow. Microbiology Ecology 92(4): fiw030. DOI: 10.1093/femsec/fiw030

Rodriguez-Amaya D.B. 2001. A guide to carotenoid analysis in foods. Washington: ILSI Press.

Saito M., Watanabe H., Sasaki M. et al. 2023. Coproduction of lipids and carotenoids by the novel green alga *Coelastrella* sp. depending on cultivation conditions. Biotechnology Reports 37: e00769. DOI: 10.1016/j.btre.2022.e00769

Seibel P.N., Müller T., Dandekar T. et al. 2006. 4SALE – a tool for synchronous RNA sequence and secondary structure alignment and editing. BMC Bioinformatics 7: 498. DOI: 10.1186/1471-2105-7-498

Solovchenko A. 2013. Physiology and adaptive significance of secondary carotenogenesis in green microalgae. Russian Journal of Plant Physiology 60(1): 1–13. DOI: 10.1134/S1021443713010081

Solovchenko A., Merzlyak M., Khozin-Goldberg I. et al. 2010. Coordinated carotenoid and lipid syntheses induced in *Parietochloris incisa* (Chlorophyta, Trebouxiophyceae) mutant deficient in Δ5 desaturase by nitrogen starvation and high light. Journal of Phycology 46: 763–772. DOI: 10.1111/j.1529-8817.2010.00849.x

Vasistha S., Khanra A., Rai M.P. 2021. Influence of microalgae-ZnO nanoparticle association on sewage wastewater towards efficient nutrient removal and improved biodiesel application: An integrated approach. Journal of Water Process Engineering 39: 101711. DOI: 10.1016/j.jwpe.2020.101711

Vonshak A. 1985. Microalgae: Laboratory growth techniques and outdoor biomass production. In: Coombs J., Hall D., Long S. et al. (Eds.), Techniques in Bioproductivity and Photosynthesis. Oxford: Pergamon Press, pp. 188–203. DOI: 10.1016/B978-0-08-031999-5.50025-X

Watanabe S., Mitsui K., Nakayama T. et al. 2006. Phylogenetic relationships and taxonomy of sarcinoid green algae: *Chlorosarcinopsis*, *Desmotetra*, *Sarcinochlamys* gen. nov.,

Neochlorosarcina, and *Chlorosphaeropsis* (Chlorophyceae, Chlorophyta). Journal of Phycology 42: 679–695. DOI: 10.1111/j.1529-8817.2006.00196.x

White T.J., Bruns T., Lee S. et al. 1990. Amplification and direct sequencing of fungal ribosomal RNA genes for phylogenetics. In: Innis M.A., Gelfand D.H., Sninsky J.J. et al. (Eds.), PCR protocols. San Diego: Academic Press, pp. 315–324.

Wongsnansilp T., Tansakul P., Arunyanart M. 2007. Factors affecting growth and betacarotene content of *Chlorosarcinopsis* sp. (PSU/CHL20) in batch culture. Kasetsart J (Nat Sci) 41(1):153–157.

Wood A.M., Everroad R.C., Wingard L.M. 2005. Measuring growth rates in microalgal cultures. In: Andersen R.A. (Ed.), Algal Culturing Techniques. Elsevier Academic Press, pp. 269-285. DOI: 10.1016/B978-012088426-1/50019-6

Original Article

LIMNOLOGY FRESHWATER BIOLOGY

Morphological and genetic features of crustaceans *Artemia parthenogenetica* and *A. tibetiana* (Crustacea, Anostraca) in different-type hypersaline lakes in the south of Western Siberia

Bezmaternykh D.M.*, Vesnina L.V., Lassyi M.V., Vesnin Yu.A., Ryabova K.K.

Institute for Water and Environmental Problems, Siberian Branch of the Russian Academy of Sciences, 1, Molodezhnaya St., Barnaul, 656038, Russia

ABSTRACT. We studied modern morphological features of parthenogenetic and bisexual *Artemia* populations from 10 different-type hypersaline lakes in the south of Western Siberia (Altai Krai). DNA barcoding of these populations revealed two *Artemia* species: *Artemia parthenogenetica* Barigozzi, 1974 and *A. tibetiana* (Abatzopoulos et al., 1998). The studies were conducted monthly from July to September 2025. Principal component analysis indicated differences in the hydrochemical composition of brine (water) of lakes inhabited by parthenogenetic and bisexual *Artemia* populations. Comparative analysis of morphological features suggested that females of *A. parthenogenetica* and *A. tibetiana* significantly differed in mean values (14 of 16 traits). Cluster analysis of 12 plastic and 4 meristic characters of *A. parthenogenetica* females demonstrated splitting of its population into three groups with different structural features of the furca: length (*fl*), number (*sf*), and length of setae (*sl*). The Spearman correlation index establishes significant statistical correlations between the morphological features of *A. parthenogenetica* and *A. tibetiana* and main environmental factors, i.e. salinity and water temperature.

Keywords: Altai Krai, salt lakes, branchiopods, populations, morphometric characteristics, salinity, environmental factors, DNA barcoding

For citation: Bezmaternykh D.M., Vesnina L.V., Lassyi M.V., Vesnin Yu.A., Ryabova K.K. Morphological and genetic features of crustaceans *Artemia parthenogenetica* and *A. tibetiana* (Crustacea, Anostraca) in different-type hypersaline lakes in the south of Western Siberia // Limnology and Freshwater Biology. 2026. - № 2. - P. 103-129. DOI: 10.31951/2658-3518-2026-A-2-103

1. Introduction

Artemia populations are found in natural and artificial salt waterbodies of tropical, subtropical, and temperate climate zones (Persoone and Sorgeloos, 1980). New habitats of this crustacean are discovered annually. However, some previously described populations of crustaceans have disappeared because of significantly increasing/decreasing water salinity (Vanhaecke et al., 1987; Triantaphyllidis et al., 1994; Van Stappen, 2002). Physiological adaptations of branchiopods to high salinity provide an effective ecological protection from predators due to much better osmoregulation, as well as the ability to synthesize respiratory pigments under low oxygen concentrations in water and to produce diapausing cysts under adverse environmental conditions (Vanhaecke et al., 1987; Van Stappen et al., 2024).

Widespread distribution of *Artemia* in isolated habitats characterized by varying ecological conditions led to the existence of numerous geographically separated and genetically distinct populations of a single species (Triantaphyllidis et al., 1994). In particular, the presence of parthenogenetic *Artemia* populations with diploid (2n), triploid (3n), tetraploid (4n) and pentaploid (5n) sets of chromosomes resulted in significant genotypic and phenotypic diversity. Some of these characteristics (nutritional value of cysts and nauplii) are subject to inter-seasonal and inter-annual variability. Other traits (cyst diameter, growth rate, and resistance to high temperatures) are relatively constant, indicating long-term adaptation to the specific living conditions of *Artemia* (Triantaphyllidis et al., 1994; Van Stappen, 2002).

Currently, the genus *Artemia* Leach, 1819 includes the following species distributed in Eurasia (Pilla and

*Corresponding author. E-mail address: bezmater@iwep.ru (D.M. Bezmaternykh)

Received: January 14, 2026;
Accepted after revised: April 07, 2026;
Available online: April 24, 2026

Beardmore, 1994; Beardmore et al., 1994; Browne and Bowen, 1991; Sainz-Escudero et al., 2021): *A. salina* (Linnaeus, 1758): Lymington, England (now extinct), the Mediterranean (formerly *A. tunisiana* (Bowen and Sterling, 1978); *A. urmiana* (Gunther, 1990): Iran (Lake Urmia), the Crimea; *A. sinica* (Cai, 1989): central and eastern China; *A. tibetiana* (Abatzopoulos et al., 1998): Lake Lagkor Ko, Tibet, China; *A. sorgeloosi* (Asem et al., 2023): Haiyan Lake, Tibet, China; and *Artemia amati* (Asem et al., 2023): Kazakhstan. Numerous parthenogenetic populations of *Artemia* found in Europe, Africa, Asia, and Australia are usually grouped under the species name *A. parthenogenetica* (Barigozzi, 1974; Bowen and Sterling, 1978).

The aim of the work was to study the modern morphological and genetic characteristics of parthenogenetic and bisexual populations in different-type hypersaline lakes in the south of Western Siberia.

2. Materials and methods

The study involved 1,021 *Artemia* specimens from 10 different-type hypersaline lakes in the south of Western Siberia (Fig. 1). Sampling for morphometric analysis was conducted monthly from July to September 2025 according to the generally accepted methods and recommendations (Manual…, 1992). Samples were collected manually using a hydrobiological net. The material was fixed in 4% formalin. Samples were processed in a Petri dish under an MBS-10 binocular microscope equipped with an ocular-micrometer. A total of 720 female adult crustaceans (561 specimens of *A. parthenogenetica* and 159 specimens of *A. tibetiana*), including 301 males of *A. tibetiana*, were measured. During sampling in the lakes with parthenogenetic *Artemia* populations, males were recorded only sporadically, which is insufficient for statistical analysis.

Brine temperature was measured using a hydrological thermometer in the surface layer (at a depth of at least 0.2 m), and brine salinity–by an optical device, a portable ATAGO refractometer (Kenco Instruments Co., USA), in the surface layer (at a depth of at least 0.2 m). Water samples for hydrochemical analysis–anions and cations (CO_3^{2-}, HCO_3^-, Cl^-, SO_4^{2-}, Ca^{2+}, Mg^{2+}, and $Na^+ + K^+$)–were collected by standard methods (Manual..., 2009; 2012) from the surface water layer (1.5 L in plastic containers). Hydrochemical samples were processed in the Laboratory of Biogeochemistry at Institute for Water and Environmental Problems, Siberian Branch of the Russian Academy of Sciences (IWEP SB RAS).

Based on the analysis of images from the "Resurs-P No. 4" and "Resurs-P No. 5" satellites, the water surface areas of the study hypersaline lakes were estimated for the period from April to October 2025. Images were taken in cloudless weather (cloud level <10%). For analysis, we employed the open-source Roscosmos Geoportal (URL: https://gptl.ru/), while, for depth measurements, we used a hydrological sounding. Some results of measurements and chemical analysis are given in Table 1.

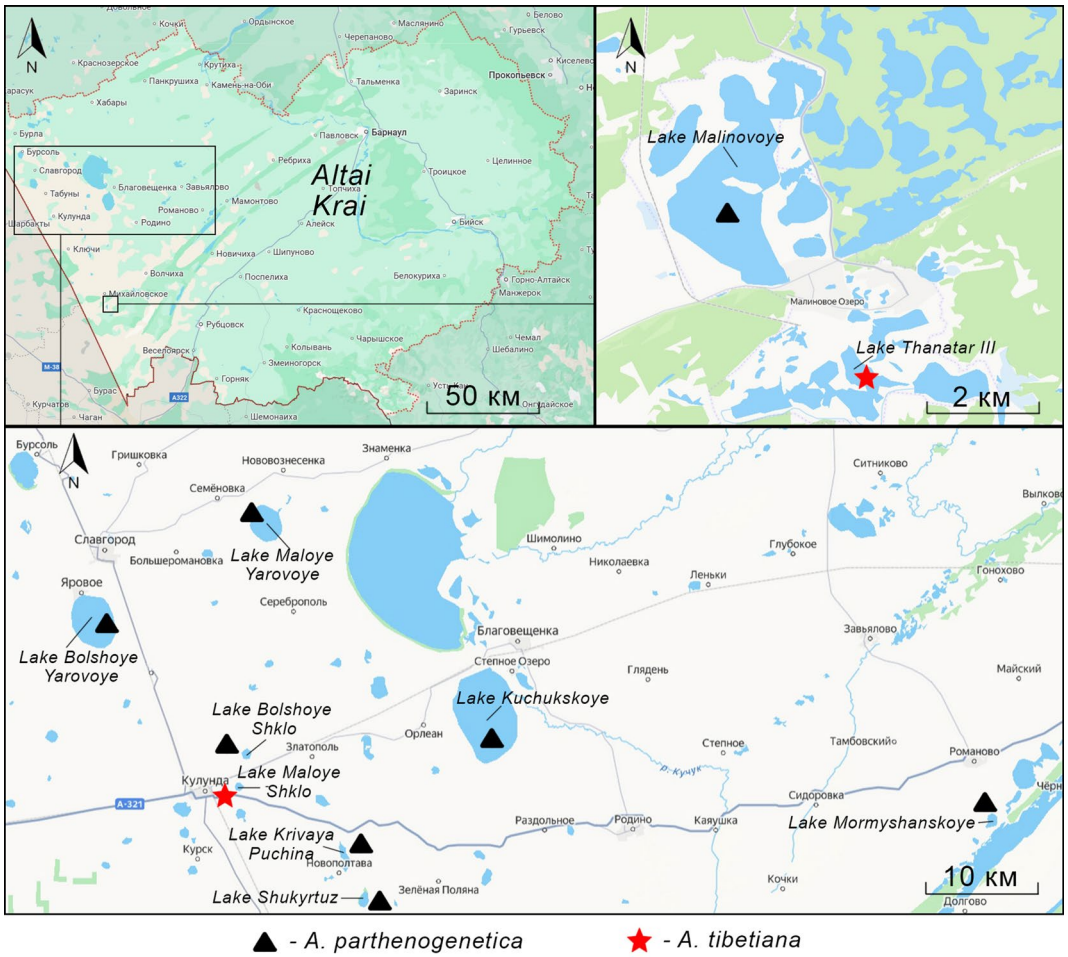

Fig.1. Study lakes and distribution of parthenogenetic and bisexual populations of *Artemia* in the south of Western Siberia.

Table 1. Main study characteristics of hypersaline lakes in the south of Western Siberia in 2025.

Lake	Geographic coordinates	Area (min–max), km ^{2}	Maximum depth (lim), m	Salinity (min–max), g/L
Bolshoye Shklo	52°37′53″ N 79°04′02″ E	3.4–3.6	1.8–2.0	65.7–91.3
Bolshoye Yarovoye	52°52′09″ N 78°36′53″ E	73.0–74.2	7.3–10.5	140.0–160.0
Krivaya Puchina	52°26′33″ N 79°21′31″ E	6.2–7.4	0.4–0.5	101.2–150.0
Kuchukskoye	52°42′06″ N 79°46′40″ E	174.6–175.7	2.4–2.9	210.9–250.0
Malinovoye	51°42′10″ N 79°44′49″ E	9.3–11.1	1.5–1.7	160.0–188.2
Maloye Shklo	52°34′20″ N 79°02′47″ E	2.1–2.5	1.1–1.3	45.9–140.0
Maloye Yarovoye	53°02′39″ N 79°07′37″ E	36.4–37.1	4.0–4.9	150.0–180.0
Mormyshanskoye	52°30′39″ N 81°16′25″ E	5.9–7.9	0.9–1.2	150.0–220.0
Thanatar III	51°39′18″ N 79°47′ 39″ E	0.8–1.0	1.6–1.9	100.0–161.6
Shukyrtuz	52°22′06″ N 79°24′54″ E	5.2–5.5	0.7 –0.9	177.6–220.0

For morphometric analysis, **plastic** characters were measured in adult females and males of *Artemia* (Fig. 2): *tl*–total body length, *al*–abdomen length, *aw*–abdomen width, *de*–distance between eyes, *ed*–eye diameter, *la*–first antenna length, *hw*–head width, *cl*–cephalothorax length, *fl*–length of furcal branch, *sl*–length of setae on furca; in males: *ml*–second antenna length, *mw*–second antenna width, as well as **meristic** characters: *sf*–number of setae on furca, ratio of cephalothorax to abdomen length (*cl/al*), ratio of abdomen to body length (*al/tl*), and ratio of furca to abdomen length (*fl/al*) (Vesnina and Vasilyeva, 2019).

Species identification of *Artemia* was implemented through DNA barcoding. The material for DNA identification was fixed in 96% ethyl alcohol and analyzed at the Department of Biotechnology of the South Siberian Botanical Garden of Altai State University. Sequencing of 30 samples was performed in two to four replicates for each lake. Total DNA from the sample was isolated using the Diamond DNA Plant kit (Altaibiotech LLC, Russia) according to the manufacturer's protocol. For species identification in the samples, a fragment of the mtDNA COI gene was amplified using polymerase chain reaction (PCR) and primer pairs–forward LCO-1490 (GGTCAACAAATCATAAAGATATTGG) and reverse HCO-2198 (TAAACTTCAGGGTGACCAAAAAATCA) (Folmer et al., 1994). PCR was conducted in a 50 μL reaction mixture with the commercial BioMaster HS-TaqPCR-Color (2×) amplification kit (Biolabmix, Russia) in the following composition per sample: 25 μL

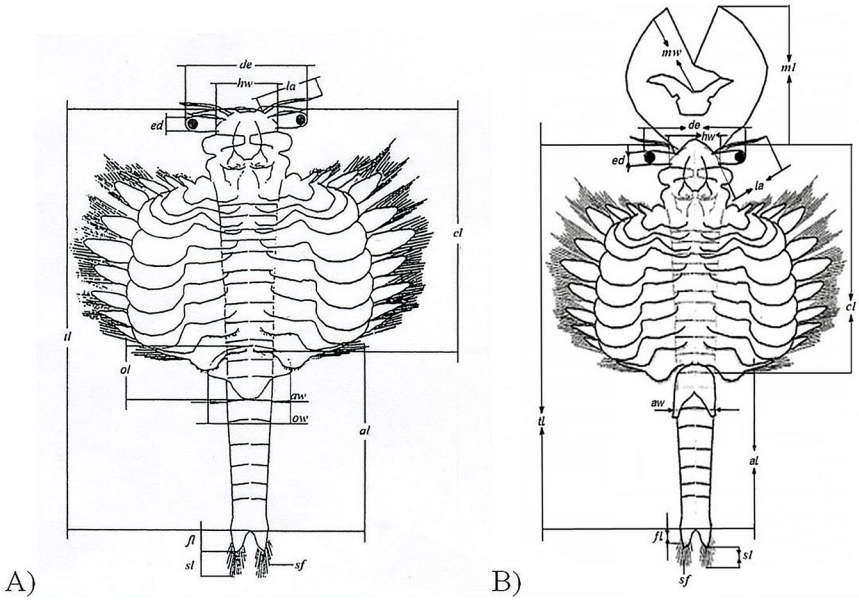

Fig.2. Scheme of morphometric measurements in *Artemia* females (A) and males (B). (Vesnina and Vasilyeva, 2019): *tl*–total body length, *al*–abdomen length, *aw*–abdomen width, *de*–distance between eyes, *ed*–eye diameter, *la*–length of the first antenna, *hw*–head width, *cl*–cephalothorax length, *fl*–length of furcal branch, *sf*–number of setae on furca, *sl*–length of setae on furca; *ml*–length of the second antenna, *mw*–width of the second antenna.

of ready-made PCR mixture (Biolabmix, Novosibirsk), 21 μL of $_{dd}H_2O$, 1 μL of 10 μM of the corresponding primers, 2 μL of DNA.

Amplification was carried out in a MyCycler thermocycler (Bio-Rad, USA) using the following cycles: an initial denaturation cycle at 94°C for 60 sec, followed by 35 cycles at 94°C for 30 sec, primer annealing at 45°C for 90 sec, extension at 72°C for 60 sec, and final extension at 72°C for 300 sec (Lobo et al., 2013).

Amplification products were separated on a 1.3% agarose gel in a horizontal electrophoresis chamber in TAE-buffer at 220 V using ethidium bromide, and their visualization was performed under transmitted UV light using the Gel Doc XR gel documentation system (Bio-Rad, USA). To determine the length of amplified fragments, we used DNA markers (Biolabmix, Novosibirsk).

MAXLIFE Magnet DNA magnetic particles (MBM-Diagnostics, Russia) were used for purification of PCR-products before sequencing with an ABI Prism 3130xl automated sequencer in accordance with the manufacturer's protocol. Final sequences were analyzed via the MEGA 11 program (Tamura et al., 2021).

To visualize the similarity of the nucleotide sequences of the mtDNA COI gene fragment in the studied samples, we constructed a dendrogram with all sequences of the species *A. parthenogenetica* and *A. tibetiana*, which was published in the GenBank database, NCBI (National Center for Biotechnology Information). Duplicate haplogroups were removed from the dendrogram. Sequences of closely related species, *A. urmiana*, served as an outgroup. Sequences were aligned by the MUSCLE algorithm (Edgar, 2004) implemented in the MEGA X program (Kumar et al., 2018). For selecting the nucleotide substitution model and constructing the dendrogram, the IQ-TREE web server with a bootstrap parameter value of 10,000 was employed. The dendrogram construction strategy was Maximum Likelihood (ML).

For statistical processing of the obtained data, we applied MS Excel 2013 and PAST 4 (Hammer et al., 2001) software packages, including such methods as Kruskal-Wallis test (*H*), Spearman's rank correlation coefficient (r), cluster analysis, and linear approximation with the coefficient of determination (R^2).

3. Results

3.1. Variability of morphometric traits in females of *A. parthenogenetica* and *A. tibetiana* in different lakes

In terms of water salinity, all studied lakes are hypersaline water bodies. This indicator ranges from 45.9 (Maloye Shklo) to 210.9 g/L (Kuchukskoye). In terms of predominant anions, they are classified as hydrocarbonate (Tanatar III), sulfate (Mormishanskoye), and chloride (Bolshoye Shklo, Bolshoye Yarovoye, Krivaya Puchina, Kulundinskoye, Kuchukskoye, Malinovoye, Maloye Shklo, Maloye Yarovoye, and Shukyrtuz) (Nikonorov, 1989).

Waters in the study lakes of sulfate and chloride types are neutral in terms of the hydrogen potential, i.e. slightly alkaline (pH = 7.5–8.8), and waters of the bicarbonate type–alkaline (pH = 9.8).

Water temperature in July fluctuated from 19.1 (Tanatar III) up to 27.0°C (Maloye Yarovoye); in August–from 16.6 (Tanatar III) to 26.8°C (Kuchukskoye); and in September–from 11.7 (Kuchukskoye) to 18.3°C (Krivaya Puchina).

In 2025, DNA barcoding (Table 2) allowed us to identify two species of *Artemia* in the stud-

Table 2. Results of DNA barcoding of *Artemia* spp. from lakes in the south of Western Siberia.

Lake	GenBank No. NCBI	% compliance	% sequence overlap
A. parthenogenetica			
Bolshoye Shklo	MT791796.1	96.83–100	99
Bolshoye Yarovoye	PV017298.1	99.70	94
	MT791796.1	100	91
	MT791710.1	99.85–100	100
Krivaya Puchina	PV017298.1	99.70	100
	MT791796.1	100	99
Kulundinskoye	MT791796.1	100	99
	MT791710.1	99.70	100
Kuchukskoye	MT791796.1	99.85	99
Malinovoye	MT791796.1	99.85–100	99
	MT791710.1	99.85	100
Maloye Yarovoye	MT791796.1	99.85	99
	MT791710.1	99.70	100
Mormyshanskoye	MT791796.1	99.55–100	91–99
Shukyrtuz	MT791796.1	99.85–100	99
A. tibetiana			
Maloye Shklo	MT 791825.1	98.94–99.25	99–100
Thanatar III	MT 791825.1	99.40–99.70	99

ied hypersaline lakes in the south of Western Siberia (Fig. 3): *A. parthenogenetica* (Bolshoye Shklo, Bolshoye Yarovoye, Krivaya Puchina, Kuchukskoye, Malinovoye, Maloye Yarovoye, Mormyshanskoye, and Shukyrtuz) and *A. tibetiana* (Maloye Shklo, and Tanatar III). *A. tibetiana* was previously determined as *Artemia* sp. (Vesnina et al., 2025).

The dendrogram of samples' similarity was constructed through the UPGMA method: unweighted pair group method using arithmetic averages with a bootstrap parameter value of 10,000 (Fig. 3). The dendrogram presents a combination of the studied samples from lakes Bolshoye Shklo, Bolshoye Yarovoye, Krivaya Puchina, Kulundinskoye, Kuchukskoye, Malinovoye, Maloye Yarovoye, Mormyshanskoye, and Shukyrtuz with *A. parthenogenetica* samples. Specimens from lakes Maloye Shklo and Tanatar III are combined in a separate clade with *A. tibetiana*.

Previous research suggests that *A. tibetiana* is a polyphyletic group (Maccari et al., 2013; Eimanifar et al., 2014; Asem et al., 2020). The studied populations from lakes in the south of Western Siberia belong to the western lineage (Pang et al., 2024). Sequences of the bisexual species, *A. sorgeloosi*, form a clearly differentiated clade, thereby confirming its species status (Asem et al., 2023). Chinese *A. sinica* and American *A. franciscana* occupy a terminal position, also forming separate clusters.

According to our data, *A. parthenogenetica* was found in seven chloride lakes and in one sulfate lake, while *A. tibetiana* was detected in one chloride lake and one hydrocarbonate lake.

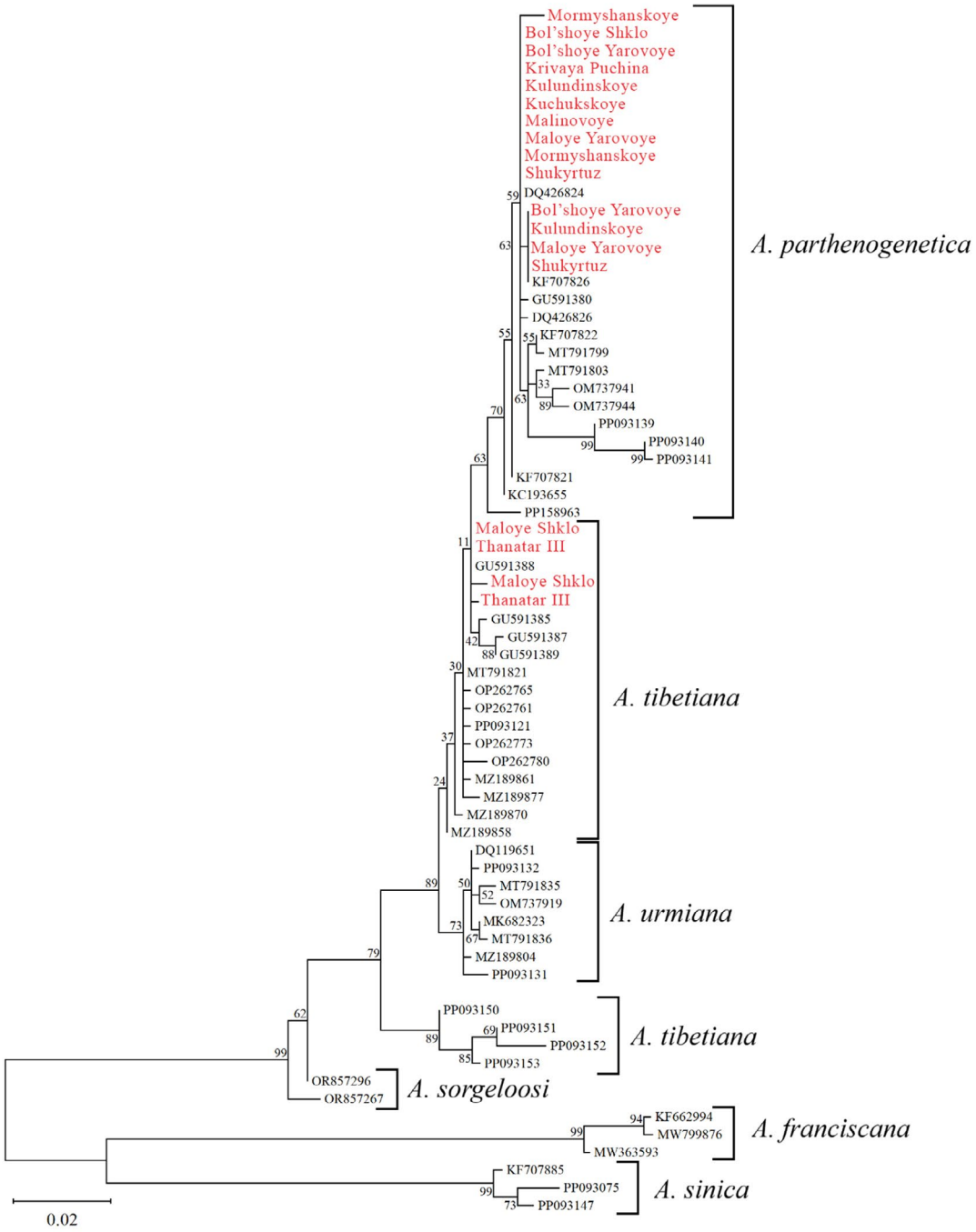

Fig.3. Dendrogram of the studied *Artemia spp.* populations and genetically similar samples from NCBI based on the COI gene fragment. Populations from lakes in the south of Western Siberia studied in 2025 are highlighted in red.

In 2025, the most variable indicators of furcal characters in *A. parthenogenetica* were identified in Lake Kuchukskoye: furca length (*fl*)–40.94%, number of setae on furcae (*sf*)–31.15%, and length of setae on furcae (*sl*)–34.24%.

The *A. parthenogenetica* crustaceans from Lake Bolshoye Yarovoye have the highest average values of morphometric parameters (7 out of 14 traits): total body length (*tl*), cephalothorax length (*cl*), abdomen width (*aw*), distance between eyes (*de*), eye diameter (*ed*), length of the first antenna (*la*), and head width (*hw*) (Table 3, Fig. 4). The lowest average values of morphometric parameters (12 out of 14) were recorded in lakes Bolshoye Shklo, Kuchukskoye, and Shukyrtuz: total body length (*tl*), abdomen length (*al*), cephalothorax length (*cl*), ratio of cephalothorax length to abdomen length (*cl/al*), ratio of abdomen length to body length (*al/tl*), distance between eyes (*de*), length of the first antenna (*la*), head width (*hw*), furcae length (*fl*), number of setae on furcae (*sf*), length of setae on furcae (*sl*), and ratio of furcae length to abdomen length (*fl/al*).

Crustaceans of Tanatar III demonstrate the highest average values of morphometric features in *A. tibetiana* (12 out of 14 signs); the smallest–in crustaceans of Lake Maloye Shklo: total body length (*tl*), cephalothorax length (*cl*), abdomen length (*al*), abdomen width (*aw*), distance between eyes (*de*), eye diameter (*ed*), length of first antenna (*la*), head width (*hw*), furcae length (*fl*), number of setae on furcae (*sf*), length of setae on furcae (*sl*), and ratio of furcae length to abdomen length (*fl/al*).

3.2. Variability of morphometric features in males of *A. tibetiana* in different lakes

The results of a comparison of plastic and meristic characters of *A. tibetiana* mature males reveal that the specimens from Lake Tanatar III are taller than those from Lake Maloye Shklo in body length (*tl:* $H = 95.14$, $p < 0.01$), cephalothorax (*cl:* $H = 89.28$, $p < 0.01$), length (*al:* $H = 56.28$, $p < 0.01$) and width (*aw:* $H = 73.21$, $p < 0.01$) of abdomen, length of the second antenna (*ml:* $H = 103.50$, $p < 0.01$), maximum (*mw* (*max*)*:* $H = 91.26$, $p < 0.01$) and minimum length of the second antenna (*mw* (*min*)*:* $H = 88.09$, $p < 0.01$), distance between eyes (*de:* $H = 95.85$, $p < 0.01$), eye diameter (*ed:* $H = 92.91$, $p < 0.01$), length of the first antenna (*la:* $H = 92.02$, $p < 0.01$), head width (*hw:* $H = 103.50$, $p < 0.01$), length of furcae (*fl:* $H = 92.70$, $p < 0.01$), length of setae on furcae (*sl:* $H = 52.77$, $p < 0.01$), number of setae on furcae (*sf:* $H = 66.08$, $p < 0.01$), and ratio

Table 3. Morphometric features of females of *A. parthenogenetica* and *A. tibetiana* in hypersaline lakes in the south of Western Siberia.

Character (Fig. 2)	*A. parthenogenetica*		*A. tibetiana*	
	Max, *M* ± SE	Min, *M* ± SE	Max, *M* ± SE	Min, *M* ± SE
tl, mm	11.51 ± 0.17 (Maloye Yarovoye)	8.27 ± 0.10 (Bolshoye Shklo)	10.01 ± 0.17 (Tanatar III)	8.24 ± 0.08 (Maloye Shklo)
al, mm	7.11 ± 0.09 (Shukyrtuz)	4.13 ± 0.07 (Bolshoye Shklo)	5.38 ± 0.14 (Tanatar III)	4.35 ± 0.06 (Maloye Shklo)
cl, mm	4.95 ± 0.08 (Bolshoye Yarovoye)	3.84 ± 0.04 (Mormishanskoye)	4.38 ± 0.06 (Tanatar III)	3.68 ± 0.04 (Maloye Shklo)
aw, mm	0.56 ± 0.01 (Bolshoye Yarovoye)	0.37 ± 0.00 (Mormishanskoye)	0.47 ± 0.01 (Tanatar III)	0.40 ± 0.01 (Maloye Shklo)
cl/al	0.95 ± 0.01 (Bolshoye Shklo)	0.56 ± 0.01 (Shukyrtuz)	0.86 ± 0.01 (Maloye Shklo)	0.84 ± 0.02 (Tanatar III)
al/tl	0.695 ± 0.021 (Kuchukskoye)	0.498 ± 0.003 (Bolshoye Shklo)	0.53 ± 0.01 (Tanatar III)	0.53 ± 0.00 (Maloye Shklo)
de, mm	1.64 ± 0.03 (Bolshoye Yarovoye)	1.16 ± 0.01 (Shukyrtuz)	1.50 ± 0.02 (Tanatar III)	1.15 ± 0.02 (Maloye Shklo)
ed, mm	0.30 ± 0.01 (Bolshoye Yarovoye)	0.23 ± 0.00 (Mormishanskoye)	0.29 ± 0.00 (Tanatar III)	0.22 ± 0.00 (Maloye Shklo)
la, mm	1.05 ± 0.03 (Bolshoye Yarovoye)	0.71 ± 0.01 (Shukyrtuz)	1.05 ± 0.02 (Tanatar III)	0.75 ± 0.02 (Maloye Shklo)
hw, mm	0.78 ± 0.01 (Bolshoye Yarovoye)	0.62 ± 0.01 (Shukyrtuz)	0.88 ± 0.01 (Tanatar III)	0.69 ± 0.01 (Maloye Shklo)
fl, mm	0.28 ± 0.01 (Krivaya Puchina)	0.05 ± 0.00 (Kuchukskoye)	0.32 ± 0.01 (Thanatar III)	0.22 ± 0.01 (Maloye Shklo)
sf, pcs.	9.98 ± 0.43 (Krivaya Puchina)	0.48 ± 0.06 (Kuchukskoye)	10.26 ± 0.35 (Tanatar III)	6.53 ± 0.26 (Maloye Shklo)
sl, mm	0.67 ± 0.02 (Bolshoye Shklo)	0.23 ± 0.01 (Kuchukskoye)	0.69 ± 0.02 (Tanatar III)	0.58 ± 0.02 (Maloye Shklo)
fl/al	0.070 ± 0.002 (Bolshoye Shklo)	0.008 ± 0.001 (Kuchukskoye)	0.061 ± 0.002 (Tanatar III)	0.052 ± 0.001 (Maloye Shklo)

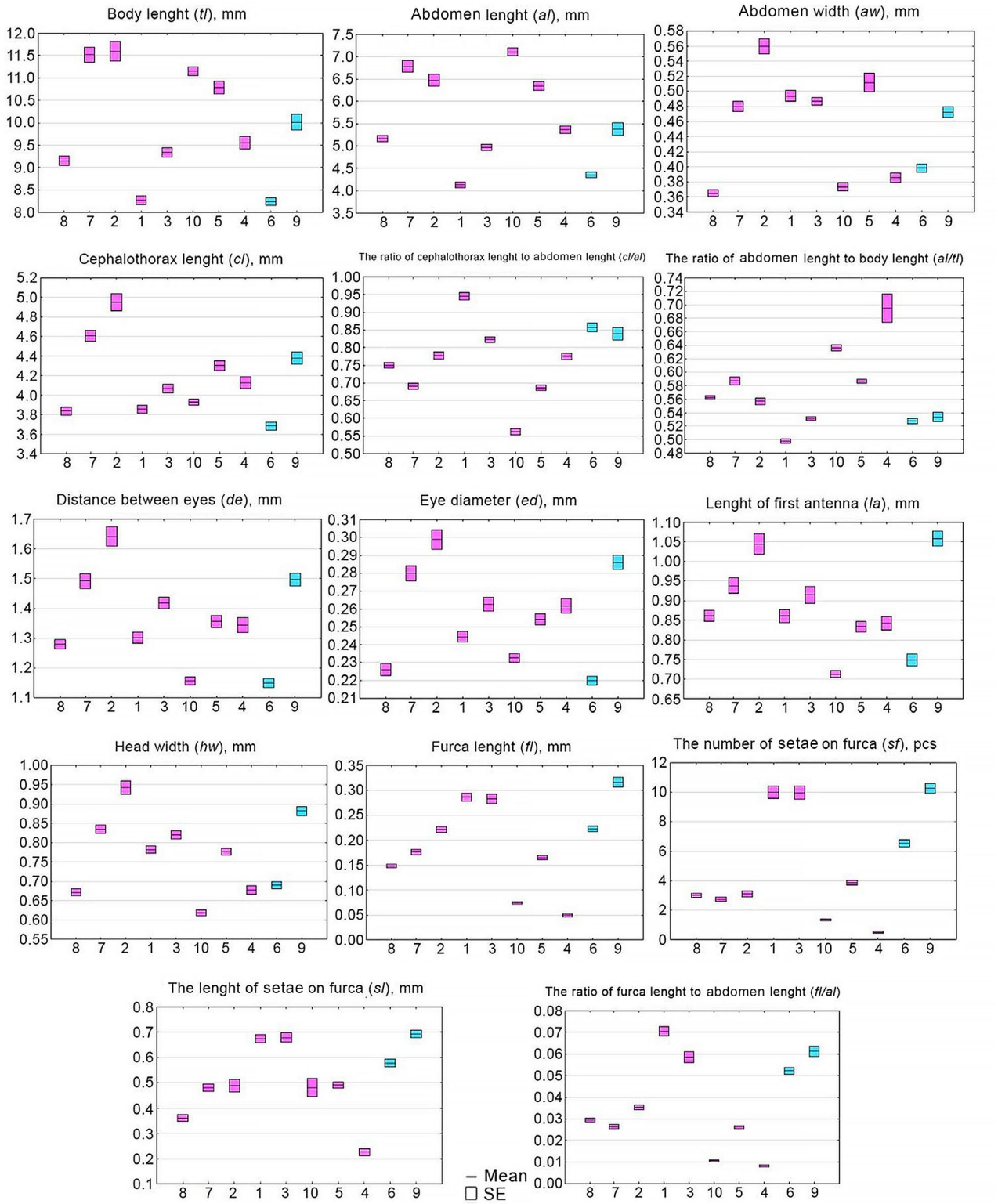

Fig.4. Morphometric features of mature females of *A. parthenogenetica* (pink) and *A. tibetiana* (blue) in the study lakes (2025): 1–Bolshoye Shklo, 2–Bolshoye Yarovoye, 3–Krivaya Puchina, 4–Kuchukskoye, 5–Malinovoye, 6–Maloye Shklo, 7–Maloye Yarovoye, 8–Mormyshanskoye, 9–Tanatar III, and 10–Shukyrtuz; Mean–average value; and SE–standard error.

of furca length to abdomen length (*fl/al:* $H = 128.50$, $p < 0.01$). Based on 13 plastic and 2 meristic characters, males *of A. tibetiana* from Lake Thanatar III have larger body proportions compared to those from Lake Maloye Shklo (Fig. 5).

The meristic character of *A. tibetiana* males from Lake Maloye Shklo is higher than that for males from Lake Tanatar III by the ratio of abdomen length to body length (*al/tl:* $H = 4.31$, $p < 0.05$). The ratio of cephalothorax length to abdomen length (*cl/al:* $H = 0.93$, $p > 0.05$) in males of *A. tibetiana* does not differ. Thus, based on one meristic character, males of *A. tibetiana* from Lake Maloye Shklo have a larger body size compared to those from Lake Tanatar III. Equivalence of meristic characters (ratio of cephalothorax length to abdomen length (*cl/al*)) morphologically unites males of bisexual species.

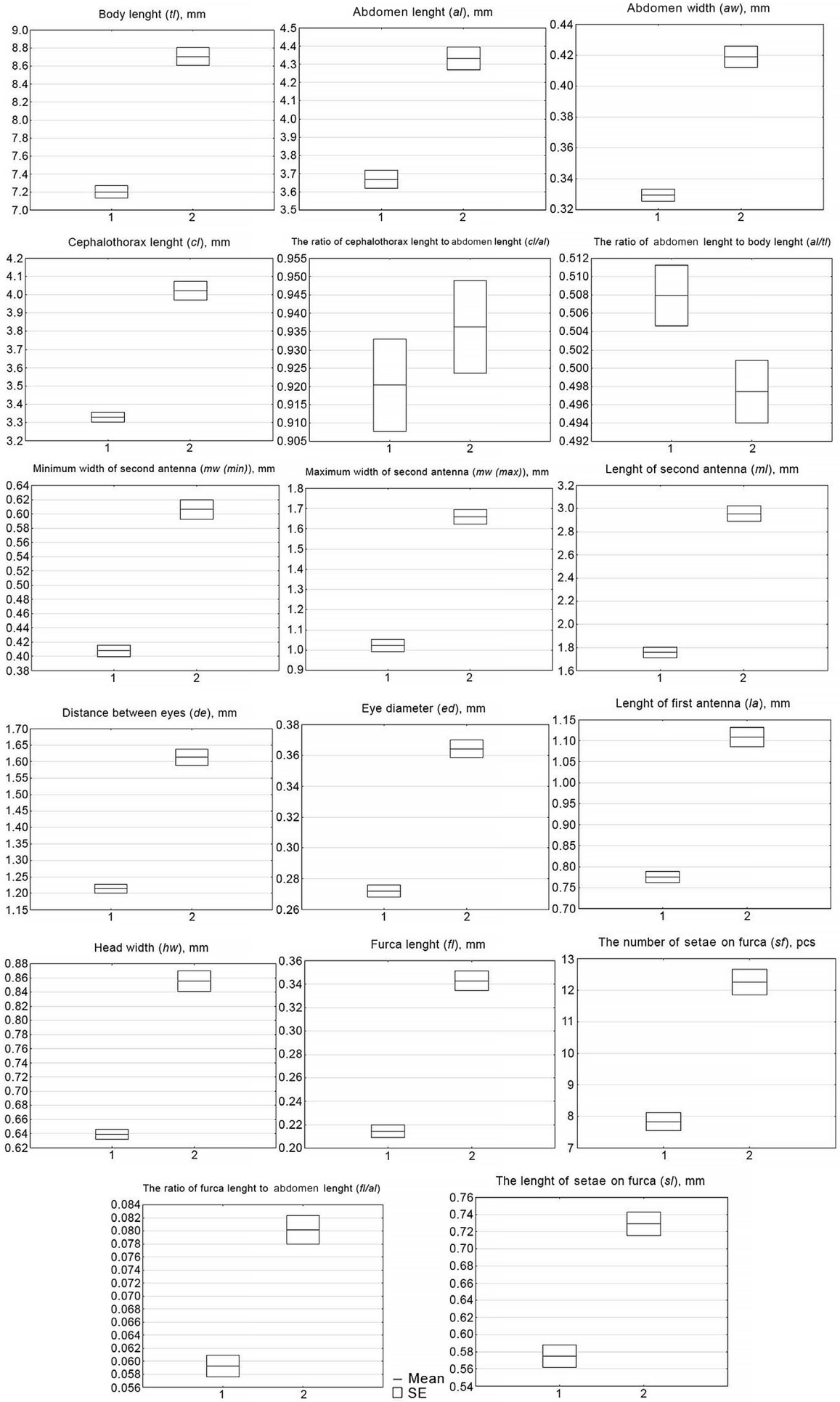

Fig.5. Morphometric features of *A. tibetiana* mature males in the study lakes (2025): 1–Maloye Shklo; 2–Tanatar III; Mean–average value; and SE–standard error.

3.3. Comparative analysis of morphological features of females and males of *A. parthenogenetica* and *A. tibetiana*

Comparative analysis of the variability of morphometric features in different species of mature females of *A. parthenogenetica* and *A. tibetiana spp.* enables us to identify the features of individual body parts (Fig. 6). Plastic and meristic characters of *A. parthenogenetica* females are higher than of *A. tibetiana* ones in terms of body length (*tl:* $H = 69.28$, $p < 0.01$), cephalothorax (*cl:* $H = 21.22$, $p < 0.01$), length (*al:* $H = 86.79$, $p < 0.01$) and width (*aw:* $H = 14.78$, $p < 0.01$) of abdomen, distance between eyes (*de:* $H = 13.28$, $p < 0.01$), eye diameter (*ed:* $H = 11.35$, $p < 0.05$), and ratio of abdomen length to body length (*al/tl:* $H = 79.75$, $p < 0.01$). Based on six plastic and one meristic characters, females of *A. parthenogenetica* have a larger body proportions than females of *A. tibetiana*.

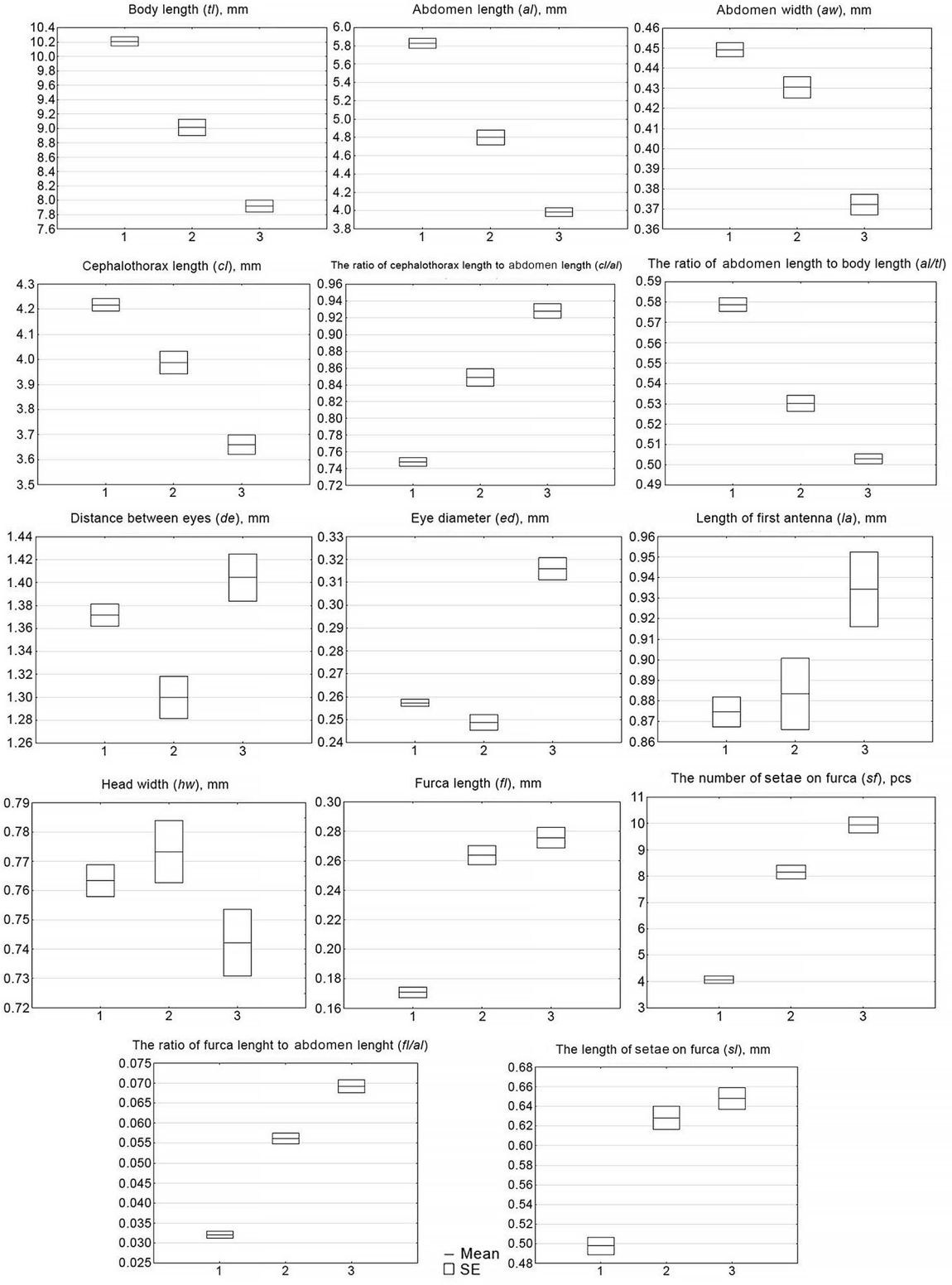

Fig.6. Morphometric features of mature females and males of *A. parhenogenetica* and *A. tibetiana* in the study lakes (2025): 1–females of *A. parthenogenetica*; 2–females of *A. tibetiana*; 3–males of *A. tibetiana;* Mean–average value; and SE–standard error.

However, plastic and meristic characters of *A. tibetiana* females are higher than for *A. parthenogenetica* females by furcae length (*fl:* H = 113.80, p < 0.01), length of setae on furcae (*sl: H* = 43.12, p < 0.01), number of setae on furcae (sf: H = 154.90, p < 0.01), ratio of cephalothorax to abdomen length (*cl/al: H* = 58.20, p < 0.01), and ratio of furcae to abdomen length (*fl/al: H* = 158.80, p < 0.01). In females, length of the first antenna (*la:* H = 0.05, p > 0.05) and head width (*hw:* H = 0.01, p > 0.05) do not differ significantly. Thus, based on two plastic and three meristic signs, females of *A. tibetiana* have a larger body size than females *of A. parthenogenetica.* Equivalence of plastic characters (length of the first antenna (*la*) and head width (*hw*)) morphologically unites parthenogenetic and bisexual species.

Comparison of plastic and meristic indices of mature females and males *of A. tibetiana* indicates that females of *A. tibetiana* have a larger body length than males *of A. tibetiana* (*tl: H* = 52.31, p < 0.01), cephalothorax (*cl: H* = 31.31, p < 0.01), length (*al: H* = 69.36, p < 0.01) and width (*aw: H* = 55.97, p < 0.01) of abdomen, length of the first antenna (*la: H* = 4.51, p < 0.05), head width (*hw: H* = 6.95, p < 0.01), and ratio of abdomen length to body length (*al/tl: H* = 39.44, p < 0.01). According to six plastic characters and one meristic character, females of *A. tibetiana* are distinguished by larger body proportions than males of *A. tibetiana.*

At the same time, plastic and meristic characters of *A. tibetiana* males are greater than in *A. tibetiana* females in terms of distance between eyes (*de: H* = 10.31, p < 0.01), eye diameter (*ed: H* = 93.32, p < 0.01), number of setae on furcae (*sf: H* = 19.66, p < 0.01), ratio of cephalothorax length to abdomen length (*cl/al: H* = 36.47, p < 0.01), and furca length to abdomen length (*fl/al: H* = 35.44, p < 0.01). Furcae length (*fl: H* = 0.74, p > 0.05) and length of setae on furcae (*sl: H* = 1.21, p > 0.05) of *A. tibetiana* males and females do not differ. Based on two plastic and three meristic characters, *A. tibetiana* males have a larger body size than *A. tibetiana* females. Equivalence of plastic characters (furca length (*fl*) and furca setae length (*sl*)) morphologically unites females and males of bisexual species.

In our opinion, water salinity, varying from 45.9 (Lake Maloye Shklo) to 210.9 g/l (Lake Kuchukskoye), mainly affects the studied plastic and meristic characters of *A. parthenogenetica* and *A. tibetiana.* Changes in water salinity affect body proportions.

4. Discussion

Obviously, studies of *Artemia* morphometric traits must take into account such factors as brine salinity and temperature. Based on the relationship between plastic/meristic characters and the mentioned factors, there are some general conclusions for populations of the *A. parthenogenetica* crustaceans (at a significance level of p < 0.05) (Table 4):

- when salinity increases, setae on the furca (*sf*) reduce along with their length (*sl*) and the length of the furca itself (*fl*);
- abdomen length (*al*) and ratio of abdomen length to body length (*al/tl*) proportionally increase with salinity;
- ratio of cephalothorax length to abdomen length (*cl/al*), furca length to abdomen length (*fl/al*), abdomen width (*aw*), length of the first antenna (*la*), and head width (*hw*) negatively correlate with salinity.

With the rise in brine temperature, cephalothorax length (*cl*) and distance between eyes (*de*) in the *A. parthenogenetica* populations reduce.

Owing to a small sample size because of the detection of *A. tibetiana* populations only in two lakes, we applied other methods for statistical analysis. Based on the Kruskal-Wallis criterion (*H*), the compared data on the average brine salinity in Lake Maloye Shklo

Table 4. Correlation analysis of plastic and meristic characters of *A. parthenogenetica* based on abiotic factors

Character	r	R^2	Dependency equation
Brine salinity, g/L			
Abdomen length (*al*)	0.41	0.24	y = 0.0094x + 4.3428
Abdomen width (*aw*)	-0.67	0.35	y = -0.0008x + 0.5901
Length of the first antenna (*la*)	-0.43	0.11	y = -0.0007x + 0.9885
Head width (*hw*)	-0.53	0.22	y = -0.001x + 0.9262
Length of furrows (*fl*)	-0.82	0.59	y = -0.0011x + 0.3492
Length of setae on furcae (*sl*)	-0.59	0.30	y = -0.0018x + 0.7715
Number of setae on furcae (*sf*)	-0.75	0.44	y = -0.0401x + 10.31
Ratio of cephalothorax length to abdomen length (*cl/al*)	-0.70	0.46	y = -0.0013x + 0.9627
Ratio of abdomen length to body length (*al/tl*)	0.86	0.63	y = 0.001x + 0.431
Ratio of furcae length to abdomen length (*fl/al*)	-0.87	0.63	y = -0.0003x + 0.077
Brine temperature, ˚C			
Cephalothorax length (*cl*)	-0.42	0.18	y = -0.0435 x + 5.1284
Distance between eyes (*de*)	-0.39	0.15	y = -0.0156x + 1.7005

Note: r is the Spearman correlation coefficient, and R^2 is the approximation coefficient.

(45.9 ± 13.8 g/l) and Lake Tanatar III (161.6 ± 48.5 g/l) demonstrate a reliable difference ($p < 0.05$). Brine temperatures in the study lakes (Lake Maloye Shklo: 21.4 ± 1.4°C; Lake Tanatar III: 16.0 ± 1.2°C) also differ significantly ($p < 0.05$).

Thus, with an increase in brine salinity by 115.7 g/L and a decrease in its temperature by 5.4°C, the morphometric characteristics of females and males of *A. tibetiana* change:

- body parameters of females and males increase: body length (*tl*), abdomen length (*al*), abdomen width (*aw*), and cephalothorax length (*cl*);
- size characteristics of the head in females and males increase: distance between eyes (*de*), eye diameter (*ed*), length of the first antenna (*la*), and head width (*hw*);
- furca parameters in females and males increase: furca length (*fl*), number of setae on furcae (*sf*), and length of setae on furcae (*sl*);
- ratio of abdomen length to body length (*al/tl*) in males decreases;
- size of the second antenna in males increases: length of the second antenna (*ml*), maximum and minimum width of the second antenna (*mw* (*max*) and *mw* (*min*)).

Cluster analysis of 12 plastic and 4 meristic characters of *A. parthenogenetica* females, based on the average seasonal values, demonstrates that populations are split into three groups with different brine salinity and furcal indicators (Fig. 7).

A separate group is formed by the *Artemia* population from lakes Bolshoye Shklo and Krivaya Puchina, crustaceans of which are characterized by the highest furcal indices in contrast to other water bodies (furcae length (*fl*), number of setae on furcae (*sf*), and length of setae on furcae (*sl*)) (see Fig. 4). The average salinity of brine in the first group of lakes is 109.9 ± 7.1 g/L. The second group combines the *Artemia* populations from lakes Kuchukskoye and Mormyshanskoye. The length of setae on the furcae (*sl*) of crustaceans of this group is the shortest in comparison with other lakes. The average salinity of this group reaches 219.1 ± 8.0 g/L. The third group involves the populations of lakes Bolshoye Yarovoye, Maloye Yarovoye, Malinovoye, and Shukyrtuz, crustaceans of which are characterized by similar setae lengths on furcae (*sl*) and differ significantly from those in other lake groups. The average salinity of brine in this group is 170.2 ± 2.8 g/L.

As shown above, we have studied the hypersaline lakes (in the south of Western Siberia) characterized by various abiotic factors affecting the vital activity of aquatic organisms. Fluctuations in temperature and salinity of lake brine influence the dynamics of quantitative indicators and differences in morphometric traits of *Artemia*, as shown in previous studies (Vesnina et al., 2023; Vesnina and Bezmaternykh, 2023; Litvinenko et al., 2024). Excessively high or low salinity of brine is manifested as inhibition of growth, development, and reproduction of *Artemia* (Vesnina et al., 2011). When brine salinity alters, not only morphology but also reproductive characteristics and sex ratio change (Vesnina et al., 2012; Syomik et al., 2024).

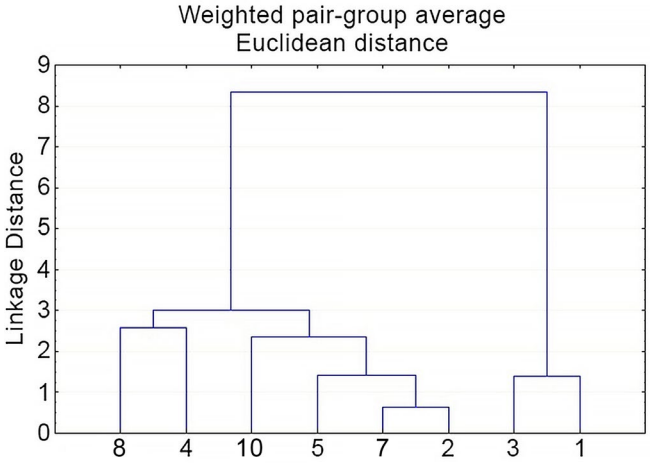

Fig.7. Dendrogram of similarity of morphometric parameters in *A. parthenogenetica* females of the studied populations from hypersaline lakes in the south of Western Siberia (single linkage method): 1–Bolshoye Shklo; 2–Bolshoye Yarovoye; 3–Krivaya Puchina; 4–Kuchukskoye; 5–Malinovoye; 7–Maloye Yarovoye; 8–Mormyshanskoye; and 10–Shukyrtuz.

Artemia is distinguished by high ecological plasticity: the species can change its size and shape depending on external factors, among which a salt concentration in water is essential (Nobile et al., 2020; Forneck et al., 2021; Van Stappen et al., 2020; Thirunavukkarasu et al., 2024). At the same time, the morphometric characters of *Artemia* are studied worldwide for differentiation and identification of species (Naganawa and Mura, 2017; Asem et al., 2020; Sainz-Escudero et al., 2021). Furthermore, the morphometric differences between individuals or populations of the same species may be due to genotypic variation (Thirunavukkarasu et al., 2021). Our data fully confirm these findings. We have revealed distinct changes in morphometric features of both studied *Artemia* species across a gradient of key environmental factors, as well as interspecific and interpopulation differences that significantly complicate taxonomic diagnosis based on morphological features.

Similar patterns were stated in previous studies. They demonstrated the differences in morphological features in some populations found in different geographic areas, particularly in the coastal areas of India, China, Europe, and Africa (Thirunavukkarasu et al., 2022; Thirunavukkarasu et al., 2021; Ruebhart et al., 2008). Scientists from India and Taiwan discovered six morphotypes of *Artemia* based on their morphometric characters (Maniatsi et al., 2009). Similar to our case, differences in morphometric parameters were revealed between females and males of *Artemia* from North America and the Caribbean coast of Colombia (Van Stappen et al., 2024). Obviously, our investigations and previous studies of morphological and size-weight characteristics of *Artemia* in different-type lakes in the south of Western Siberia are not sufficient for reliable differentiation of *Artemia* populations of various species (Litvinenko et al., 2024; Vesnina et al., 2025).

The analysis of plastic and meristic characters of mature *Artemia* specimens from different-type hypersaline lakes in Altai Krai confirms that furcal indices are the most variable characteristics in *Artemia* females (Vesnina et al., 2025).

5. Conclusions

We studied modern morphological features of parthenogenetic and bisexual populations of *Artemia* in 10 different hyperhaline lakes in the south of Western Siberia. DNA barcoding allowed us to identify two species of *Artemia* in the studied hyperhaline lakes of Altai Krai: *A. parthenogenetica* and *A. tibetiana. A. parthenogenetica* was found in chloride (Bolshoye Shklo, Bolshoye Yarovoye, Krivaya Puchina, Kuchukskoye, Malinovoye, Maloye Yarovoye, and Shukyrtuz) and sulfate (Mormishanskoye) lakes, while *A. tibetiana*–in the chloride (Maloye Shklo) and hydrocarbonate lakes (Tanatar III).

The comparative analysis of morphological features demonstrated that females of *A. parthenogenetica* and *A. tibetiana* have significant differences in the average values (14 out of 16 traits studied): body length, abdomen length, ratio of abdomen length to body length, abdomen width, distance between eyes, eye diameter, cephalothorax length, ratio of cephalothorax length to abdomen length, furcal branch length, number of setae on furca, length of setae on furca, and ratio of furca length to abdomen length.

The analysis of 12 plastic and 4 meristic characters in *A. parthenogenetica* females revealed the splitting of its populations into three groups, which differ in the furca structure: length, number of setae, and setae length. The Spearman correlation index demonstrated strong statistical relationships between the morphological traits of *A. parthenogenetica* and *A. tibetiana* and main environmental factors, i.e. brine salinity and temperature.

Acknowledgements

The research was supported by the Russian Science Foundation grant No. 25-26-00148 (https://rscf.ru/en/project/25-26-00148/).

Conflict of interest

The authors declare no conflict of financial or personal interest.

References

Asem A., Eimanifar A., Rastegar-Pouyani N. et al. 2020. An overview on the nomenclatural and phylogenetic problems of native Asian brine shrimps of the genus Artemia Leach, 1819 (Crustacea, Anostraca). Zookeys 902: 1.

Asem A., Yang C., Eimanifar A. et al. 2023. Phylogenetic analysis of problematic Asian species of Artemia Leach, 1819 (Crustacea, Anostraca), with the descriptions of two new species. Journal of Crustacean Biology 83(1): 1–25. DOI: 10.1093/jcbiol/ruad002

Beardmore J.A., Pilla E.J., Thomas K.M. 1994. Genetic variation in *Artemia*: speciation, reproductive mode and potential for exploitation. In: Gajardo G., Coutteau P. (Eds.), Book of Abstracts of Contributions. Puerto Montt.

Browne R.A., Bowen S.T. 1991. Taxonomy and population genetics of *Artemia*. In: Browne R.A., Sorgeloos P., Trotman C.N.A. (Eds.), *Artemia* Biology. Boston: CRC Press, pp. 221–235.

Edgar R.C. 2004. MUSCLE: multiple sequence alignment with high accuracy and high throughput. Nucleic Acids Research 32(5): 1792. DOI: 10.1093/nar/gkh340

Eimanifar A., Van Stappen G., Marden B. et al. 2014. *Artemia* biodiversity in Asia with the focus on the phylogeography of the introduced American species *Artemia franciscana* Kellogg, 1906. Molecular Phylogenetics Evolution 79: 392–403.

Folmer O., Black M., Hoeh W. et al. 1994. DNA primers for amplification of mitochondrial cytochrome coxidase subunit I from diverse metazoan invertebrates. Molecular Marine Biology and Biotechnology 3(5): 294–299.

Forneck S.C., Dutra F.M., de Camargo M.P. et al. 2021. Aquaculture facilities drive the introduction and establishment of non-native Oreochromis niloticus populations in Neotropical streams. Hydrobiologia 848(9): 1955–1966. DOI: 10.1007/s10750-020-04430-8

Hammer Ø., Harper D.A.T., Ryan P.D. 2001. PAST: Paleontological Statistics Software Package for Education and Data Analysis. Palaeontologia Electronica.

Kumar S., Stecher G., Li M. et al. 2018. MEGA X: Molecular evolutionary genetics analysis across computing platforms. Molecular Phylogenetics Evolution 35: 1547. DOI: 10.1093/molbev/msy096

Litvinenko L.I., Korentovich M.A., Boyko E.G. et al. 2024. *Artemia* in the hypersaline water bodies of Russia (geography, biodiversity, ecology, biology, and practical use). Tyumen: GAU Severnogo Zaural'ya. (in Russian)

Lobo J., Costa P., Teixeira M. et al. 2013. Enhanced primers for amplification of DNA barcodes from a broad range of marine metazoans. BMC ecology 13: 1.

Maccari M., Amat F., Gómez A. 2013. Origin and Genetic Diversity of Diploid Parthenogenetic *Artemia* in Eurasia. PLoS ONE 8(12): e83348.

Maniatsi S., Baxevanis A.D., Abatzopoulos T.J. 2009. The intron 2 of p26 gene: a novel genetic marker for discriminating the two most commercially important *Artemia franciscana* subspecies. Journal of Biological Research 11: 73–82. DOI: 10.3390/ijms10125455

Manual for the Chemical Analysis of Land Surface Waters. Part 1. 2009. In: Boeva L.V. (Ed.). Rostov-on-Don. (in Russian)

Manual for the Chemical Analysis of Land Surface Waters. Part 2. 2012. In: Boeva L.V. (Ed.). Rostov-on-Don. (in Russian)

Manual on Hydrobiological Monitoring of Freshwater Ecosystems. 1992. SPb.: Gidrometeoizdat. (in Russian)

Naganawa H., Mura G. 2017. Two new cryptic species of *Artemia* (Brachiopoda, Anostraca) from Mongolia and the possibility of invasion and disturbance by the aquaculture industry in East Asia. Crustaceana 90(14): 1679–1698. DOI: 10.1163/15685403-00003744

Nikonorov A.M. 1989. Handbook of Hydrochemistry. Leningrad: Gidrometeoizdat. (in Russian)

Nobile A.B., Cunico A.M., Vitule J.R. et al. 2020. Status and recommendations for sustainable freshwater aquaculture in Brazil. Reviews in Aquaculture 12(3): 1495–1517. DOI: 10.1111/raq.12393

Pang H., Zheng K., Wang W. et al. 2024.The Morphological Differentiation and Evolutionary Origins of *Artemia* in China. Diversity 16(3): 144.

Persoone G., Sorgeloos P. 1980. General aspects of

the ecology and biogeography of *Artemia*. In: Persoone G., Sorgeloos P., Roels O., Jaspers E. (Eds.). The brine shrimp *Artemia*. Ecology, culturing, use in aquaculture 3: Universa Press, Wetteren, Belgium, pp. 3–24.

Pilla E.J.S., Beardmore J.A. 1994. Genetic and morphometric differentiation in Old World bisexual species of the brine shrimp (*Artemia*). Heredity 72: 47–56. DOI: 10.1038/hdy.1994.97

Ruebhart D.R., Cock I.E., Shaw G.R. 2008. Invasive character of the brine shrimp *Artemia* franciscana Kellogg 1906 (Branchiopoda: Anostraca) and its potential impact on Australian inland hypersaline waters. Marine & Freshwater Research 59(7): 587–595. DOI: 10.1071/MF07221

Sainz-Escudero L., López-Estrada E.K., Rodríguez-Flores P.C. et al. 2021. Settling taxonomic and nomenclatural problems in brine shrimps, *Artemia* (Crustacea: Branchiopoda: Anostraca), by integrating mitogenomics, marker discordances and nomenclature rules. PeerJ: 62. DOI: 10.7717/peerj.10865

Syomik A.M., Zamyatina E.A., Parshin-Chudin A.V. et al. 2024. Comparative analysis of the population of the *Artemia* genus in the hypersaline lakes of Crimea based on morphometric characteristics. Rybovodstvo i rybnoe hozyajstvo [Fish farming and fisheries] 12: 862–875. DOI: 10.33920/sel-09-2412-03 (in Russian)

Tamura K., Stecher G., Kumar S. 2021. MEGA11: Molecular Evolutionary Genetics Analysis Version 11. Molecular Biology and Evolution 38(7): 3022. DOI: 10.1093/molbev/msab120

Thirunavukkarasu S., Karunasagaran G., Munuswamy N. 2021. Genetic diversity and population structure of *Artemia franciscana* from southeast coast of India. Journal of Sea Research 178: 102127. DOI: 10.1016/j.seares.2021.102127

Thirunavukkarasu S., Karunasagaran G., Munuswamy N. 2022. Morphometric and phylogenetic analysis of morphotypes in *Artemia franciscana* Kellogg, 1906 (Crustacea: Anostraca). Regional Studies in Marine Science 54: 102411. DOI: 10.1016/j.rsma.2022.102411

Thirunavukkarasu S., Murugan G., Hwang J.-S. et al. 2024. Morphology and morphometry of morphotypes in the population of *Artemia franciscana* (Kellogg, 1906) from salterns of the southeastern coast of India. Heliyon 10(1): 1–13. DOI: 10.1016/j.heliyon.2024.e29796

Triantaphyllidis G.V., Zhang B., Zhu L. et al. 1994. International Study on *Artemia*. L. Review of the literature on *Artemia* from salt lakes in the People's Republic of China. International Journal of Salt Lake Research 3: 1–12. DOI: 10.1007/BF01990645

Van Stappen G. 2002. Chapter IV. Zoogeography. In: Abatzopoulos T.J., Beardmore J.A., Clegg J.S., Sorgeloos P. (Eds.), *Artemia*: Basic and applied biology. Dordrecht, the Netherlands, Kluwer Academic Publishers, pp. 286.

Van Stappen G., Sorgeloos P., Rombaut G. 2024. Manual on *Artemia* production and use. FAO Fisheries and Aquaculture Technical Papers. Rome. DOI: 10.4060/cd0313en

Van Stappen G., Sui L., Hoa V.N. et al. 2020. Review on integrated production of the brine shrimp *Artemia* in solar salt ponds. Reviews in Aquaculture 12(2): 1054–1071. DOI: 10.1111/raq.12371

Vanhaecke P., Tackaert W., Sorgeloos P. 1987. The biogeography of *Artemia*: an updated review. In: Sorgeloos P., Bengtson D.A., Decleir W. et al. (Eds.), *Artemia* research and Its applications. Morphology, genetics, strain characterisation, toxicology. Wetteren, Belgium, Universa Press.

Vesnina L.V., Bezmaternykh D.M. 2023. Influence of Environmental Factors on the Dynamics of Zooplankton in Lake Kulunda (Western Siberia). Russian Journal of Ecology 54(3): 243–250. DOI: 10.1134/S1067413623030086

Vesnina L.V., Bezmaternykh D.M., Lassyi M.V. et al. 2025. Morphometric Characteristics and DNA Barcoding of Branchiopod Crustaceans of the Genus *Artemia* (Crustacea: Anostraca) from the Lakes of the Kulunda Lowland of Altai Krai. Inland Water Biology 18(5): 980–990. DOI: 10.1134/S1995082925600978

Vesnina L.V., Ronzhina T.O., Permyakova G.V. et al. 2011. Altai Starter Feeds: Yesterday, Today, and Tomorrow. Akvakul'tura central'noj i vostochnoj Evropy: nastoyashchee i budushchee [Proceedings of the II International Scientific Conference Aquaculture in Central and Eastern Europe: Present and Future]: 48–53. (in Russian)

Vesnina L.V., Ronzhina T.O., Permyakova G.V. et al. 2012. Technology for producing starter feed from *Artemia* from the salt lakes of the Altai krai. Rybovodstvo i rybnoe hozyajstvo [Fish farming and fisheries] 3: 52–59. (in Russian)

Vesnina L.V., Vasileva A.S. 2019. The current state of the Artemia population during the desalination of hypersaline lakes (Lake Kulundinskoye as an example). Vodnye bioresursy, akvakul'tura i ekologiya vodoemov [Proceedings of the IV International Scientific Conference Aquatic biological resources, aquaculture, and water ecology] 6: 108–118. (in Russian)

Vesnina L.V., Vesnin Yu.A., Romanova N.S. et al. 2023. The role of brackish-water fauna and the state of the bioresources of the hypersaline Kulundinskoye Lake ecosystem in the transgression phase (Altai Krai) Rybnoe hozyaystvo [Fisheries] 2: 65–72. (in Russian)

Оригинальная статья

LIMNOLOGY FRESHWATER BIOLOGY

Морфологические и генетические особенности рачков *Artemia parthenogenetica* и *A. tibetiana* (Crustacea, Anostraca) в разнотипных гипергалинных озерах юга Западной Сибири

Безматерных Д.М.*, Веснина Л.В., Лассый М.В., Веснин Ю.А., Рябова К.К.

Институт водных и экологических проблем Сибирского отделения Российской академии наук, ул. Молодежная, 1, Барнаул, 656038, Россия

АННОТАЦИЯ. Изучены современные морфологические характеристики партеногенетических и двуполых популяций артемии в 10 разнотипных гипергалинных озерах юга Западной Сибири (Алтайский край). ДНК-баркодинг этих популяций позволил выявить два вида артемии: *Artemia parthenogenetica* Barigozzi, 1974 и *A. tibetiana* (Abatzopoulos et al., 1998). Исследования проводили ежемесячно, с июля по сентябрь 2025 г. С помощью метода главных компонент показаны различия гидрохимического состава рапы озер, в которых обитают партеногенетические и двуполые популяции артемии. Сравнительный анализ морфологических признаков показал, что самки *A. parthenogenetica* и *A. tibetiana* имеют значимые отличия средних величин – 14 из 16 признаков. Кластерный анализ 12 пластических и 4 меристических признаков самок *A. parthenogenetica* показал, что её популяции разделяются на 3 группы, которые различаются особенностями строения фурки: длиной (*fl*), количеством щетинок (*sf*), длиной щетинок (*sl*). Индекс корреляции Спирмена выявил значимые статистические зависимости морфологических признаков *A. parthenogenetica* и *A. tibetiana* от основных экологических факторов – минерализации и температуры рапы.

Ключевые слова: Алтайский край, соленые озера, жаброногие рачки, популяции, морфометрические признаки, минерализация, экологические факторы, ДНК-баркодинг

Для цитирования: Безматерных Д.М., Веснина Л.В., Лассый М.В., Веснин Ю.А., Рябова К.К. Морфологические и генетические особенности рачков *Artemia parthenogenetica* и *A. tibetiana* (Crustacea, Anostraca) в разнотипных гипергалинных озерах юга Западной Сибири // Limnology and Freshwater Biology. 2026. - № 2. - С. 103-129. DOI: 10.31951/2658-3518-2026-A-2-103

1. Введение

Популяции артемии обнаружены как в естественных, так и в искусственных соленых водоемах тропических, субтропических и умеренных климатических зон (Persoone and Sorgeloos, 1980). Ежегодно выявляются новые места обитания этого рачка. При этом некоторые ранее описанные популяции рачков исчезли из-за значительного повышения или понижения минерализации рапы (Vanhaecke et al., 1987; Triantaphyllidis et al., 1994; Van Stappen, 2002). Физиологические адаптации жаброногов к высокой солености обеспечивают эффективную экологическую защиту от хищников, поскольку они обладают более эффективной осморегуляцией; способностью синтезировать дыхательные пигменты при низком содержании кислорода в рапе; способностью производить диапаузирующие цисты при негативных условиях среды обитания (Vanhaecke et al., 1987; Van Stappen et al., 2024).

Широкое распространение артемии в изолированных местообитаниях, характеризующихся различными экологическими условиями, привело к существованию многочисленных географически разделенных и генетически различающихся популяций одного вида (Triantaphyllidis et al., 1994). В частности, наличие партеногенетических популяций артемии с ди-, три-, тетра- и пентаплоидией

*Автор для переписки. Адрес e-mail: bezmater@iwep.ru (Д.М. Безматерных)

Поступила: 14 января 2026;
Принята после доработки: 07 апреля 2026;
Опубликована online: 24 апреля 2026

привело к большому генотипическому и фенотипическому разнообразию. Некоторые из этих характеристик (пищевая ценность цист и науплий) подвержены межсезонной и межгодовой изменчивости. Другие признаки (диаметр цист, скорость роста, устойчивость к высокой температуре) относительно постоянны и являются проявлением долговременной адаптации к особым условиям обитания артемии (Triantaphyllidis et al., 1994; Van Stappen, 2002).

В настоящее время род *Artemia* Leach, 1819 включает следующие виды, распространенные в Евразии (Pilla and Beardmore, 1994; Beardmore et al., 1994; Browne and Bowen, 1991; Sainz-Escudero et al., 2021): *A. salina* (Linnaeus, 1758): Лимингтон, Англия (ныне вымерший), Средиземноморье (в прошлом называлась *A. tunisiana* (Bowen and Sterling, 1978); *A. urmiana* (Gunther, 1990): Иран (озеро Урмия), Крым; *A. sinica* (Cai, 1989): центральный и восточный Китай; *A. tibetiana* (Abatzopoulos et al., 1998): озеро Лагкор Ко, Тибет, Китай; *A. sorgeloosi* (Asem et al., 2023): озеро Хайян, Тибет, Китай; *Artemia amati* (Asem et al., 2023): Казахстан. Многочисленные партеногенетические популяции артемии, встречающиеся в Европе, Африке, Азии и Австралии, обычно объединяются под названием вида *A. parthenogenetica* (Barigozzi, 1974; Bowen and Sterling, 1978).

Целью работы было изучение современных морфологических и генетических характеристик партеногенетических и двуполых популяций в разнотипных гипергалинных озерах юга Западной Сибири.

2. Материалы и методы

Объектом исследования послужили 1021 экземпляр жаброногого рачка *Artemia* с 10 разнотипных гипергалинных озер юга Западной Сибири (Рис. 1). Отбор проб на морфометрический анализ рачка артемии проводили ежемесячно в период с июля по сентябрь 2025 г. по общепринятым методикам и рекомендациям (Руководство…, 1992). Пробы отбирали вручную с помощью гидробиологического сачка. Материал фиксировали 4%-ным формалином. Пробы обрабатывали в чашке Петри под бинокуляром МБС–10, оборудованным окуляр-микрометром. Всего было промерено 720 самок взрослого рачка, в том числе 561 экземпляр *A. parthenogenetica* и 159 экземпляров *A. tibetiana*, а также 301 самец *A. tibetiana*. При отборе проб в озерах с партеногенетическими популяциями артемии самцы регистрировалась единично, что недостаточно для статистического анализа.

Температура рапы измерялась с помощью гидрологического термометра в поверхностном слое (на глубине не менее 0,2 м); минерализация рапы – с помощью оптического прибора – портатив-

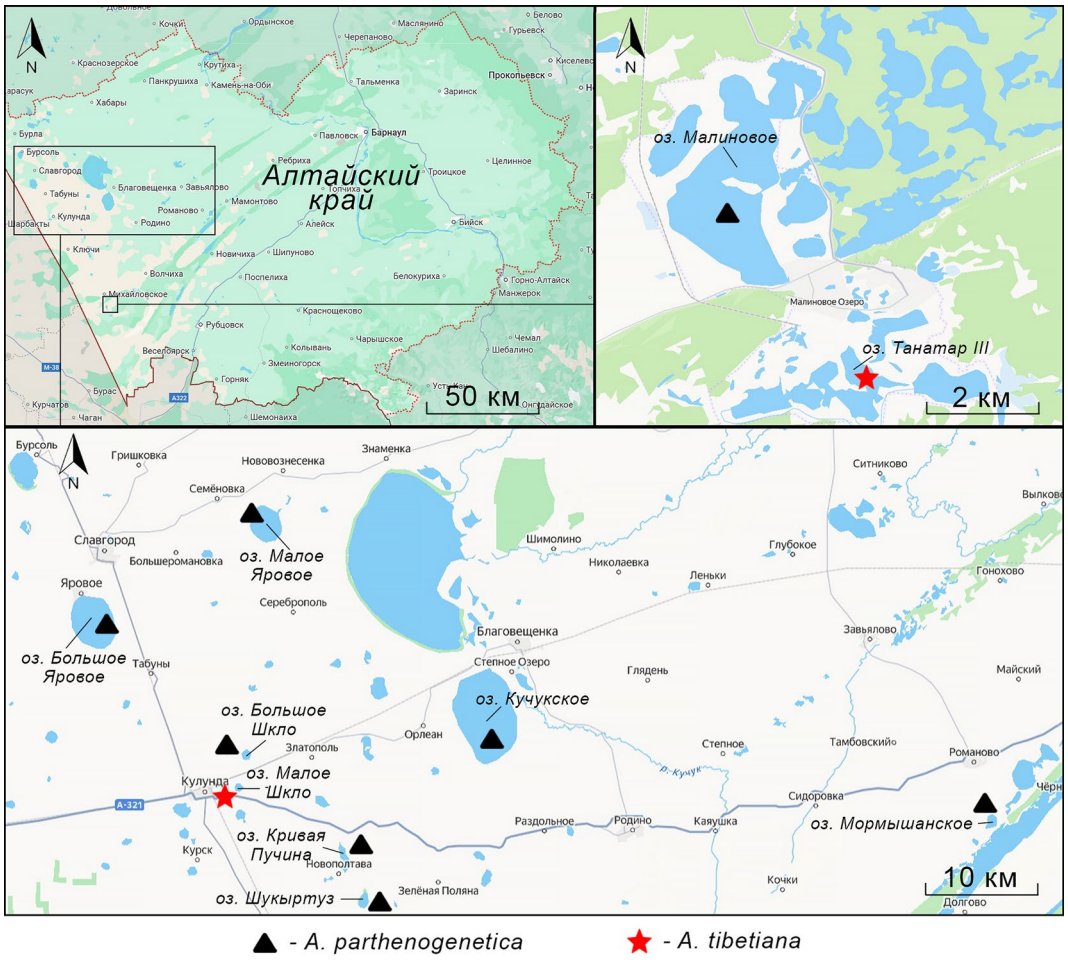

Рис.1. Изученные озера и распространение партеногенетических и двуполых популяций рачка *Artemia* юга Западной Сибири.

ного рефрактометра ATAGO (Kenco Instruments Co., USA) в поверхностном слое (на глубине не менее 0,2 м). Пробы воды для гидрохимического анализа – анионов и катионов (CO_3^{2-}, HCO_3^-, Cl^-, SO_4^{2-}, Ca^{2+}, Mg^{2+}, $Na^+ + K^+$), отбирали стандартными методами (Руководство…, 2009; 2012) из приповерхностного слоя воды (по 1,5 л в пластиковую тару). Камеральная обработка гидрохимических проб выполнена в Лаборатории биогеохимии ИВЭП СО РАН.

На основе анализа космоснимков, полученных спутниками «Ресурс-П» №4 и «Ресурс-П» №5, оценены площади водной поверхности исследуемых гипергалинных озер в период с апреля по октябрь 2025 г. Использованы снимки, сделанные в безоблачную погоду (уровень облачности менее 10%). Анализ проводился через открытый источник Геопортала Роскосмоса (URL: https://gptl.ru/). Измерение глубины исследуемых озер осуществлялось с помощью гидрологического лота. Некоторые результаты измерений и химического анализа представлены в Таблице 1.

Для морфометрического анализа у взрослых самок и самцов рачка артемии измеряли **пластические** признаки (Рис. 2): *tl* – общую длину тела, *al* – длину абдомена, *aw* – ширину абдомена, *de* – расстояние между глазами, *ed* – диаметр глаза, *la* – длину первой антенны, *hw* – ширину головы, *cl* – длину цефалоторакса, *fl* – длину фуркальной ветви, *sl* – длину щетинок на фурке; у самцов: *ml* – длину второй антенны, *mw* – ширину второй антенны, и **меристические** признаки: *sf* – количество щетинок на фурке, отношение длины цефалоторакса к длине абдомена (*cl/al*), отношение длины абдомена к длине тела (*al/tl*), отношение длины фурки к длине абдомена (*fl/al*) (Веснина и Васильева, 2019).

Видовую идентификацию рачка артемии проводили с помощью ДНК-баркодинга. Материал для ДНК-идентификации фиксировали 96%-ным этиловым спиртом. Анализ проводили в Отделе биотехнологий Южно-Сибирского ботанического сада Алтайского государственного университета. Для каждого озера секвенирование выполняли в двух-четырех повторностях, общее число исследованных образцов составило 30. Тотальную ДНК из пробы выделяли с использованием набора Diamond DNA Plantkit (ООО “Алтайбиотех”, Россия) по протоколу фирмы-изготовителя. Для видовой идентификации образцов амплифицировали фрагмент гена COI мтДНК с помощью полимеразной цепной реакции (ПЦР) и использованием пар праймеров – прямой LCO-1490 (GGTCAACAAATCATAAAGATATTGG) и обратный HCO-2198 (TAAACTTCAGGGTGACCAAAAAATCA) (Folmer et al., 1994). ПЦР проводили в 50 мкл реакционной смеси с применением коммерческого набора для амплификации БиоМастер HS-TaqПЦР-Color (2×) (Биолабмикс, Россия) в следующем составе на один образец: 25 мкл готовой PCR–смеси (ООО “Биолабмикс”, Новосибирск), 21 мкл $_{dd}H_2O$, по 1 мкл 10 мкМ соответствующих праймеров, 2 мкл ДНК.

Амплификацию проводили на амплификаторе MyCycler (Bio-Rad, USA) по следующей программе: начальная денатурация при 94˚C – 60 с; 35 циклов с денатурацией при 94˚C – 30 с, отжиг праймеров при 45˚C – 90 с, элонгация при 72˚C – 60 с; финальная элонгация при 72˚C – 300 с (Lobo et al., 2013).

Продукты амплификации разделяли в 1.3%-ном агарозном геле в горизонтальной электрофорезной камере в ТАЕ-буфере при 220V с при-

Таблица 1. Основные характеристики исследованных гипергалинных озер юга Западной Сибири в 2025 г.

Озеро	Географические координаты	Площадь (min–max), км²	Максимальная глубина (lim), м	Минерализация (min–max), г/л
Большое Шкло	52˚37′53″ N 79˚04′02″ E	3,4–3,6	1,8–2,0	65,7–91,3
Большое Яровое	52˚52′09″ N 78˚36′53″ E	73,0–74,2	7,3–10,5	140,0–160,0
Кривая Пучина	52˚26′33″ N 79˚21′31″ E	6,2–7,4	0,4–0,5	101,2–150,0
Кучукское	52˚42′06″ N 79˚46′40″ E	174,6–175,7	2,4–2,9	210,9–250,0
Малиновое	51˚42′10″ N 79˚44′49″ E	9,3–11,1	1,5–1,7	160,0–188,2
Малое Шкло	52˚34′20″ N 79˚02′47″ E	2,1–2,5	1,1–1,3	45,9–140,0
Малое Яровое	53˚02′39″ N 79˚07′37″ E	36,4–37,1	4,0–4,9	150,0–180,0
Мормышанское	52˚30′39″ N 81˚16′25″ E	5,9–7,9	0,9–1,2	150,0–220,0
Танатар III	51˚39′18″ N 79˚47′39″ E	0,8–1,0	1,6–1,9	100,0–161,6
Шукыртуз	52˚22′06″ N 79˚24′54″ E	5,2–5,5	0,7–0,9	177,6–220,0

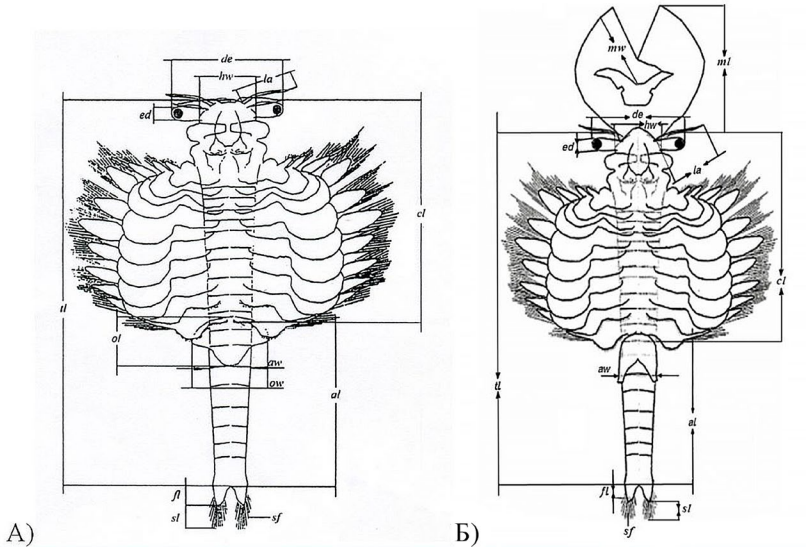

Рис.2. Схема морфометрических измерений самок (А) и самцов (Б) рачка *Artemia* spp. (Веснина и Васильева, 2019): *tl* – общая длина тела, *al* – длина абдомена, *aw* – ширина абдомена, *de* – расстояние между глазами, *ed* – диаметр глаза, *la* – длина первой антенны, *hw* – ширина головы, *cl* – длина цефалоторакса, *fl* – длина фуркальной ветви, *sf* – количество щетинок на фурке, *sl* – длина щетинок на фурке; *ml* – длина второй антенны, *mw* – ширина второй антенны.

менением бромистого этидия. Визуализацию продуктов амплификации проводили в проходящем УФ-излучении с помощью системы гель-документирования Gel Doc XR (Bio-Rad, USA). Для определения длины амплифицированных фрагментов использовали ДНК-маркеры (ООО «Биолабмикс», Новосибирск).

Очистку ПЦР-продукта перед секвенированием проводили с помощью магнитных частиц MAXLIFE Magnet DNA (MBM-Диагностик, Россия) по протоколу фирмы-изготовителя. Для секвенирование использовали автоматический секвенатор ABI Prism 3130xl. Полученные последовательности анализировали с помощью программы MEGA 11 (Tamura et al., 2021).

Для визуализации схожести нуклеотидных последовательностей фрагмента гена COI мтДНК изучаемых образцов была построена дендрограмма, включающая все последовательности видов *A. parthenogenetica* и *A. tibetiana*, опубликованные в базе данных GenBank NCBI (National Center for Biotechnology Information). Повторяющиеся гаплогруппы удаляли из дендрограммы. В качестве внешней группы использовали последовательности близкородственного вида *A. urmiana*. Выравнивание участка проводили с помощью алгоритма MUSCLE (Edgar, 2004), реализованного в программе MEGA X (Kumar et al., 2018). Для подбора модели нуклеотидных замен и построения дендрограммы использовали веб-сервер IQ-TREE со значением параметра бутстрэпа 10000. Стратегия построения дендрограммы – Maximum Likelihood (ML).

Статистическая обработка полученных данных проводилась с помощью пакетов компьютерных программ MS Excel – 2013 и PAST – 4 (Hammer et al., 2001). Использованы следующие методы: критерий Краскела-Уоллиса (*H*), коэффициент ранговой корреляции Спирмена (r), кластерный анализ, линейная аппроксимация с коэффициентом детерминации (R^2).

3. Результаты

3.1. Изменчивость морфометрических признаков у самок *A. parthenogenetica* и *A. tibetiana* в различных озерах

Все изученные озера по величине солености воды относились к гипергалинным. Величина их солености колебалась от 45,9 (оз. Малое Шкло) до 210,9 г/л (оз. Кучукское). По преобладающим анионам гипергалинные озера относились к 3 типам (Никоноров, 1989): гидрокарбонатные (Танатар III), сульфатные (Мормышанское) и хлоридные (Большое Шкло, Большое Яровое, Кривая Пучина, Кулундинское, Кучукское, Малиновое, Малое Шкло, Малое Яровое, Шукыртуз).

Вода исследуемых озер сульфатного и хлоридного типов по величине водородного потенциала была нейтральной – слабощелочной (pH = 7,5–8,8), а гидрокарбонатного типа – щелочной (pH = 9,8).

Температура воды в июле изменялась от 19,1 (оз. Танатар III) до 27,0°C (оз. Малое Яровое); в августе – от 16,6 (оз. Танатар III) до 26,8°C (оз. Кучукское); в сентябре – от 11,7 (оз. Кучукское) до 18,3°C (оз. Кривая Пучина).

В 2025 г. использование ДНК-баркодинга (Таблица 2) позволило определить в изученных гипергалинных озерах юга Западной Сибири два вида артемии (Рис. 3): *A. parthenogenetica* (Большое Шкло, Большое Яровое, Кривая Пучина, Кучукское, Малиновое, Малое Яровое, Мормышанское, Шукыртуз) и *A. tibetiana* (Малое Шкло, Танатар III). *A. tibetiana* ранее нами определялась как к *Artemia* sp. (Vesnina et al., 2025).

Дендрограмма сходства образцов была построена методом UPGMA: невзвешенной попарной группировки с усреднением (unweighted pair group method using arithmetic averages) со значением параметра бутстрэпа 10000 (Рис. 3). На дендрограмме прослеживается объединение изу-

Таблица 2. Результаты ДНК-баркодинга *Artemia* spp. из озер юга Западной Сибири.

Озеро	№ GenBank NCBI	% соответствия	% перекрывания последовательностей
A. parthenogenetica			
Большое Шкло	MT791796.1	96,83–100	99
Большое Яровое	PV017298.1	99,70	94
	MT791796.1	100	91
	MT791710.1	99,85–100	100
Кривая Пучина	PV017298.1	99,70	100
	MT791796.1	100	99
Кулундинское	MT791796.1	100	99
	MT791710.1	99,70	100
Кучукское	MT791796.1	99,85	99
Малиновое	MT791796.1	99,85–100	99
	MT791710.1	99,85	100
Малое Яровое	MT791796.1	99,85	99
	MT791710.1	99,70	100
Мормышанское	MT791796.1	99,55–100	91–99
Шукыртуз	MT791796.1	99,85–100	99
A. tibetiana			
Малое Шкло	MT791825.1	98,94–99,25	99–100
Танатар III	MT791825.1	99,40–99,70	99

ченных образцов из озер Большое Шкло, Большое Яровое, Кривая Пучина, Кулундинское, Кучукское, Малиновое, Малое Яровое, Мормышанское, Шукыртуз с образцами *A. parthenogenetica*. Пробы из озер Малое Шкло и Танатар III объединены в отдельном кладе с *A. tibetiana*.

Как показали предыдущие исследования, *A. tibetiana* является полифилетической группой (Maccari et al., 2013; Eimanifar et al., 2014; Asem et al., 2020). Изученные популяции озер юга Западной Сибири принадлежат к западной линии (Pang et al., 2024). Последовательности двуполого вида *A. sorgeloosi* образуют четко дифференцированную кладу, что подтверждает его видовой статус (Asem et al., 2023). Китайская *A. sinica* и американская *A. franciscana* занимают терминальное положение, также образуя отдельные кластеры.

По нашим данным *A. parthenogenetica* выявлена в семи озерах хлоридного типа минерализации и в одном озере сульфатного типа, в то время как *A. tibetiana* встречена в одном хлоридном и в одном гидрокарбонатном озере.

В 2025 г. самые вариабельные показатели по фуркальным признакам *A. parthenogenetica* были выявлены в оз. Кучукское: длина фурки (*fl*) – 40,94 %, количество щетинок на фурках (*sf*) – 31,15 %, длина щетинок на фурках (*sl*) – 34,24 %.

Наибольшими средними значениями морфометрических показателей *A. parthenogenetica* обладают рачки из озера Большое Яровое – по 7 признакам из 14: общей длине тела (*tl*), длине цефалоторакса (*cl*), ширине абдомена (*aw*), расстоянию между глазами (*de*), диаметру глаза (*ed*), длине первой антенны (*la*), ширине головы (*hw*) (Таблица 3, Рис. 4). Наименьшие средние значения морфометрических показателей (12 признаков из 14) зарегистрированы в озерах Большое Шкло, Кучукское, Шукыртуз по общей длине тела (*tl*), длине абдомена (*al*), длине цефалоторакса (*cl*), отношению длины цефалоторакса к длине абдомена (*cl/al*), отношению длины абдомена к длине тела (*al/tl*), расстоянию между глазами (*de*), длине первой антенны (*la*), ширине головы (*hw*), длине фурок (*fl*), количеству щетинок на фурках (*sf*), длине щетинок на фурках (*sl*), отношению длины фурки к длине абдомена (*fl/al*).

Наибольшими средними значениями морфометрических показателей *A. tibetiana* (12 признаков из 14) обладают рачки озера Танатар III, наименьшими – рачки озера Малое Шкло: общая длина тела (*tl*), длина цефалоторакса (*cl*), длина абдомена (*al*), ширина абдомена (*aw*), расстояние между глазами (*de*), диаметр глаза (*ed*), длина первой антенны (*la*), ширина головы (*hw*), длина фурок (*fl*), количество щетинок на фурках (*sf*), длина щетинок на фурках (*sl*), отношение длины фурки к длине абдомена (*fl/al*).

3.2. Изменчивость морфометрических признаков у самцов *A. tibetiana* в различных озерах

Результаты сравнения пластических и меристических показателей половозрелых самцов *A. tibetiana* показали, что самцы оз. Танатар III выше таковых самцов оз. Малое Шкло по длине тела (*tl*: $H = 95{,}14$, $p < 0{,}01$), цефалоторакса (*cl*: $H = 89{,}28$,

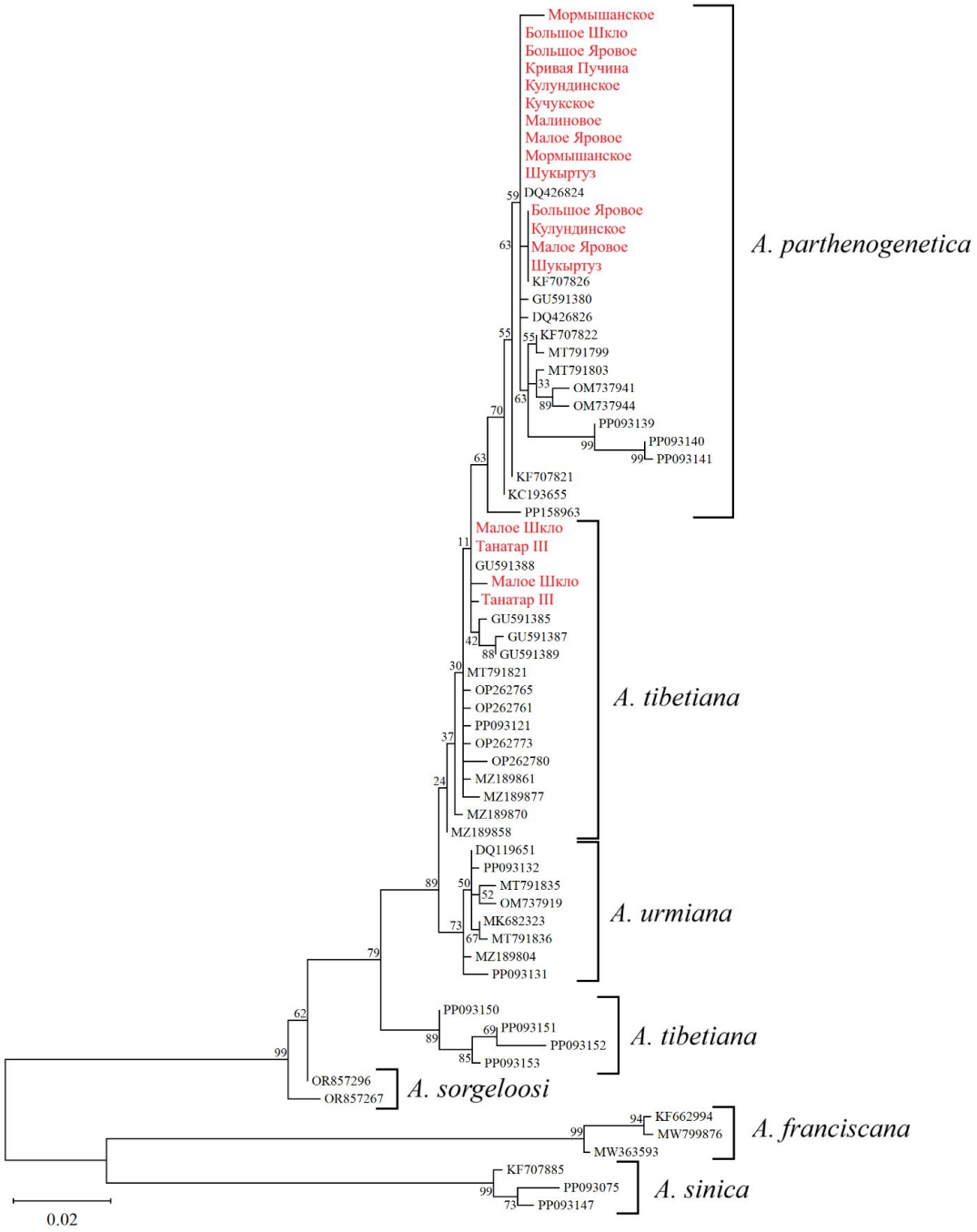

Рис.3. Дендрограмма изученных популяций *Artemia* spp. и генетически схожих образцов из NCBI на основе фрагмента гена COI. Популяции из изученных в 2025 г. озер юга Западной Сибири выделены красным.

$p < 0,01$), длине (*al*: $H = 56,28$, $p < 0,01$) и ширине (*aw*: $H = 73,21$, $p < 0,01$) абдомена, длине второй антенны (*ml*: $H = 103,50$, $p < 0,01$), максимальной (*mw (max)*: $H = 91,26$, $p < 0,01$) и минимальной длине второй антенны (*mw (min)*: $H = 88,09$, $p < 0,01$), расстоянию между глазами (*de*: $H = 95,85$, $p < 0,01$), диаметру глаза (*ed*: $H = 92,91$, $p < 0,01$), длине первой антенны (*la*: $H = 92,02$, $p < 0,01$), ширине головы (*hw*: $H = 103,50$, $p < 0,01$), длине фурок (*fl*: $H = 92,70$, $p < 0,01$), длине щетинок на фурках (*sl*: $H = 52,77$, $p < 0,01$), количеству щетинок на фурках (*sf*: $H = 66,08$, $p < 0,01$) и отношению длины фурки к длине абдомена (*fl/al*: $H = 128,50$, $p < 0,01$). Таким образом, самцы *A. tibetiana* оз. Танатар III имеют более крупные пропорции тела по сравнению с самцами оз. Малое Шкло на основании 13 пластических и 2 меристических признаков (Рис. 5).

Однако, меристический признак самцов *A. tibetiana* оз. Малое Шкло выше таковых у самцов из оз. Танатар III по отношению длины абдомена к длине тела (*al/tl*: $H = 4,31$, $p < 0,05$). Отношение длины цефалоторакса к длине абдомена (*cl/al*: $H = 0,93$, $p > 0,05$) между самцами *A. tibetiana* не имело отличия. Таким образом, самцы *A. tibetiana* оз. Малое Шкло имеют более крупные пропорции тела по сравнению с самцами оз. Танатар III на основании 1 меристического признака. Равнозначность меристического признака (отношение длины цефалоторакса к длине абдомена (*cl/al*)) объединяет морфологически самцов двуполых видов.

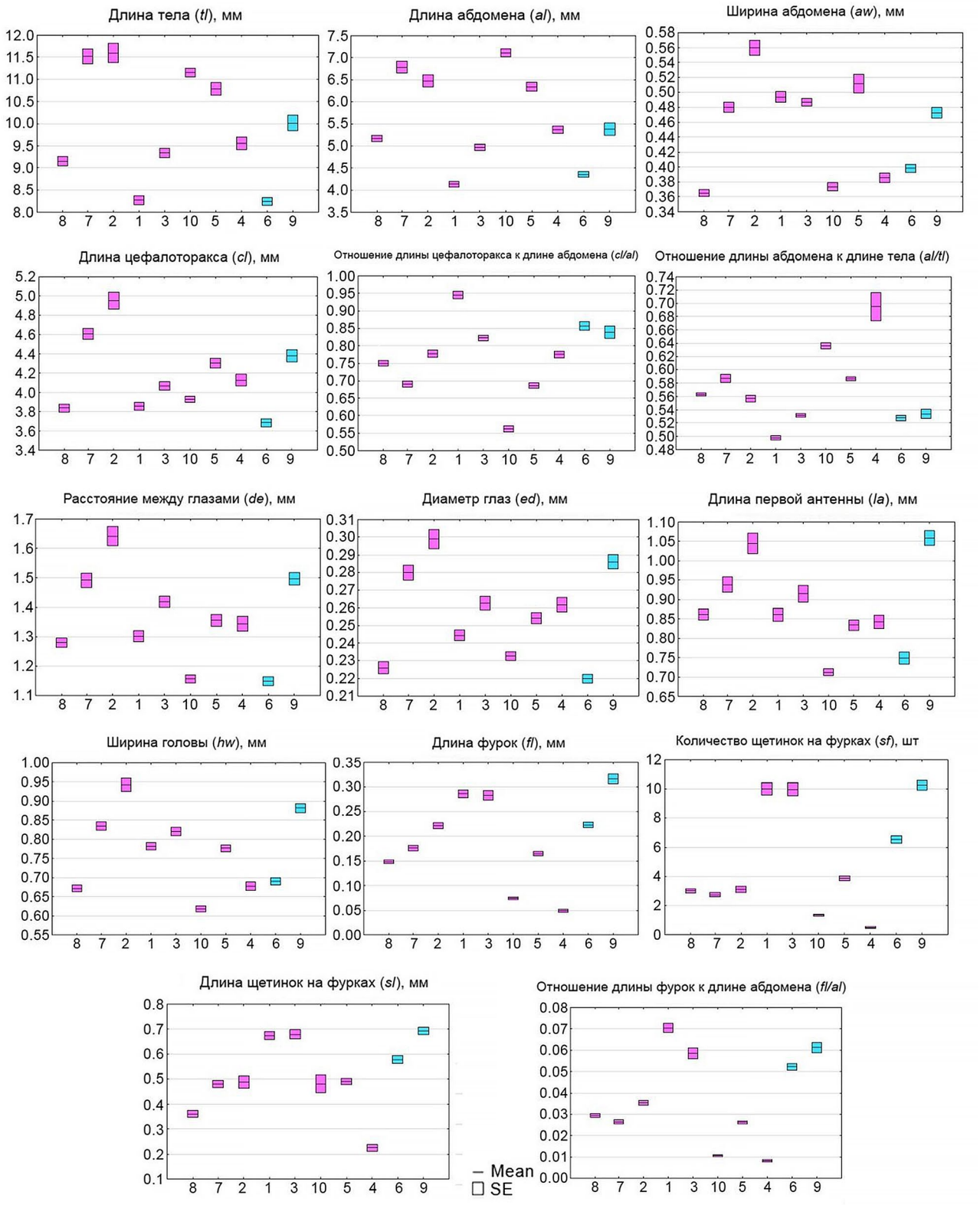

Рис.4. Морфометрические признаки половозрелых самок *A. parthenogenetica* (розовый цвет) и *A. tibetiana* (голубой цвет) в исследованных озерах, 2025 г.: 1 – Большое Шкло, 2 – Большое Яровое, 3 – Кривая Пучина, 4 – Кучукское, 5 – Малиновое, 6 – Малое Шкло, 7– Малое Яровое, 8 – Мормышанское, 9 – Танатар III, 10 – Шукыртуз; Mean – среднее значение; SE – стандартная ошибка.

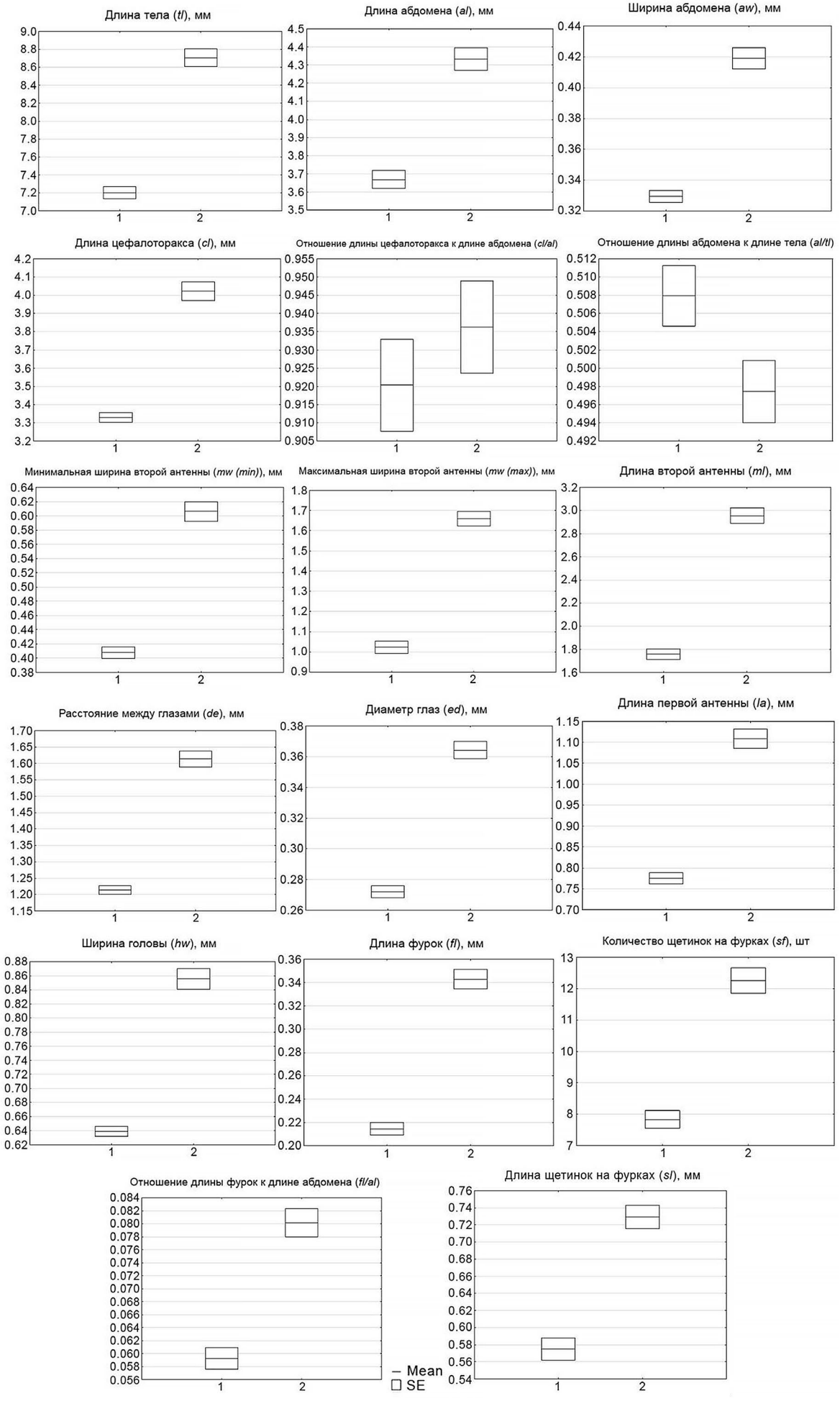

Рис.5. Морфометрические признаки половозрелых самцов *A. tibetiana* в исследованных озерах, 2025 г.: 1 – Малое Шкло; 2 – Танатар III; Mean – среднее значение; SE – стандартная ошибка.

Таблица 3. Морфометрические признаки самок *A. parthenogenetica* и *A. tibetiana* в гипергалинных озерах юга Западной Сибири.

Признак (рис. 2)	*A. parthenogenetica*		*A. tibetiana*	
	Max, $M \pm SE$	Min, $M \pm SE$	Max, $M \pm SE$	Min, $M \pm SE$
tl, мм	11,51 ± 0,17 (Малое Яровое)	8,27 ± 0,10 (Большое Шкло)	10,01 ± 0,17 (Танатар III)	8,24 ± 0,08 (Малое Шкло)
al, мм	7,11 ± 0,09 (Шукыртуз)	4,13 ± 0,07 (Большое Шкло)	5,38 ± 0,14 (Танатар III)	4,35 ± 0,06 (Малое Шкло)
cl, мм	4,95 ± 0,08 (Большое Яровое)	3,84 ± 0,04 (Мормышанское)	4,38 ± 0,06 (Танатар III)	3,68 ± 0,04 (Малое Шкло)
aw, мм	0,56 ± 0,01 (Большое Яровое)	0,37 ± 0,00 (Мормышанское)	0,47 ± 0,01 (Танатар III)	0,40 ± 0,01 (Малое Шкло)
cl/al	0,95 ± 0,01 (Большое Шкло)	0,56 ± 0,01 (Шукыртуз)	0,86 ± 0,01 (Малое Шкло)	0,84 ± 0,02 (Танатар III)
al/tl	0,695 ± 0,021 (Кучукское)	0,498 ± 0,003 (Большое Шкло)	0,53 ± 0,01 (Танатар III)	0,53 ± 0,00 (Малое Шкло)
de, мм	1,64 ± 0,03 (Большое Яровое)	1,16 ± 0,01 (Шукыртуз)	1,50 ± 0,02 (Танатар III)	1,15 ± 0,02 (Малое Шкло)
ed, мм	0,30 ± 0,01 (Большое Яровое)	0,23 ± 0,00 (Мормышанское)	0,29 ± 0,00 (Танатар III)	0,22 ± 0,00 (Малое Шкло)
la, мм	1,05 ± 0,03 (Большое Яровое)	0,71 ± 0,01 (Шукыртуз)	1,05 ± 0,02 (Танатар III)	0,75 ± 0,02 (Малое Шкло)
hw, мм	0,78 ± 0,01 (Большое Яровое)	0,62 ± 0,01 (Шукыртуз)	0,88 ± 0,01 (Танатар III)	0,69 ± 0,01 (Малое Шкло)
fl, мм	0,28 ± 0,01 (Кривая Пучина)	0,05 ± 0,00 (Кучукское)	0,32 ± 0,01 (Танатар III)	0,22 ± 0,01 (Малое Шкло)
sf, шт,	9,98 ± 0,43 (Кривая Пучина)	0,48 ± 0,06 (Кучукское)	10,26 ± 0,35 (Танатар III)	6,53 ± 0,26 (Малое Шкло)
sl, мм	0,67 ± 0,02 (Большое Шкло)	0,23 ± 0,01 (Кучукское)	0,69 ± 0,02 (Танатар III)	0,58 ± 0,02 (Малое Шкло)
fl/al	0,070 ± 0,002 (Большое Шкло)	0,008 ± 0,001 (Кучукское)	0,061 ± 0,002 (Танатар III)	0,052 ± 0,001 (Малое Шкло)

3.3. Сравнительный анализ морфологических признаков самок и самцов *A. parthenogenetica* и *A. tibetiana*

Сравнительный анализ изменчивости морфометрических признаков у разных видов половозрелых самок *A. parthenogenetica* и *A. tibetiana* позволил выявить особенности отдельных частей тела (Рис. 6). Пластические и меристические признаки самок *A. parthenogenetica* выше таковых у самок *A. tibetiana* по длине тела (*tl*: $H = 69{,}28$, $p < 0{,}01$), цефалоторакса (*cl*: $H = 21{,}22$, $p < 0{,}01$), длине (*al*: $H = 86{,}79$, $p < 0{,}01$) и ширине (*aw*: $H = 14{,}78$, $p < 0{,}01$) абдомена, расстоянию между глазами (*de*: $H = 13{,}28$, $p < 0{,}01$), диаметру глаз (*ed*: $H = 11{,}35$, $p < 0{,}05$) и отношению длины абдомена к длине тела (*al/tl*: $H = 79{,}75$, $p < 0{,}01$). Таким образом, самки *A. parthenogenetica* имеют более крупные пропорции тела по сравнению с самками *A. tibetiana* на основании 6 пластических и 1 меристического признака.

Однако пластические и меристические признаки самок *A. tibetiana* выше таковых у самок *A. parthenogenetica* по длине фурок (*fl*: $H = 113{,}80$, $p < 0{,}01$), длине щетинок на фурках (*sl*: $H = 43{,}12$, $p < 0{,}01$), количеству щетинок на фурках (*sf*: $H = 154{,}90$, $p < 0{,}01$), отношению длины цефалоторакса к длине абдомена (*cl/al*: $H = 58{,}20$, $p < 0{,}01$) и длины фурки к длине абдомена (*fl/al*: $H = 158{,}80$, $p < 0{,}01$). Длина первой антенны (*la*: $H = 0{,}05$, $p > 0{,}05$) и ширина головы (*hw*: $H = 0{,}01$, $p > 0{,}05$) между самками не имели значительного отличия. Таким образом, самки *A. tibetiana* имеют более крупные пропорции тела по сравнению с самками *A. parthenogenetica* на основании 2 пластических и 3 меристических признаков. Равнозначность пластических признаков (длина первой антенны (*la*) и ширина головы (*hw*)) объединяют морфологически партеногенетических и двуполых видов.

Результаты сравнения пластических и меристических показателей половозрелых самок и самцов *A. tibetiana* показали, что самки *A. tibetiana* больше самцов *A. tibetiana* по длине тела (*tl*: $H = 52{,}31$, $p < 0{,}01$), цефалоторакса (*cl*: $H = 31{,}31$, $p < 0{,}01$), длине (*al*: $H = 69{,}36$, $p < 0{,}01$) и ширине (*aw*: $H = 55{,}97$, $p < 0{,}01$) абдомена, длине первой антенны (*la*: $H = 4{,}51$, $p < 0{,}05$), ширине головы (*hw*: $H = 6{,}95$, $p < 0{,}01$) и отношению длины абдомена к длине тела (*al/tl*: $H = 39{,}44$, $p < 0{,}01$). Таким образом, самки *A. tibetiana* имеют более крупные пропорции тела по сравнению с самцами *A. tibetiana* на основании 6 пластических и 1 меристического признака.

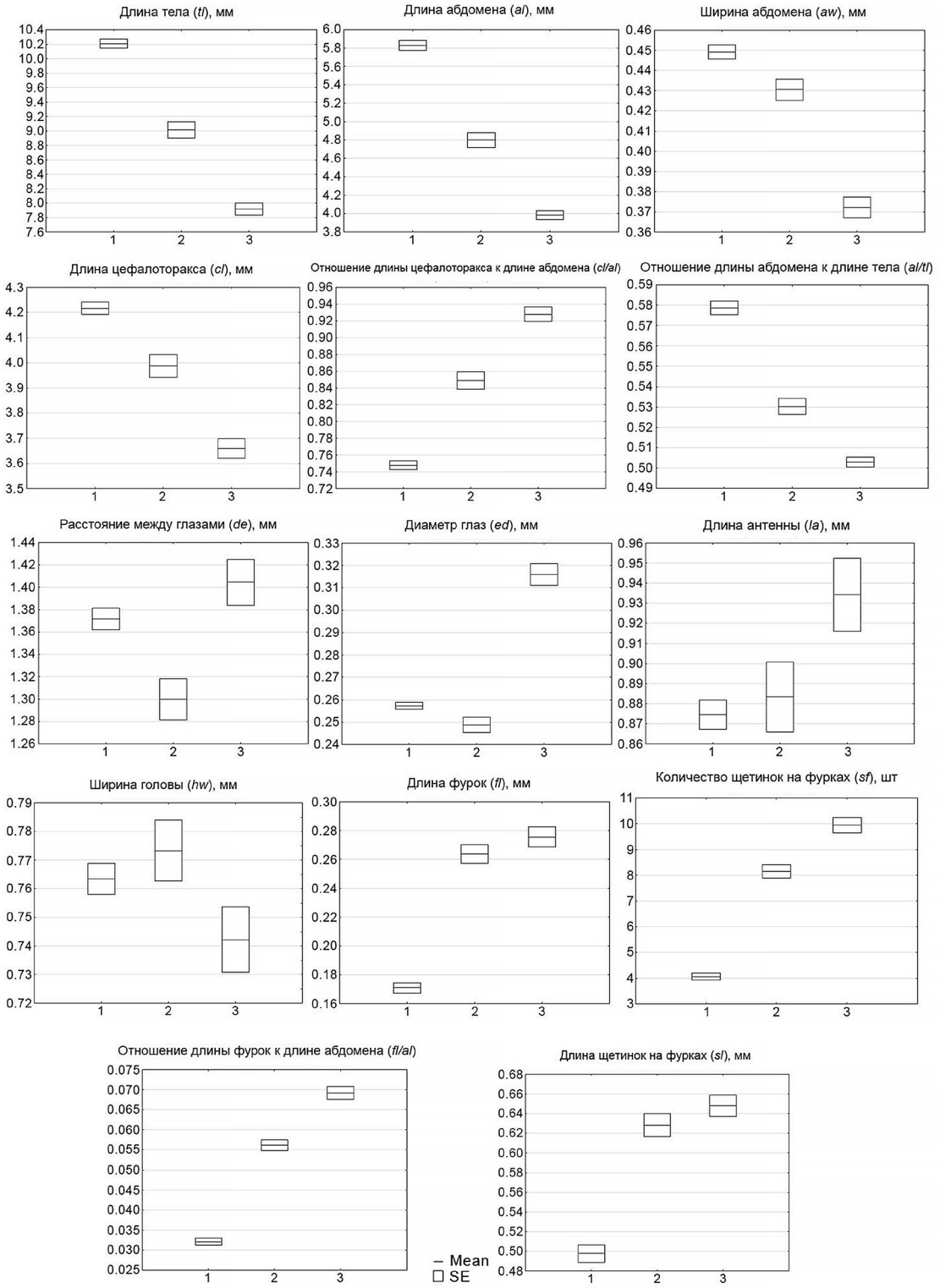

Рис.6. Морфометрические признаки половозрелых самок и самцов рачка *A. parhenogenetica* и *A. tibetiana* в исследованных озерах, 2025 г.: 1 – самки *A. parthenogenetica*; 2 – самки *A. tibetiana*; 3 – самцы *A. tibetiana*; Mean – среднее значение; SE – стандартная ошибка.

Однако пластические и меристические признаки самцов *A. tibetiana* выше таковых самок *A. tibetiana* по расстоянию между глазами (*de*: $H = 10{,}31$, $p < 0{,}01$), диаметру глаз (*ed*: $H = 93{,}32$, $p < 0{,}01$), количеству щетинок на фурках (*sf*: $H = 19{,}66$, $p < 0{,}01$), отношению длины цефалоторакса к длине абдомена (*cl/al*: $H = 36{,}47$, $p < 0{,}01$), длины фурки к длине абдомена (*fl/al*: $H = 35{,}44$, $p < 0{,}01$). Длина фурок (*fl*: $H = 0{,}74$, $p > 0{,}05$) и длина щетинок на фурках (*sl*: $H = 1{,}21$, $p > 0{,}05$) самок и самцов *A. tibetiana* не имели отличия. Таким образом, самцы *A. tibetiana* имеют более крупные пропорции тела по сравнению с самками *A. tibetiana* на основании 2 пластических и 3 меристических признаков. Равнозначность пластических признаков (длина фурки (*fl*) и длина щетинок на фурках (*sl*)) объединяют морфологически самок и самцов двуполых видов.

По нашему мнению, изученные нами пластические и меристические признаки *A. parthenogenetica* и *A. tibetiana* в основном изменялись под воздействием минерализации рапы в исследуемых озерах, которая менялась от 45,9 (оз. Малое Шкло) до 210,9 г/л (оз. Кучукское). Отмечено, что изменения солености воды сказываются на пропорциях тела.

4. Обсуждение

Очевидно, что для понимания особенностей формирования морфометрических признаков артемии, необходимо рассматривать ее развитие во взаимосвязи с факторами минерализации и температуры рапы. Характер связей пластических и меристических признаков с этими факторами позволяет сделать ряд общих выводов для популяций рачка *A. parthenogenetica* (при уровне значимости $p < 0,05$) (Таблица 4):

- при увеличении минерализации происходит редукция щетинок на фурке (*sf*) с уменьшением их длины (*sl*) и уменьшение длины самой фурки (*fl*);
- длина абдомена (*al*) и отношение длины абдомена к длине тела (*al/tl*) увеличиваются пропорционально солености;
- отношение длины цефалоторакса к длине абдомена (*cl/al*), длины фурок к длине абдомена (*fl/al*), ширина абдомена (*aw*), длина первой антенны (*la*) и ширина головы (*hw*) отрицательно коррелируют с минерализацией.

При увеличении температуры рапы в исследованный период происходит уменьшение длины цефалоторакса (*cl*) и расстояния между глазами (*de*) в популяциях рачка *A. parthenogenetica*.

Поскольку популяции *A. tibetiana* отмечены только в двух озерах, из-за малой выборки для статистического анализа были использованы другие методы. Сравнение средних данных минерализации рапы оз. Малое Шкло (45,9 ±13,8 г/л) и оз. Танатар III (161,6 ± 48,5 г/л) по критерию Краскела-Уоллиса (*H*) показало достоверное различие ($p < 0,05$). Температура рапы рассматриваемых озер (оз. Малое Шкло: 21,4 ± 1,4 ˚C; оз. Танатар III: 16,0 ± 1,2 ˚C) также значимо отличалась ($p < 0,05$).

Таким образом, при увеличении минерализации рапы на 115,7 г/л и уменьшении ее температуры на 5,4 ˚C изменились морфометрические признаки самок и самцов рачка *A. tibetiana*:

- увеличились параметры тела самок и самцов: длина тела (*tl*), длина абдомена (*al*), ширина абдомена (*aw*), длина цефалоторакса (*cl*);
- увеличились размерные характеристики головы самок и самцов: расстояние между глазами (*de*), диаметр глаза (*ed*), длина первой антенны (*la*), ширина головы (*hw*);
- увеличились показатели фурок самок и самцов: длина фурки (*fl*), количество щетинок на фурках (*sf*), длина щетинок на фурках (*sl*);
- уменьшилось отношение длины абдомена к длине тела (*al/tl*) самцов;
- увеличились размеры второй антенны самцов: длина второй антенны (*ml*), максимальная и минимальная ширина второй антенны (*mw (max)*, *mw (min)*).

Кластерный анализ 12 пластических и 4 меристических признаков самок *A. parthenogenetica* по среднесезонным значениям показал принадлежность популяций к 3 группам, различающимся по минерализации рапы, а также по особенностям фуркальных показателей (Рис. 7).

Отдельная группа образована популяцией артемии из озер Большое Шкло и Кривая Пучина.

Таблица 4. Корреляционный анализ пластических и меристических признаков *A. parthenogenetica* по абиотическим факторам.

Признак	r	R^2	Уравнение зависимости
Минерализация рапы, г/л			
Длина абдомена (*al*)	0,41	0,24	y = 0,0094x + 4,3428
Ширина абдомена (*aw*)	-0,67	0,35	y = -0,0008x + 0,5901
Длина первой антенны (*la*)	-0,43	0,11	y = -0,0007x + 0,9885
Ширина головы (*hw*)	-0,53	0,22	y = -0,001x + 0,9262
Длина фурок (*fl*)	-0,82	0,59	y = -0,0011x + 0,3492
Длина щетинок на фурках (*sl*)	-0,59	0,30	y = -0,0018x + 0,7715
Количество щетинок на фурках (*sf*)	-0,75	0,44	y = -0,0401x + 10,31
Отношение длин цефалоторакса к длине абдомена (*cl/al*)	-0,70	0,46	y = -0,0013x + 0,9627
Отношение длины абдомена к длине тела (*al/tl*)	0,86	0,63	y = 0,001x + 0,431
Отношение длины фурок к длине абдомена (*fl/al*)	-0,87	0,63	y = -0,0003x + 0,077
Температура рапы, ˚C			
Длина цефалоторакса (*cl*)	-0,42	0,18	y = -0,0435x + 5,1284
Расстояние между глазами (*de*)	-0,39	0,15	y = -0,0156x + 1,7005

Примечание: r – коэффициент корреляции Спирмена, R^2 – коэффициент аппроксимации.

Рачки, обитающие в этих озерах, характеризуются наиболее высокими фуркальными показателями по сравнению с остальными озерами (длина фурок (*fl*), количество щетинок на фурках (*sf*), длина щетинок на фурках (*sl*)) (см. Рис. 4). Средняя минерализация рапы первой группы озер составляет 109.9 ± 7.1 г/л. Вторая группа объединила популяции артемии озер Кучукское и Мормышанское. Длина щетинок на фурках (*sl*) рачков этой группы самая короткая по сравнению с остальными озерами. Средняя минерализация этой группы озер составляет 219,1 ± 8,0 г/л. Третья группа образована популяциями артемии из озер Большое Яровое, Малое Яровое, Малиновое, Шукыртуз. Рачки этих озер характеризуются схожей между собой длиной щетинок на фурках (*sl*), которая значительно отличается от таковых остальных групп озер. Средняя минерализация рапы этой группы озер составила 170,2 ± 2,8 г/л.

Как было показано выше, изученные нами гипергалинные озера юга Западной Сибири характеризуются различными абиотическими факторами, которые оказывают воздействие на жизнедеятельность гидробионтов. Изменение температуры и минерализации рапы в озерах оказывает воздействие на динамику численных показателей, а также различий морфометрических признаков артемии, что было отмечено в ранее проведенных исследованиях (Веснина и др., 2023; Vesnina and Bezmaternykh, 2023; Литвиненко и др., 2024). Слишком высокая или низкая минерализация рапы проявляется в угнетении роста, развития и размножения артемии (Веснина и др., 2011). При изменении минерализации рапы меняется не только морфология, но и особенности размножения и соотношение полов (Веснина и др., 2012; Сёмик и др., 2024).

Как известно, артемия характеризуется высокой экологической пластичностью и может менять свои размеры и форму в зависимости от внешних факторов, основным из которых многие исследователи считают концентрацию солей в воде (Nobile et al., 2020; Forneck et al., 2021; Van Stappen et al., 2020; Thirunavukkarasu et al., 2024). При этом морфометрические признаки артемии изучаются во всем мире для дифференциации и идентификации видов (Naganawa and Mura, 2017; Asem et al., 2020; Sainz-Escudero et al., 2021). Кроме того, эти морфометрические различия между особями или популяциями одного и того же вида могут быть обусловлены генотипической изменчивостью (Thirunavukkarasu et al., 2021). Наши данные полностью подтверждают эти выводы. Выявлены как явные изменения морфометрических признаков обоих изученных видов артемии по градиенту важнейших экологических факторов, так межвидовые и межпопуляционные отличия, которые существенно осложняют таксономическую диагностику по морфологическим признакам.

Подобные закономерности отмечены в ранее проведённых исследованиях, которые показали различия морфологических признаков ряда популяций, обнаруженных в разных географических районах, особенно в прибрежных районах Индии, Китая, Европы и Африки (Thirunavukkarasu et al., 2022; Thirunavukkarasu et al., 2021; Ruebhart et al., 2008). Авторы из Индии и Тайваня на основе изучения их морфометрических признаков обнаружили 6 морфотипов артемии (Maniatsi et al., 2009). По морфометрическим показателям так же, как и в нашем случае, были выявлены отличия самок и самцов артемии Северной Америки и Карибского побережья Колумбии (Van Stappen et al., 2024). Очевидно, наших и ранее проведенных исследований морфологических и размерно-весовых характеристик артемии из разнотипных озер юга Западной Сибири пока недостаточно для достоверной дифференциации популяций артемии разных видов (Литвиненко и др., 2024; Vesnina et al., 2025).

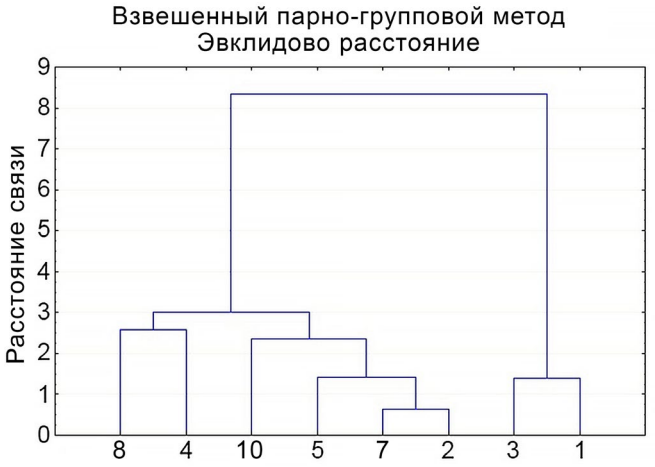

Рис.7. Дендрограмма сходства комплекса морфометрических показателей самок исследованных популяций *A. parthenogenetica* из гипергалинных озер юга Западной Сибири (метод одиночной связи): 1 – Большое Шкло; 2 – Большое Яровое; 3 – Кривая Пучина; 4 – Кучукское; 5 – Малиновое; 7 – Малое Яровое; 8 – Мормышанское; 10 – Шукыртуз.

Выполненный анализ пластических и меристических признаков половозрелых особей артемии из разнотипных гипергалинных озер Алтайского края подтвердил, что наиболее вариабельными признаками у самок рачка артемии являются фуркальные показатели (Vesnina et al., 2025).

5. Выводы

Изучены современные морфологические характеристики партеногенетических и двуполых популяций артемии в 10 разнотипных гипергалинных озерах юга Западной Сибири. Использование ДНК-баркодинга позволило определить в изученных гипергалинных озерах Алтайского края два вида артемии: *A. parthenogenetica* и *A. tibetiana.* В хлоридных (Большое Шкло, Большое Яровое, Кривая Пучина, Кучукское, Малиновое, Малое Яровое, Шукыртуз) и сульфатном (Мормышанское) озерах выявлена *A. parthenogenetica*, а в хлоридном (Малое Шкло) и в гидрокарбонатном (Танатар III) – *A. tibetiana*.

Сравнительный анализ морфологических признаков показал, что самки *A. parthenogenetica* и

A. tibetiana имеют значимые отличия средних величин – 14 из 16 изученных признаков: длина тела, длина абдомена, отношение длины абдомена к длине тела, ширина абдомена, расстояние между глазами, диаметр глаза, длина цефалоторакса, отношение длины цефалоторакса к длине абдомена, длина фуркальной ветви, количество щетинок на фурке, длина щетинок на фурке, отношение длины фурки к длине абдомена.

Анализ 12 пластических и 4 меристических признаков самок *A. parthenogenetica* показал, что её популяции разделяются на 3 группы, различающиеся особенностями строения фурки: длиной, количеством щетинок, длиной щетинок. Индекс корреляции Спирмена выявил значимые статистические зависимости морфологических признаков *A. parthenogenetica* и *A. tibetiana* от основных экологических факторов – минерализации и температуры рапы.

Благодарности

Работа выполнена в рамках гранта Российского научного фонда, проект №25-26-00148 (https://rscf.ru/en/project/25-26-00148/).

Конфликт интересов

Авторы заявляют об отсутствии конфликта финансовых и личных интересов.

Список литературы

Веснина Л.В., Васильева А.С. 2019. Современное состояние популяции рачка артемии в период опреснения гипергалинных озер (на примере озера Кулундинское). Водные биоресурсы, аквакультура и экология водоемов: материалы VII Международной научной конференции 6: 108–118.

Веснина Л.В., Веснин Ю.А., Романова Н.С. и др. 2023. Роль солоноватоводной фауны и состояние биоресурса экосистемы гипергалинного озера Кулундинское в фазе трансгрессии (Алтайский край). Рыбное хозяйство 2: 65–72.

Веснина Л.В., Ронжина Т.О., Пермякова Г.В. и др. 2011. Алтайские стартовые корма: вчера, сегодня, завтра. В: Аквакультура центральной и восточной Европы: настоящее и будущее: материалы II Международной научной конференции, С. 48–53.

Веснина Л.В., Ронжина Т.О., Пермякова Г.В. и др. 2012. Технология получения стартовых кормов из артемии соленых озер Алтайского края. Рыбоводство и рыбное хозяйство 3: 52–59.

Литвиненко Л.И., Корентович М.А., Бойко Е.Г. и др. 2024. Артемия в гипергалинных водоемах России (география, биоразнообразие, экология, биология и практическое использование). Тюмень: ГАУ Северного Зауралья.

Никоноров А.М. 1989. Справочник по гидрохимии. Л.: Гидрометеоиздат.

Руководство по гидробиологическому мониторингу пресноводных экосистем. 1992. СПб.: Гидрометеоиздат.

Руководство по химическому анализу поверхностных вод суши. Часть 1. 2009. В: Боева Л.В. (ред.). Ростов-на-Дону.

Руководство по химическому анализу поверхностных вод суши. Часть 2. 2012. В: Боева Л.В. (ред.). Ростов-на-Дону.

Семик А.М., Замятина Е.А., Паршин-Чудин А.В. и др. 2024. Сравнительный анализ популяции жаброногого рачка рода *Artemia* в гипергалинных озерах Крыма по морфометрическим признакам. Рыбоводство и рыбное хозяйство 12: 862–875. DOI: 10.33920/sel-09-2412-03

Asem A., Eimanifar A., Rastegar-Pouyani N. et al. 2020. An overview on the nomenclatural and phylogenetic problems of native Asian brine shrimps of the genus Artemia Leach, 1819 (Crustacea, Anostraca). Zookeys 902: 1.

Asem A., Yang C., Eimanifar A. et al. 2023. Phylogenetic analysis of problematic Asian species of Artemia Leach, 1819 (Crustacea, Anostraca), with the descriptions of two new species. Journal of Crustacean Biology 83(1): 1–25. DOI: 10.1093/jcbiol/ruad002

Beardmore J.A., Pilla E.J., Thomas K.M. 1994. Genetic variation in *Artemia*: speciation, reproductive mode and potential for exploitation. In: Gajardo G., Coutteau P. (Eds.), Book of Abstracts of Contributions. Puerto Montt.

Browne R.A., Bowen S.T. 1991. Taxonomy and population genetics of *Artemia*. In: Browne R.A., Sorgeloos P., Trotman C.N.A. (Eds.), *Artemia* Biology. Boston: CRC Press, pp. 221–235.

Edgar R.C. 2004. MUSCLE: multiple sequence alignment with high accuracy and high throughput. Nucleic Acids Research 32(5): 1792. DOI: 10.1093/nar/gkh340

Eimanifar A., Van Stappen G., Marden B. et al. 2014. *Artemia* biodiversity in Asia with the focus on the phylogeography of the introduced American species *Artemia franciscana* Kellogg, 1906. Molecular Phylogenetics Evolution 79: 392–403.

Folmer O., Black M., Hoeh W. et al. 1994. DNA primers for amplification of mitochondrial cytochrome coxidase subunit I from diverse metazoan invertebrates. Molecular Marine Biology and Biotechnology 3(5): 294–299.

Forneck S.C., Dutra F.M., de Camargo M.P. et al. 2021. Aquaculture facilities drive the introduction and establishment of non-native Oreochromis niloticus populations in Neotropical streams. Hydrobiologia 848(9): 1955–1966. DOI: 10.1007/s10750-020-04430-8

Hammer Ø., Harper D.A.T., Ryan P.D. 2001. PAST: Paleontological Statistics Software Package for Education and Data Analysis. Palaeontologia Electronica.

Kumar S., Stecher G., Li M. et al. 2018. MEGA X: Molecular evolutionary genetics analysis across computing platforms. Molecular Phylogenetics Evolution 35: 1547. DOI: 10.1093/molbev/msy096

Lobo J., Costa P., Teixeira M. et al. 2013. Enhanced primers for amplification of DNA barcodes from a broad range of marine metazoans. BMC ecology 13: 1.

Maccari M., Amat F., Gómez A. 2013. Origin and Genetic Diversity of Diploid Parthenogenetic *Artemia* in Eurasia. PLoS ONE 8(12): e83348.

Maniatsi S., Baxevanis A.D., Abatzopoulos T.J. 2009. The intron 2 of p26 gene: a novel genetic marker for discriminating the two most commercially important *Artemia franciscana* subspecies. Journal of Biological Research 11: 73–82. DOI: 10.3390/ijms10125455

Naganawa H., Mura G. 2017. Two new cryptic species of *Artemia* (Brachiopoda, Anostraca) from Mongolia and the possibility of invasion and disturbance by the aquaculture industry in East Asia. Crustaceana 90(14): 1679–1698. DOI: 10.1163/15685403-00003744

Nobile A.B., Cunico A.M., Vitule J.R. et al. 2020. Status and recommendations for sustainable freshwater aquaculture in Brazil. Reviews in Aquaculture 12(3): 1495–1517. DOI: 10.1111/raq.12393

Pang H., Zheng K., Wang W. et al. 2024.The Morphological

Differentiation and Evolutionary Origins of *Artemia* in China. Diversity 16(3): 144.

Persoone G., Sorgeloos P. 1980. General aspects of the ecology and biogeography of *Artemia*. In: Persoone G., Sorgeloos P., Roels O., Jaspers E. (Eds.). The brine shrimp *Artemia*. Ecology, culturing, use in aquaculture 3: Universa Press, Wetteren, Belgium, pp. 3–24.

Pilla E.J.S., Beardmore J.A. 1994. Genetic and morphometric differentiation in Old World bisexual species of the brine shrimp (*Artemia*). Heredity 72: 47–56. DOI: 10.1038/hdy.1994.97

Ruebhart D.R., Cock I.E., Shaw G.R. 2008. Invasive character of the brine shrimp *Artemia* franciscana Kellogg 1906 (Branchiopoda: Anostraca) and its potential impact on Australian inland hypersaline waters. Marine & Freshwater Research 59(7): 587–595. DOI: 10.1071/MF07221

Sainz-Escudero L., López-Estrada E.K., Rodríguez-Flores P.C. et al. 2021. Settling taxonomic and nomenclatural problems in brine shrimps, *Artemia* (Crustacea: Branchiopoda: Anostraca), by integrating mitogenomics, marker discordances and nomenclature rules. PeerJ: 62. DOI: 10.7717/peerj.10865

Tamura K., Stecher G., Kumar S. 2021. MEGA11: Molecular Evolutionary Genetics Analysis Version 11. Molecular Biology and Evolution 38(7): 3022. DOI: 10.1093/molbev/msab120

Thirunavukkarasu S., Karunasagaran G., Munuswamy N. 2021. Genetic diversity and population structure of *Artemia franciscana* from southeast coast of India. Journal of Sea Research 178: 102127. DOI: 10.1016/j.seares.2021.102127

Thirunavukkarasu S., Karunasagaran G., Munuswamy N. 2022. Morphometric and phylogenetic analysis of morphotypes in *Artemia franciscana* Kellogg, 1906 (Crustacea: Anostraca). Regional Studies in Marine Science 54: 102411. DOI: 10.1016/j.rsma.2022.102411

Thirunavukkarasu S., Murugan G., Hwang J.-S. et al. 2024. Morphology and morphometry of morphotypes in the population of *Artemia franciscana* (Kellogg, 1906) from salterns of the southeastern coast of India. Heliyon 10(1): 1–13. DOI: 10.1016/j.heliyon.2024.e29796

Triantaphyllidis G.V., Zhang B., Zhu L. et al. 1994. International Study on *Artemia*. L. Review of the literature on *Artemia* from salt lakes in the People's Republic of China. International Journal of Salt Lake Research 3: 1–12. DOI: 10.1007/BF01990645

Van Stappen G. 2002. Chapter IV. Zoogeography. In: Abatzopoulos T.J., Beardmore J.A., Clegg J.S., Sorgeloos P. (Eds.), *Artemia*: Basic and applied biology. Dordrecht, the Netherlands, Kluwer Academic Publishers, pp. 286.

Van Stappen G., Sorgeloos P., Rombaut G. 2024. Manual on *Artemia* production and use. FAO Fisheries and Aquaculture Technical Papers. Rome. DOI: 10.4060/cd0313en

Van Stappen G., Sui L., Hoa V.N. et al. 2020. Review on integrated production of the brine shrimp *Artemia* in solar salt ponds. Reviews in Aquaculture 12(2): 1054–1071. DOI: 10.1111/raq.12371

Vanhaecke P., Tackaert W., Sorgeloos P. 1987. The biogeography of *Artemia*: an updated review. In: Sorgeloos P., Bengtson D.A., Decleir W. et al. (Eds.), *Artemia* research and Its applications. Morphology, genetics, strain characterisation, toxicology. Wetteren, Belgium, Universa Press.

Vesnina L.V., Bezmaternykh D.M. 2023. Influence of Environmental Factors on the Dynamics of Zooplankton in Lake Kulunda (Western Siberia). Russian Journal of Ecology 54(3): 243–250. DOI: 10.1134/S1067413623030086

Vesnina L.V., Bezmaternykh D.M., Lassyi M.V. et al. 2025. Morphometric Characteristics and DNA Barcoding of Branchiopod Crustaceans of the Genus *Artemia* (Crustacea: Anostraca) from the Lakes of the Kulunda Lowland of Altai Krai. Inland Water Biology 18(5): 980–990. DOI: 10.1134/S1995082925600978

Short communication

LIMNOLOGY FRESHWATER BIOLOGY

Seasonal dynamics of rotifer community in relation to water quality at Pravara-Godavari river confluence (Ahmednagar, MS, India)

Zaware R.V.*, Harkal A.D.

Department of Zoology and Research Centre, New Arts Commerce and Science College, Ahmednagar-414001, Maharashtra, Affiliated with Savitribai Phule Pune University, Pune, Maharashtra, India

ABSTRACT. This study reports the diversity, abundance, and seasonal dynamics of the rotifer community in the Pravara-Godavari river confluence, Ahmednagar, throughout a year, from November 2024 to October 2025. Seasonal sampling was conducted to assess rotifer species composition and density, and to measure key physicochemical water parameters, including temperature, pH, dissolved oxygen, turbidity, alkalinity, hardness, and chloride. A total of 19 rotifer species, representing 4 genera and 3 families, were recorded in the study area. Strong temporal variation in population structure was indicated by the rotifer community's noticeable seasonal variations in both species richness and density. The summer period recorded the highest rotifer diversity and abundance. At the same time, the monsoon season had the lowest values, perhaps due to a dilution effect, increased water turbulence, and altered habitat stability. Furthermore, correlation analysis showed that important physicochemical parameters such as pH, water temperature, turbidity, alkalinity, total hardness, chloride concentration, and dissolved oxygen had a significant impact on rotifer species richness. These results demonstrate that even small changes in water quality can significantly impact the composition of rotifer communities. Overall, the study highlights rotifers' sensitivity to environmental factors and underscores their value as reliable bioindicators for evaluating freshwater ecosystems.

Keywords: species diversity, bioindicator, rotifer abundance, water quality, freshwater ecosystem

For citation: Zaware R.V., Harkal A.D. Seasonal dynamics of rotifer community in relation to water quality at Pravara-Godavari river confluence (Ahmednagar, MS, India) // Limnology and Freshwater Biology. 2026. - № 2. - P. 130-134. DOI: 10.31951/2658-3518-2026-A-2-130

1. Introduction

Rotifers (Phylum Rotifera) are among the oldest metazoan groups (Barnes, 1993) and dominate zooplankton assemblages in freshwater ecosystems. They exhibit distinct seasonal dynamics closely regulated by physicochemical parameters, confirming their ecological sensitivity and reliability as bioindicators for assessing freshwater quality and environmental change (Arora and Mehra, 2003). A rotifer taxon of considerable diversity is frequently found in various types of stabilization ponds, polluted rivers, and lentic ecosystems such as village ponds (Sládeček, 1983). Rotifer species composition and abundance are suggested to be strongly associated with ecosystem health status, and individual species may reflect the level of eutrophication (Rogozin, 2021). In tropical and subtropical regions such as India, seasonal variations, including the Monsoon, Post-Monsoon, Winter, and Summer, play a pivotal role in shaping aquatic environments. The present study aims to investigate seasonal variation in rotifer diversity and abundance at the Pravara-Godavari river confluence in Ahmednagar (Ahilyanagar) district, Maharashtra, India. We also analyze the influence of key physicochemical parameters on their distribution. River confluences create dynamic environmental gradients that strongly influence the distribution, diversity, and metabolic activity of microorganisms, making these zones critical for understanding microbial ecology and river health (Hui et al., 2022). By examining these interactions across different seasons, the study provides important baseline data. It enhances our understanding of how environmental variability shapes zooplankton communities in freshwater ecosystems.

*Corresponding author. E-mail address: rajashrizaware1@gmail.com (R.V. Zaware)

Received: February 06, 2026;
Accepted after revised: April 08, 2026;
Available online: April 24, 2026

The study of the Godavari River at Kaygaon Toka and Kopargaon revealed significant seasonal and spatial variations in water quality, with several parameters at Kopargaon exceeding drinking water standards, indicating localized pollution impacts (Rathod and Shinde, 2011). The study by Thitame et al. (2010) examines seasonal variations in physicochemical parameters and irrigation suitability of water from the Pravara River at Sangamner, Ahmednagar district. Overall, research on the seasonal dynamics of rotifer communities, particularly at the Pravara–Godavari river confluence, is limited. Most available studies are either broader zooplankton surveys, general diversity assessments, or seasonal studies in other freshwater bodies and water quality contexts. The Pravara–Godavari river confluence is an ecologically significant zone where seasonal runoff, hydrological mixing, and watershed activities influence water quality and biological communities. Despite its importance, detailed studies on rotifer dynamics remain limited. Assessing seasonal variations of rotifers in relation to physicochemical parameters provides essential baseline data for understanding community responses, evaluating water quality, and supporting sustainable management under increasing anthropogenic pressure.

Ahmednagar (Ahilyanagar) is the largest district in terms of area. It is situated in the middle of western Maharashtra, India. The district has a total area of 17196 sq. km, making it the largest district in Maharashtra. The Pravara-Godavari river confluence is located at Pravaranagar in Ahmednagar district, Maharashtra, where the Pravara and Godavari rivers meet. The Pravara River is about 200-208 km long in Ahmednagar, flowing eastward and gathering tributaries such as the Mula and Mahalungi before meeting the Godavari at Pravara Sangam. The region falls within the semi-arid zone and experiences a tropical monsoon climate, characterized by three major seasons: the Monsoon (July to November) Winter (December to February) and Summer (March to June).

2. Materials and Methods

2.1. Study area

The study was conducted at the Pravara–Godavari river confluence in Ahmednagar (Ahilyanagar) district, Maharashtra, India. Two sampling sites were selected at the confluence zone: site 1 (latitude 19.621814° N; longitude 75.018419° E) and site 2 (latitude 19.622778° N; longitude 75.015309° E). The geographic locations were recorded using GPS, and a site map was prepared to depict the sampling stations.

2.2. Sample collection and analysis

Rotifer samples were collected seasonally from both sites. Sampling was carried out using a standard plankton net with a 40 μm mesh size over the period of one year (October 2024 to September 2025). The plankton net was pulled horizontally at ~1 m below the water surface and towed for a distance of 10 m. The collected samples were transferred to clean polyethene bottles and preserved in 4% formalin for laboratory analysis. Physicochemical parameters were analysed according to standard methods. Water temperature and pH were measured on-site using portable field instruments. Dissolved oxygen (DO) was measured in situ and later determined in the laboratory using Winkler's method. Turbidity was measured using a Secchi disc. Other chemical parameters, such as alkalinity, hardness, and chloride, were analysed using standard titrimetric and laboratory procedures.

All zooplankton were left to settle at the bottom. The concentrated sample was examined using a LABOMED Lx 300 binocular microscope. Microphotographs were taken using a digital camera attached to the microscope. A micrometre was used to measure the organism's size. All rotifers were identified based on external morphological characters. The latest standard taxonomic keys and relevant literature were used for identification, including Sharma (1987; 2005), Dhanapathi (2000), Koste (1987), and Segers (2007). For quantitative estimation, counting was performed using the Sedgwick-Rafter method. Rotifer community structure was evaluated using standard ecological indices such as the Shannon–Wiener Diversity Index (H'), Simpson's Diversity Index (D), and Evenness Index (E). Statistical analysis was performed using Microsoft Excel. The association between physicochemical parameters and rotifer abundance was evaluated through direct seasonal comparison of measured values, and the relationships were interpreted based on concurrent fluctuations.

3. Results

In 2024–2025, a total of 19 rotifer species from four genera and three families were identified in the present research from the Pravara-Godavari river confluence. With nine species, Brachionidae was the most prevalent family. Lecanidae and *Trichocercidae* followed with four and two species, respectively. About the genus-wise seasonal distribution, Brachionus had the most significant number of species in every season (six in the Monsoon, eight in the Winter, and six in the Summer). In contrast, *Keratella* had between one and two species, *Lecane* had between one and four species, and *Trichocerca* was only found in the Winter and Summer. The number of species increased from nine during the Monsoon to thirteen during the Summer (Table 1).

Summer had the highest diversity, followed by Monsoon and Winter, according to the Shannon-Wiener diversity index (H') values. At the same time, Pielou's Evenness (E) was highest in Summer, indicating a more uniform distribution of species, and lowest in Winter. Simpson's index (D) revealed the lowest dominance in Summer and higher dominance in Monsoon and Winter (Table 2).

Rotifer population density also varied seasonally in the water sample analysis. Summer showed the highest abundance (1760 ind./L), followed by Winter (1520 ind./L) and Monsoon (1120 ind./L) (Fig. 1).

The pH value ranged from 7.5 to 7.9, the water temperature peaked in the Summer (29°C), the turbidity

Table 1. Rotifer species recorded from the water samples of the Pravara-Godavari river confluence (November 2024-October 2025).

No.	Family	Species	Monsoon	Winter	Summer
1.	Brachionidae	*Brachionus diversicornis* Daday, 1883	+	+	+
2.		*Brachionus plicatilis plicatilis* Müller, 1786	+	–	–
3.		*Brachionus quadridentatus melhemi* Barrois & Daday, 1894	–	+	+
4.		*Brachionus calyciflorus* Pallas, 1766	+	+	+
5.		*Brachionus falcatus* Zacharias, 1898	+	+	+
6.		*Brachionus variabilis* Hempel, 1896	–	+	–
7.		*Brachionus forficula* Wierzejski, 1891	+	–	–
8.		*Brachionus caudatus* Barrois & Daday, 1894	+	+	+
9.		*Brachionus angularis* Gosse, 1851	–	+	+
10.		*Keratella tropica* Apstein, 1907	–	+	+
11.		*Keratella valga* Ehrenberg, 1834	–	+	–
12.		*Keratella procurva* Thorpe, 1891	–	+	–
13.		*Keratella cochlearis* Gosse, 1851	–	–	+
14.	Lecanidae	*Lecane physalis* Wulfert, 1939	–	–	+
15.		*Lecane leontina* Turner, 1892	+	–	+
16.		*Lecane lunaris* Ehrenberg, 1832	+	–	+
17.		*Lecane bulla bulla* Gosse, 1851	–	+	+
18.	Trichocercidae	*Trichocerca siamensis* Segers & Pholpunthin, 1997	–	–	+
19.		*Trichocerca tigris* Müller, 1786	–	+	–

ranged from 1.5 to 1.8 NTU, and the dissolved oxygen slightly dropped in the Summer (7.3 mg/L) compared to the Monsoon (8.8 mg/L). These physicochemical parameters showed minor seasonal variations. Higher rotifer abundance was associated with increases in hardness, alkalinity, and chloride concentrations from Monsoon to Summer (Table 3, Fig. 2).

Table 2. Diversity indices of rotifer abundance at the Pravara-Godavari river confluence.

No.	Season	Shannon H'	Simpson D	Evenness E
1.	Monsoon	0.932	0.444	0.673
2.	Winter	0.918	0.439	0.662
3.	Summer	1.190	0.282	0.859

4. Discussion

At the Pravara-Godavari river confluence, seasonal variation had a significant impact on rotifer diversity and abundance. The Summer period recorded the highest levels of species richness, diversity, and evenness. At the same time, the Monsoon season showed the lowest levels. Increased temperature also improved feeding efficiency and nutrient assimilation, leading to rapid population turnover. In addition, relatively stable hydrological conditions during Summer increased water residence time, allowing plankton communities to establish and proliferate. The Monsoon season exhibited reduced diversity and abundance due to hydrological disturbance. Heavy rainfall increased turbidity and reduced light penetration, thereby indirectly limiting phytoplankton availability. Monsoonal runoff also diluted nutrients. These combined stressors explain the observed decline in richness and community stability. A lower Simpson's dominance in the Summer further indicated a more uniform distribution of species.

Perhaps as a result of lower temperatures and different dissolved oxygen levels, Winter supported moderate diversity but lower evenness, indicating

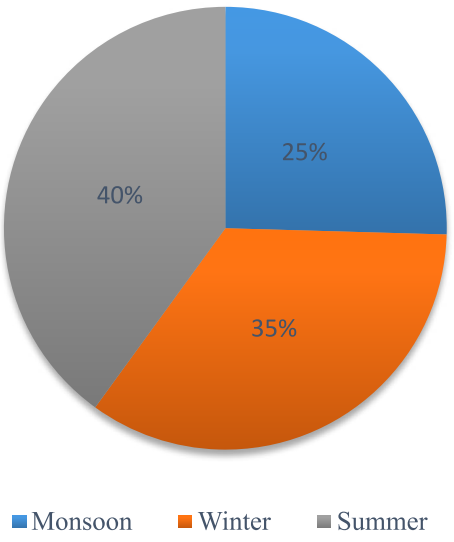

Fig.1. Seasonal percent contribution of rotifer density (ind./L) in the Pravara-Godavari river confluence.

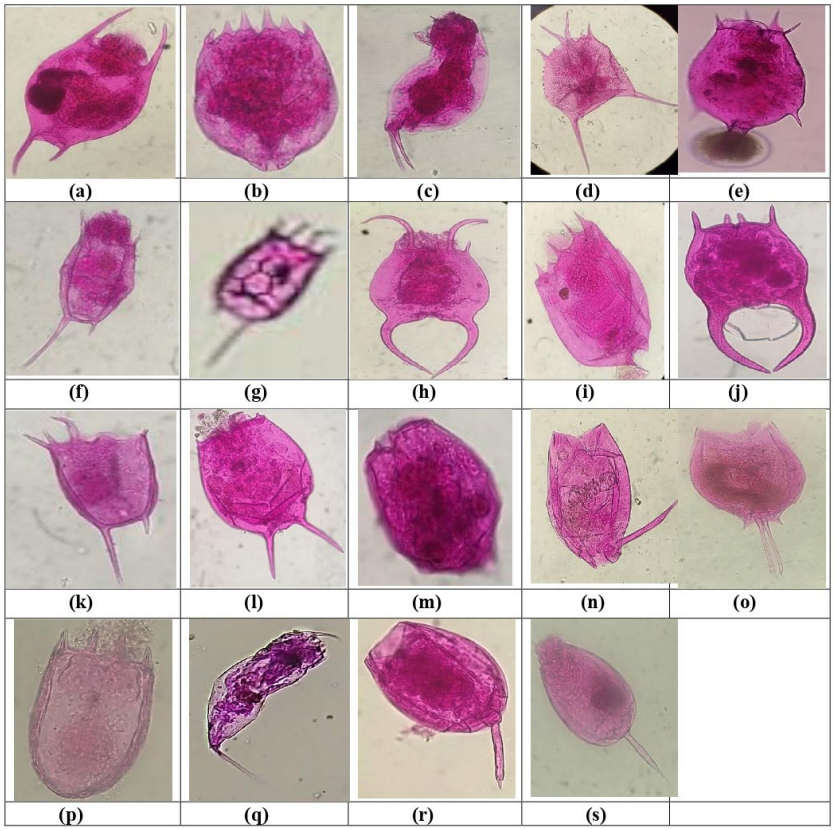

Fig.2. a) *B. diversicornis*; b) *B. plicatilis plicatilis*; c) *Trichocerca tigris*; d) *B. quadridentatus melhemi*; e) *B. calyciflorus*; f) *K. tropica*; g) *K. procurva*; h) *B. falcatus*; i) *B. variabilis*; j) *B. forficula*; k) *K. valga*; l) *B. caudatus*, 1894; m) *B. angularis*; n) *L. physalis*; o) *L. leontina*; p) *K. cochlearis*; q) *Trichocerca siamensis*; r) *L. lunaris*; and s) *L. bulla bulla*.

dominance by fewer genera. Perennial dominance of Brachionus species demonstrates their ecological adaptability across a range of physicochemical conditions. The ecological success of *Brachionus* in semi-arid freshwater ecosystems is attributed to its high reproductive rate, broad tolerance to environmental variations, and ability to utilize nutrient-rich conditions. Many species thrive in alkaline, moderately eutrophic waters, which are common in reservoirs and river systems in Maharashtra. Consequently, the consistent dominance of *Brachionus* indicates its role as a bioindicator of productive and nutrient-enriched freshwater habitats. The seasonal pattern observed in the Pravara–Godavari river confluence, where rotifer diversity and abundance peaked during Summer and declined during the Monsoon, is consistent with observations from other freshwater bodies of Maharashtra, such as Shanoor Dam (Gadhikar and Sawale, 2016), Dnyaneshwar Sagar (Kawade and Pandarkar, 2014), and Visapur Dam (Bhalsing and Pokale, 2023). Thus, the similarity between the present findings and previous studies indicates that seasonal hydrological dynamics play a crucial role in structuring rotifer communities in freshwater ecosystems of Maharashtra. Rotifers are sensitive to environmental changes, as indicated by correlations between rotifer community structure and physicochemical parameters such as temperature, dissolved oxygen, turbidity, alkalinity, hardness, and chloride. These results support the application of rotifers as useful bioindicators of ecological status and water quality in semi-arid freshwater ecosystems.

5. Conclusion

According to the study, rotifer diversity in the Pravara-Godavari river confluence is seasonal, with the highest levels of species richness, diversity, and evenness occurring in the Summer. The dominant family, Brachionidae, demonstrates the ecological adaptability of certain rotifers to changing environmental conditions. Continuous monitoring of rotifer populations and water quality assessments may contribute to ecological management and provide essential baseline data for research on freshwater biodiversity. These findings contribute to our understanding of the dynamics of planktonic communities in the freshwater ecosystems of Ahmednagar, Maharashtra. They can serve as a guide for future ecological and conservation research.

Table 3. Physicochemical profile of the Pravara-Godavari river confluence.

No.	Season	pH	Water Temp (°C)	Turbidity (NTU)	DO (mg/L)	Hardness (mg/L as $CaCO_3$)	Alkalinity (mg/L)	Chloride (mg/L)
1.	Monsoon	7.5	27	1.8	8.8	204	124	84.57
2.	Winter	7.7	25	1.5	8.4	255	135	95.32
3.	Summer	7.9	29	1.6	7.3	276	168	102.84

Acknowledgments

The authors are thankful to the Department of Zoology, New Arts, Commerce and Science College, Ahilyanagar, for providing facilities for conducting research.

Conflict of interest

The author declares no conflicts of interest.

References

Arora J., Mehra N.K. 2003. Seasonal dynamics of rotifers in relation to physical and chemical conditions of the river Yamuna (Delhi), India. Hydrobiologia 491(1): 101-109. DOI: 10.1023/A:1024490805310

Barnes K.E. 1993. A study of the zooplankton community of Ratcliff Lake in the Davy Crockett National Forest, Texas. Stephen F. Austin State University.

Bhalsing D.G., Pokale S.N. 2023. Occurrence of Some Freshwater Rotifers from Visapur Dam, Ahmednagar, Maharashtra, India. Uttar Pradesh Journal of Zoology 44(16): 100-106. DOI: 10.56557/upjoz/2023/v44i163583

Dhanapathi M.V.S. S. S. 2000. Taxonomic notes on the rotifers from India. Hyderabad, India: Indian Association of Aquatic Biologists.

Gadhikar Y.A., Sawale S.P. 2016. Seasonal abundance and diversity of rotifers of Shahanoor dam, Amravati District, India. Universal journal of environmental research and technology 6(2): 82-90.

Hui C., Li Y., Liao Z. et al. 2022. Confluences characteristics determine the influence scope of microbial community from confluence hydrodynamic zone on river network. Journal of Hydrology 612: 128288. DOI: 10.1016/j.jhydrol.2022.128288

Kawade S.A., Pandarkar A.K. 2014. Study of interrelationship between water parameters and zooplankton diversity of Dnyaneshwar Sagar, Ahmednagar, Maharashtra. Journal of Experimental Zoology 17(2): 737-742.

Koste W., Shiel R.J. 1987. Rotifera from Australian inland waters. II. Epiphanidae and brachionidae (Rotifera: Monogononta). Invertebrate taxonomy 1(7): 949-1021. DOI: 10.1071/IT9870949

Rathod S.R., Shinde S.E. 2011. Comparative study of the physio-chemical parameter of water from Godavari river at Kaygaon Toka and Kopargaon. Bioinfolet 8(4): 452-454.

Rogozin A.G. 2021. Materials on the fauna and ecology of rotifers in the Urals, family Brachionidae (Rotifera, Eurotatoria, Ploima), genera Kellicottia, Plationus, and Platyias. Biology Bulletin 48(7): 950-958. DOI: 10.1134/S1062359021070244

Segers H. 2007. Annotated checklist of the rotifers (Phylum Rotifera), with notes on nomenclature, taxonomy and distribution. Zootaxa 1564(1): 1-104.

Sharma B.K. 1987. Rotifera: Eurotatoria: Monogononta (Freshwater). Fauna of Orissa: State Fauna Series 1(1): 323-340.

Sharma B.K., Sharma S. 2005. Biodiversity of freshwater rotifers (Rotifera, Eurotatoria) from North-Eastern India. Zoosystematics and Evolution 81(1): 81-88.

Sládeček V. 1983. Rotifers as indicators of water quality. Hydrobiologia 100(1): 169-201. DOI: 10.1007/BF00027429

Thitame S.N., Pondhe G.M. 2010. Assessment of seasonal variation in physico-chemical characteristics and quality of Pravara River water for irrigation use in Sangamner, Dist Ahmednagar, Maharashtra. Journal of Chemical and Pharmaceutical Research 2(2): 316-320.